Aus dem Walther-Straub-Institut für Pharmakologie und Toxikologie

Institut der Ludwig-Maximilians-Universität München

Vorstand: Prof. Dr. med. Thomas Gudermann

Roles of Transient Receptor Potential (TRP) Cation Channels in Primary Pulmonary Fibroblasts

Dissertation
zum Erwerb des Doktorgrades der Naturwissenschaften

an der Medizinischen Fakultät der

Ludwig-Maximilians-Universität München

vorgelegt von

Fabienne Angela Geiger

aus

Bayreuth

2023

Mit Genehmigung der Medizinischen Fakultät

der Universität München

Betreuer: Prof. Dr. rer. nat. Alexander Dietrich

Zweitgutachter: Prof. Dr. rer. nat. Alexander Faußner

Dekan: Prof. Dr. med. Thomas Gudermann

Tag der mündlichen Prüfung: 21.09.2023

Affidavit

Affidavit

Geiger, Fabienne

_____
Surname, first name

_____
Street

_____
Zip code, town, country

I hereby declare, that the submitted thesis entitled:

Roles of Transient Receptor Potential (TRP) Cation Channels in Primary Pulmonary Fibroblasts

is my own work. I have only used the sources indicated and have not made unauthorised use of services of a third party. Where the work of others has been quoted or reproduced, the source is always given.

I further declare that the dissertation presented here has not been submitted in the same or similar form to any other institution for the purpose of obtaining an academic degree.

Munich, November 4, 2023   Fabienne Geiger
place, date   Signature doctoral candidate

Table of contents

Table of Figures

List of abbreviations

Å	Angstrom
AA	Amino acid
AITC	Allyl isothiocyanate
Akt	Protein kinase B
AR	Ankyrin repeat
ARD	Ankyrin repeat domain
AT1/2	Alveolar epithelial cells type 1/2
α-SMA	alpha Smooth muscle actin
Ca^{2+}	Calcium ions
$[Ca^{2+}]$	Ca^{2+} concentration
$[Ca^{2+}]_e$	Extracellular Ca^{2+} concentration
$[Ca^{2+}]_i$	Intracellular Ca^{2+} concentration
CC	Coiled-coil
CD	Coupling domain
Chr	Chromosome
CIRB	Calmodulin and IP_3-receptor binding site
COL1A1	Collagen type 1A1
Cryo-EM	Cryogenic Electron Microscopy
CTD	C-terminal domain
DAG	Diacylglycerol
ECM	Extracellular matrix
ER	Endoplasmic reticulum
ERK	Extracellular signal-regulated kinase
FEPS	Familial episodic pain syndrome
FMD	Fibroblast to myofibroblast differentiation
FN1	Fibronectin 1
GPCR	G protein coupled receptor
HEK-293	Human embryonic kidney 293
HLF	Human lung fibroblasts
hTRP	Human TRP channel
I_{CRAC}	Ca^{2+} release-activated Ca^{2+} current
IP_3	Inositol triphosphate

IV

KD	Knockdown
KO	Knockout
MAPK	Mitogen-activated protein kinase (MAPK)
Mg^{2+}	Magnesium ions
MH2	Mad homology 2
MMP	Matrix metalloproteases
mTRP	murine TRP channel
MRC5	Fetal human lung fibroblast cell line
NFAT	Nuclear factor of activated T cells
NFκB	Nuclear factor 'kappa-light-chain-enhancer' of activated B-cells
pmLF	Primary murine lung fibroblasts
RNAseq	RNA sequencing
ROS	Reactive oxygen species
PAI-1	Plasminogen activator inhibitor 1
PDGF	Platelet-derived growth factor
PF	Pulmonary Fibrosis
PI3K	Phosphatidylinositol 3-kinase
PIP_2	Phosphatidylinositol-4,5-biphosphate
PLC	Phospholipase C
ROCE	Receptor operated Ca^{2+} entry
siRNA	Small interfering RNA
SOCE	Store operated Ca^{2+} entry
STIM	Stromal interaction molecule
Tg	Thapsigargin
TGF-β1	Transforming growth factor-beta 1
TMD	Transmembrane domain
TNBS	Trinitrobenzene sulfonic acid
TRP	Transient receptor potential
TRPA	Transient receptor potential ankyrin
TRPC	Transient receptor potential canonical/classical
TRPM	Transient receptor potential melastatin
µM	micro Molar
u/tPA	Urokinase or tissue plasminogen activator

VSLD	Voltage-sensor-like domain
WT	Wild type
Zn^{2+}	Zinc ion

List of publications

Research papers included in this dissertation

Research Paper I [1]

Geiger F, Zeitlmayr S, Staab-Weijnitz CA, Rajan S, Breit A, Gudermann T, Dietrich A. An inhibitory function of TRPA1 Channels in TGF-β1-driven Fibroblast to Myofibroblast Differentiation. American Journal of Respiratory Cell and Molecular Biology. 2023; 68: 314-325. https://doi.org/10.1165/rcmb.2022-0159OC

Research Paper II [2]

Bendiks L, **Geiger F**, Gudermann T, Feske S, Dietrich A. Store-operated Ca^{2+} entry in primary murine lung fibroblasts is independent of classical transient receptor potential (TRPC) channels and contributes to cell migration. Scientific Reports. 2020; 10(1): 6812. https://doi.org/10.1038/s41598-020-63677-2

Research Paper III [3]

Zeitlmayr S, Zierler S, Staab-Weijnitz CA, Dietrich A., **Geiger F**, Horgen FD, Gudermann T, Breit A. TRPM7 restrains plasmin activity and promotes transforming growth factor-β1 signaling in primary human lung fibroblasts. Archives of Toxicology. 2022; 96(10): 2767-83. https://doi.org/10.1007/s00204-022-03342-x

Research papers not included in this dissertation

Maurus K, Hufnagel A, **Geiger F.** *et al.* The AP-1 transcription factor FOSL1 causes melanocyte reprogramming and transformation. Oncogene; 2017; 36: 5110-21. https://doi.org/10.1038/onc.2017.135

Rak-Raszewska A, Reint G, **Geiger F.** *et al.* Deciphering the minimal quantity of mouse primary cells to undergo nephrogenesis ex vivo. Developmental Dynamics. 2022; 251(3): 536-50. https://doi.org/10.1002/dvdy.418

Review articles not included in this dissertation

Rajan S, Schremmer C, Weber J, Alt P, **Geiger F**, Dietrich A. Ca^{2+} Signaling by TRPV4 Channels in Respiratory Function and Disease. Cells**.** 2021; 10: 822. https://doi.org/10.3390/cells10040822

Müller I, Alt P, Rajan S, Schaller L, **Geiger F**, Dietrich A. Transient Receptor Potential (TRP) Channels in Airway Toxicity and Disease: An Update. Cells. 2022; 11: 2907. https://doi.org/10.3390/cells11182907

Published Abstracts

Geiger F, Tumbev Y, Groeber-Becker FK, Berberich-Siebelt F. 358 Human-based T cell-skin models for graft-versus-host disease. Journal of Investigative Dermatology. 2019; 139 (9): S276. https://doi.org/10.1016/j.jid.2019.07.360

Geiger F, Staab-Weijnitz CA, Gudermann T, Dietrich A. TRPA1 function in human pulmonary fibroblasts. The FASEB Journal. 2021; 35. https://doi.org/10.1096/fasebj.2021.35.S1.03394

Conferences

6th German Pharm-Tox Summit
March 1st – 3rd 2021
Oral presentation
Digital
TRPA1 function in human pulmonary fibroblasts

Experimental Biology 2021
April 27th – 30th 2021
Poster presentation
Digital
TRPA1 function in human pulmonary fibroblasts
Abstract available

7th German-Pharm-Tox Summit
March 7th – 10th 2022
Oral presentation
Digital
An inhibitory function of TRPA1 channels in TGF-β1-driven Fibroblast to Myofibroblast Differentation

European Calcium Channel Conference
May 24th – 28th 2022
Alpbach, Austria
Poster presentation

Summary

Transient receptor potential (TRP) cation channel-mediated signaling constitutes important pathways for ion homeostasis in mammalian cells. The only member of the ankyrin family of TRP channels, TRPA1, harbors a high number of ankyrin repeat domains (ARDs) in its N-terminus. We showed in paper I that this channel is highly expressed in primary human lung fibroblasts (HLFs) and prevented transforming growth factor beta 1 (TGF-β1)-induced fibroblast to myofibroblast differentiation (FMD) in these cells. FMD is a hallmark in the progression of pulmonary fibrosis (PF) in human patients. *TRPA1* mRNA expression was markedly reduced in myofibroblasts and knockdown (KD) of the channel resulted in increased expression of fibrosis markers (e.g. collagen 1A1 (COL1A1), fibronectin 1 (FN1), alpha smooth muscle actin (α-SMA) and plasminogen activator inhibitor 1 (PAI-1)). TRPA1-mediated inhibition of expressed myofibroblast specific proteins was orchestrated by a tight regulation of extracellular signal-regulated kinase 1/2 (ERK1/2) and SMAD2-linker phosphorylation and depended on the availability of extracellular calcium ions (Ca^{2+}). As one of the major second messengers, Ca^{2+} concentrations in cells underlie a rigid control to ensure the specificity of signals and avoid Ca^{2+}-mediated toxicity. Ca^{2+} influx into cells occurs either through receptor-operated calcium entry (ROCE) or through store-operated calcium entry (SOCE). Whereas some groups suggested involvement of canonical TRP channels 1 and 6 (TRPC1/6) in SOCE, paper II showed that TRPC1/6 in primary murine lung fibroblasts (pmLFs) contribute exclusively to ROCE and not to SOCE. TRP melastatin 7 (TRPM7) channels differ from TRPA1 and TRPC1/6 in that they exhibit higher selectivity for magnesium ions (Mg^{2+}) than for Ca^{2+}. Activation of TRPM7 channels supported the development of cardiac fibrosis by enhancing TGF-β1-triggered synthesis of extracellular matrix (ECM). Paper III showed that inhibition of TRPM7 in HLFs increased plasmin activity and reduced fibrosis marker expression. Therefore, the results of paper I and III suggest that activation of TRPA1 and blocking of TRPM7 channels may be promising therapeutic strategies in patients suffering from pulmonary fibrosis.

Zusammenfassung

Die Signaltransduktion durch "Transient receptor potential" (TRP) Kationen Kanäle ist für die Aufrechterhaltung des Ionengleichgewichts in Säugerzellen äußerst wichtig. Das einzige Mitglied der „Ankyrin"-Familie von TRP-Kanälen, TRPA1, exprimiert eine große Zahl an „Ankyrin Repeat" Domänen (ARDs) im N-Terminus. Wir konnten in „Paper I" zeigen, dass der aktive Kanal in primären humanen Lungen Fibroblasten (HLF) stark exprimiert ist und in diesen Zellen die durch den transformierenden Wachstumsfaktor beta 1 (TGF-β1) ausgelöste Fibroblasten-zu-Myofibroblasten-Differenzierung als essentiellen Schritt für die Entwicklung einer Lungenfibrose in Patienten verhindern kann. Die Produktion von *TRPA1* mRNS war in Myofibroblasten deutlich reduziert und eine verminderte Produktion des Kanals führte zu einer verstärken Expression von Fibrose Markern (z.B.: Kollagen, Fibronektin, alpha glattes Muskelaktin und „plasminogen activator inhibitor 1"). Die TRPA1-vermittelte Inhibition der Expression Myofibroblastenspezifischer Proteine wurde durch eine direkte Regulation der ERK1/2- und SMAD2/3-Linker-Phosphorylierung induziert und hing von der Verfügbarkeit von extrazellulärem Kalzium Ionen (Ca^{2+}) ab. Als einer der wichtigsten sekundären Botenstoffe unterliegt die Ca^{2+}-Konzentration in den Zellen einer strengen Kontrolle, um die Spezifität der Signale zu gewährleisten und um eine Ca^{2+}-vermittelte Toxizität zu vermeiden. Die Erhöhung der intrazellulären Ca^{2+}-Konzentration erfolgt entweder durch einen rezeptorgesteuerten Einstrom von Kalzium Ionen („receptor-operated Ca^{2+} entry, ROCE") oder durch den Ausstrom von Ca^{2+} aus den internen Ca^{2+}-Speichern („store-operated Ca^{2+} entry, SOCE"). Während einige Gruppen eine Beteiligung der kanonischen TRP-Kanäle 1 und 6 (TRPC1/6) am SOCE vorschlugen, zeigte Paper II, dass TRPC1/6 Kanäle in primären murinen Lungenfibroblasten (pmLFs) ausschließlich zum „ROCE" und nicht zum „SOCE" beitragen. TRP-Melastatin 7 (TRPM7) Kanäle unterscheiden sich von TRPA1 und TRPC1/6 Proteinen durch ihre höhere Selektivität für Magnesium Ionen (Mg^{2+}) im Vergleich zu Ca^{2+}. Eine Aktivierung von TRPM7-Kanälen förderte die Entwicklung einer Herzfibrose und verstärkte die durch TGF-β1 ausgelöste Synthese der extrazellulären Matrix (ECM). Paper III zeigte, dass die Hemmung von TRPM7 in HLFs die Plasminaktivität erhöhte und die Expression von Fibrosemarkern reduzierte. Die Ergebnisse von Paper I und III zeigen also, dass eine Aktivierung von TRPA1- und eine Blockade von TRPM7-Kanälen vielversprechende therapeutische Strategien für Patienten darstellen, die an einer pulmonalen Fibrose leiden.

1. *Contribution to the publications*

1.1 Contribution to paper I

Fibroblast to myofibroblast differentiation (FMD) is assumed to crucially contribute to the development of pulmonary fibrosis (PF). A former Ph.D. student (Katharina Hofmann) of our research group showed that transforming growth factor beta 1 (TGF-β1) treatment of wild type (WT) primary murine lung fibroblasts (pmLFs) led not only to myofibroblast differentiation of the cells, but also induced an upregulation of classical transient receptor potential 6 (TRPC6) mRNA and protein expression [4]. Furthermore, TRPC6 knockout (KO) in mice ameliorated bleomycin-induced lung fibrosis compared to WT mice. Now, we set out to analyze the role of TRP channels in FMD in a more translational approach. To obtain a detailed overview on the effects of TGF-β1-treatment on primary human lung fibroblasts (HLFs) and more specifically on TRP channel expression, I prepared HLF samples of three healthy donors either treated with TGF-β1 or solvent for RNA sequencing (RNAseq). I performed a preliminary analysis of the RNAseq data and noticed a clear trend towards a TGF-β1-mediated downregulation of mRNA expression from the *transient receptor potential A1* (*TRPA1*) gene in HLFs. After verification of the TGF-β1-induced reduction of *TRPA1* on mRNA level using quantitative reverse transcription PCR (qRT-PCR), I started investigating the role of the channel in HLFs more closely. As all tested TRPA1 antibodies failed to detect endogenous levels of the protein in HLFs, I verified the TGF-β1- and small interfering RNA (siRNA)-mediated reduction of TRPA1 channels on a functional level in Ca^{2+}-imaging experiments. While qRT-PCRs as well as immunoblotting, immunofluorescence staining or a plasmin activity assay confirmed TGF-β1-mediated upregulation of fibrosis markers (e.g. *ACTA2*/α-SMA, FN1, COL1A1 and *SERPINE1*/PAI-1), activation of TRPA1 channels by the specific agonists AITC or JT010 counteracted this TGF-β1-mediated upregulation of myofibroblast markers. Moreover, knockdown (KD) of TRPA1 mRNA by siRNAs led to increased levels of the above mentioned fibrosis markers. With the use of antibodies recognizing phosphorylated proteins and a luciferase reporter assay, I was able to demonstrate an involvement of the phosphorylated Extracellular signal-regulated kinase1/2 (ERK1/2) and SMAD2/3 in TRPA1 signaling in HLFs as KD and inhibition of TRPA1 diminished phosphorylation levels. Moreover, ERK1/2 and SMAD2-linker phosphorylation strongly depended on the availability of extracellular Ca^{2+} as its depletion dampened the phosphorylation levels.

Additional to my role in designing and conducting all laboratory work as well as the statistical analysis of the experiments using GraphPad PRISM (Version 9.4) (except the thorough analysis of the RNAseq data), I also took part in drafting and revising the manuscript of paper I.

1.2 Contribution to paper II

Ca^{2+} signaling plays an essential role in multiple cellular functions. Two mechanistically distinct processes can mediate Ca^{2+} entry in cells – receptor operated Ca^{2+} entry (ROCE) and store operated Ca^{2+} entry (SOCE). TRPC channels are known to be involved in ROCE. However, there is a dispute in the scientific community if – in addition to STIM and ORAI proteins – TRPCs also contribute to SOCE. In this publication, we aimed to assess the role of TRPC1/6 to SOCE in pmLFs.

My contribution to paper II included a thorough revision and critical discussion of the manuscript as well as the clarification of the effect of TRPC1/6-KO in pmLFs on STIM1/2 (protein and mRNA) and *Orai1-3* (mRNA) expression levels. During the peer-review process of the manuscript, one of the reviewers pointed out the need to reevaluate STIM1/2 protein levels in TRPC1/6$^{-/-}$ pmLFs compared to WT cells. Additional to already analyzed samples, I used cell lysates from freshly isolated pmLFs of WT and TRPC1/6$^{-/-}$ C57BL/6 mice (three of each genotype) for immunoblots. These results confirmed that KO

of TRPC1/6 does not alter STIM1/2 protein expression levels in pmLFs. Quantitative RT-PCR revealed a slightly reduced *Stim1/2* gene expression in TRPC1/6-deficient mice compared to WT mice, while *Orai1-3* mRNA expression was not affected by the TRPC1/6 KO.

1.3 Contribution to paper III

Inhibition of transient receptor potential melastatin 7 (TRPM7) signaling reduced TGF-β1-mediated production of collagen and α-SMA in MRC5 cells [5]. My colleague Sarah Zeitlmayr from the lab of Dr. Andreas Breit was able to demonstrate in this publication that application of TRPM7 antagonists result in decreased expression of myofibroblast markers as well as plasminogen activator inhibitor-1 (PAI-1). I contributed to this research by transferring our methods for the isolation and handling of murine and human primary fibroblasts and helped to draft and revise the manuscript.

2. *Introduction*

2.1 **Transient Receptor Potential Cation Channels**

In 2021, the Nobel Prize award for two transient receptor potential (TRP) researchers David Julius and Ardem Patapoutian underlined the importance of TRP cation channels. The first *Trp* gene was cloned in drosophila [6], but the channels are also highly expressed in mammalian cells, where they serve a plethora of biological functions (reviewed in [7]). The 28 mammalian TRP channels are grouped into six subfamilies: TRPC (for canonical or classical), TRPM (for melastatin), TRPV (for vanilloid), TRPA (for ankyrin), TRPML (for mucolipin) und TRPP (for polycystin) (see Fig. 1A) [7]. The human *TRPC2* gene, however, contains a premature stop codon and as a pseudogene does not code for a functional protein [8].
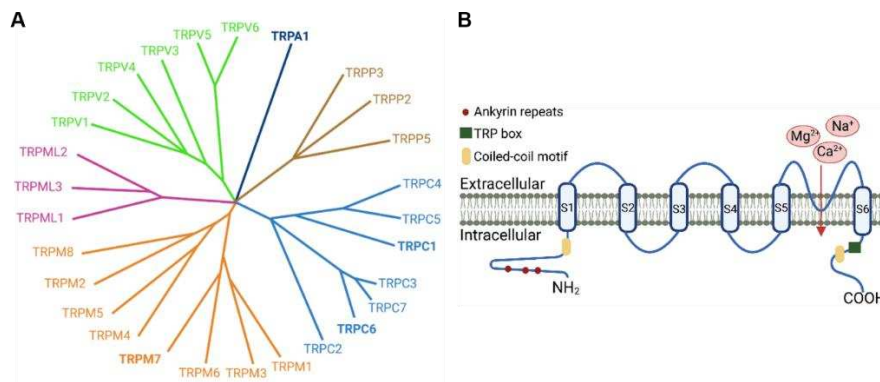

Figure 1: The Superfamily of TRP channels. A: Phylogenetic tree of the 28 mammalian members of TRP channels in six families: C for canonical, V for vanilloid, M for melastatin, A for ankyrin, P for polycystin and ML for mucolipin (created with BioRender, modified from [9]). **B:** Schematic view of the TRP subunit structure. The structure includes N-terminal: ankyrin repeat domains (ARDs) and a coiled-coil (CC) motif (not present in all TRP channels); six transmembrane segments, a pore loop through which mostly cations (e.g. Ca^{2+}, Na^+, Mg^{2+}) enter; and C-terminal: a TRP-(L) box and a CC motif (not present in all TRP channels) (created with BioRender, adapted from [10]).

Although mammalian TRP channels share merely 20 % sequence homology [11], the general structures of TRP channels are similar (see Fig. 1B). TRP channels possess six transmembrane-spanning domains, with the fifth (S5) and sixth (S6) segment forming a cation permeable pore. Typical structural characteristics for the intracellular N- and C-termini of TRPs include ankyrin repeat domains (ARDs) and a TRP box domain, respectively (reviewed in [12]). The TRP box is highly conserved and consists of a proline-rich 24 amino acid (AA) motif [12] that might be pivotal for TRP channel gating [13, 14].

Depending on the protein, the homo- or heterotetrameric TRP channels are localized either in the plasma membrane or intracellularly in lysosomal membranes. Activation occurs through a wide variety of stimuli such as diacylglycerol (DAG), temperature, reactive oxygen species (ROS) or chemicals [7]. Lanthanoids, such as La^{3+} and Gd^{3+}, inhibit most TRP channels [15, 16]. Most TRP channels are non-selective cation channels with permeability for calcium ions (Ca^{2+}) (reviewed in [17]), which serve as ubiquitous second messengers. Only TRPM4 [18] and TRPM5 [19] are impermeable for Ca^{2+}, while TRPV5 [20] and TRPV6 [21] show the highest selectivity for Ca^{2+}. Although TRP channels are expressed throughout the entire organism [7], the work presented here investigates the role of TRP channels in human and murine primary lung fibroblasts.

2.1.1 **Transient Receptor Potential Ankyrin 1 Channel**

The only member of the ankyrin family of TRP channels, TRPA1, received its name from the high number of ankyrin repeats (ARs) located at the N-terminus of the protein. In humans, the *ANKTM1* gene is

localized on chromosome (Chr) 8q21.11 and contains 29 exons [22]. In mice, the gene with 27 exons is found on Chr1 [23]. The two orthologues share 79 % sequence identity [24]. TRPA1 is a non-selective cation channel [25] with high permeability for Ca^{2+} [26, 27] and expressed throughout the entire body. The TRPA1 cDNA was first cloned from cultured human lung fibroblasts (HLFs) [28]. The channel, however, is not expressed in primary murine lung fibroblasts (pmLFs) of C57BL/6 mice (unpublished result from our RNA-Seq. data). Most research focuses on TRPA1 function in sensory neurons, where its expression is relatively high and often occurs in combination with TRPV1 [29-31]. As a noxious sensor, TRPA1 plays a role in airway diseases (e.g. cough [32] and smoking related responses [33]), itch [34, 35], pain sensation and inflammatory pain ([36-38], reviewed in [31, 39]).

The first high resolution (~ 4 Å) cryo-electron microscopy (EM) structure of the 1119 AA-long human TRPA1 cation channel by Paulsen *et al*. in 2015 confirmed the homo-tetrameric assembly of the channel [40, 41]. In contrast to previous assumptions, the TRPA1 C-terminus contains a TRP-like domain, which can function as a site for allosteric modulation of the protein and is involved in channel gating [39, 40, 42]. In the recent cryo-EM structures, only the last five ARs could be resolved sufficiently and the presence of eleven additional N-terminal ARs is predicted. The ARs might enhance interactions between the four TRPA1 subunits [40] and communicate with the pore region [43, 44] (see Fig. 2A).
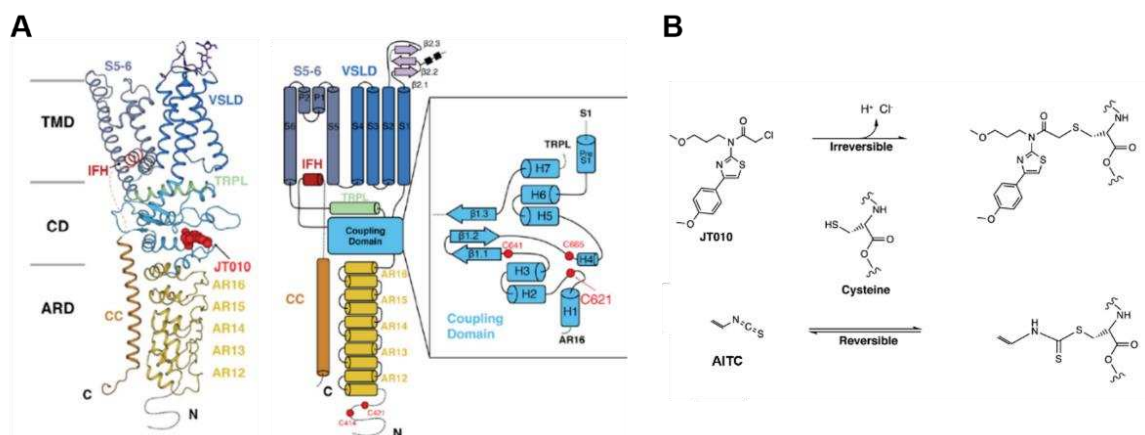

Figure 2: TRPA1 channel structure and electrophilic activation. A: Protein structure of a TRPA1 channel monomer. The protein structure can be subdivided into three parts: The transmembrane domain (TMD), the coupling domain (CD) and the ankyrin repeat domain (ARD). The TMD contains a voltage-sensor-like domain (VSLD), which comprises the first four transmembrane segments (S1-S4), and a pore domain (S5, S6 including the pore helices P1 and P2), which are connected via domain-swapping interactions. An ARD contains ARs (N-terminal) and the C-terminal coiled-coil motif (CC). The CD serves as connection for the TMD and the ARD. Reactive cysteine residues C621, C641 and C665 [45], which serve as putative binding sites for TRPA1 agonists, are located in the CD [46]. **B:** Binding of the TRPA1 channel agonists JT010 and AITC to reactive cysteine residues of TRPA1 (adapted from the supplementary information of [46]).

The protein structures furthered our understanding of the electrophilic activation and Ca^{2+}-selectivity of TRPA1. It is activated by a variety of electrophiles, including allyl isothiocyanate (AITC) in wasabi [29], garlic [47] and cinnamaldehyde [48], which covalently modify N-terminal cysteine residues [45, 49, 50] in both reversible (Thiol-Michael adduct formation e.g. by AITC) and irreversible reactions (SN2 reaction, e.g. by JT010) (see Fig. 2B) [45, 46]. Many studies have identified AA residue C621 [40, 46, 49, 50] as a hotspot for rapid, electrophilic activation of TRPA1. Ion conduction through the TRPA1 pore occurs via two gates. The lower gate is formed by AA I957 and V961 [42, 46], which form a hydrophobic seal to prevent permeation of rehydrated cations [40]. The upper gate/ selectivity filter is formed by AA G914 and D915, whereby the latter determines Ca^{2+} selectivity due to its negative charge [26, 40].

Patients suffering from Familial Episodic Pain Syndrome (FEPS), currently the only known TRPA1-related so called "channelopathy", carry the gain-of-function missense mutation N855S located in the S4 TMD which disturbs the Ca^{2+}-mediated activation of TRPA1 [51, 52]. In fact, Ca^{2+} plays a crucial role for

TRPA1 modulation. While extracellular Ca^{2+} is not a prerequisite for TRPA1 activation, its presence potentiates activation of the channel [29, 30] and also leads to desensitization. Both potentiation and deactivation by extracellular Ca^{2+} require Ca^{2+} entry into the cell [26]. Yet, the mechanisms occur independently from each other and a much lower intracellular Ca^{2+} concentration ($[Ca^{2+}]_i$) is sufficient for activation ($[Ca^{2+}]_i <$ 1mM [53, 54]) than for inactivation ($[Ca^{2+}]_i >$ 1 mM [26]). This mechanism ensures that desensitization does not precede potentiation [26]. Two studies, using TRPA1 overexpressing systems, identified the channel as a sensor for noxious cold [25, 48]. However, this was soon disputed in a TRPA1$^{-/-}$ mouse model in which the animals did not display alterations in their sensitivity to cold [38]. The role of hTRPA1 in noxious cold sensation is particularly difficult to assess, as there might be functional changes depending on the native environment of the channel [55-57]. A recent study performed patch-clamp bilayer recordings with truncated hTRPA1 proteins [58]. A form of the hTRPA1 protein lacking the N-terminal ARD (Δ1-688) exhibited an increased sensitivity to cold (< 15 °C) and heat (> 30 °C) compared to the full-length protein. hTRPA1 also lacking the VSLD (Δ1-854) was more sensitive to cold, but showed decreased sensitivity to high temperatures [58]. Although there are some data available that TRPA1 acts as a mechanosensory transducer in nociceptive sensory neurons [59-61], its mechanosensitivity is still a matter of dispute and requires further experimental investigations (discussed in [39, 57]).

The S5 TMD contains a small tilt, whose movement upon channel pore opening alters the conformation of the selectivity filter and thereby allows communication of the two gates [42]. Interestingly, the highly selective TRPA1 antagonist A-967079 binds in close proximity to this bend and the pore helices [40, 42]. HC-030031, another TRPA1 antagonist, does not bind to the same domain, as investigated by mutagenesis studies [40], but its exact binding site remains unknown. Therefore, electrophilic TRPA1 agonists appear to function in a similar manner, while blocking of TRPA1 can occur through different mechanisms.

2.1.2 Transient Receptor Potential Canonical 1 and 6 Channels

The family of classical or canonical TRP channels comprises seven members, wherein TRPC3/6/7 and TRPC4/5 form subgroups due to their sequence homology and corresponding functions [62, 63]. TRPC channels assemble as homo- or hetero-tetramers, the latter form mostly within the TRPC subgroups [62]. The existence of functional, homo-tetrameric TRPC1 channels is not conclusively clarified [64]. TRPC1 mostly forms hetero-tetramers with TRPC4/5, but TRPC1/3, TRPC1/6 and TRPC1/7 complexes have also been reported [62, 65]. TRPC1 was the first mammalian TRPC channel to be identified in 1995 [8, 66]. Two years later, the *mTrpc6* gene was cloned from mouse brain [67] and the *hTRPC6* gene from human placenta in 1999 [68]. The *hTRPC1* gene is localized on Chr3q13, *mTrpc1* on Chr9 and the genes are comprised of 16 [69] and 15 exons [70], respectively. While the existence of five murine and four human splice variants of *TRPC1* was reported, only the α-, β-, and ε-variant were shown to be functional (reviewed in [71]). *TRPC1* mRNA expression was detected in many tissues, including lungs, kidney, liver and brain [72]. Structurally, TRPC1 is predicted to have a similar molecular makeup to the other TRP channels [73], however, no structure of the channel is available.

The *hTRPC6* gene [68] is located on Chr11q21-q22 and contains 13 exons [74]. Human and murine TRPC6 (on Chr 9) share 93 % sequence identity [67] and comprise 931 and 930 AAs, respectively [75]. Single cell RNAseq detected high *hTRPC6* expression levels in inhibitory neurons and smooth muscle cells [76]. In mice, *Trpc6* is found in the lungs and the brain [67] and the human channel is highly expressed in lungs, spleen, ovary, placenta [77] and also in kidneys [78].

The N-terminus of TRPC6 contains four ARs and a CC. These domains interact with a second CC, localized in the C-terminus of the protein [75, 79], to stabilize the channel structure [80]. The C-terminus

includes the conserved TRP box and a Calmodulin and IP$_3$-receptor binding site (CIRB) [75, 79]. TRPC6 has, in contrast to other TRPC channels like TRPC3, a low basal activity due to two extracellular glycosylation sites at AA N473 and N561 [81], and shows a five times higher ion permeability for Ca^{2+} than for Na$^+$ [68]. The selectivity filter of TRPC6 contains a negatively charged E687 on the extracellular site [80], which might be responsible for the gating of divalent cations [80, 82]. The lower gate is formed by the polar residues N728 and Q732 as well as the hydrophobic residue I724 [80]. A tightly controlled extracellular Ca^{2+} concentration ([Ca^{2+}]$_e$) is pivotal for TRPC6 channel function, as full depletion of [Ca^{2+}]$_e$ abolished cation currents in smooth muscle cells, but an increase of [Ca^{2+}]$_e$ to 2 mM also diminished the currents [83]. [Ca^{2+}]$_e$ ranging from 50 to 200 µM facilitated maximal potentiation of TRPC6 currents [83] in a voltage independent manner [84]. [Ca^{2+}]$_i$ <200 nM increased and [Ca^{2+}]$_i$ >200 nM decreased TRPC6 current densities, implying that [Ca^{2+}]$_i$ might also regulate TRPC6 activity [84]. DAG and its membrane permeable analog OAG activate TRPC6, as well as TRPC3 and 7 [68]. The binding site of OAG/DAG is not yet identified, but TRPC6 binds another agonist, AM-0883, between S6 of one channel monomer and the pore helix of the neighboring subunit [85]. Binding sites for two TRPC6 antagonists (BTMD and AM-1473) were also identified [80, 85]. BTMD binds to the channel between the S5-S6 pore domain and the S1-S4 TMD, which blocked channel opening [80] and AM-1473 binding was observed within a pocket in the S1-S4 TMD [85].

2.1.3 Transient Receptor Potential Melastatin 7 Channel

Sequence analysis allows subdivision of TRPM channels into two groups: TRPM2/4/5/8 and TRPM1/3/6/7 [15]. TRPM2, TRPM6 and TRPM7 are the only mammalian TRP channels that harbor an enzymatically active kinase moiety [86-93]. The *hTRPM7* gene with 43 exons is located on Chr15q21.2 [94] and its murine ortholog on Chr2 with 42 exons [95]. *TRPM7* mRNA is ubiquitously expressed throughout the human body with overall higher expression levels than the other TRPM family members [96]. Single cell RNAseq analysis revealed high expression in excitatory and inhibitory neurons as well as in astrocytes and oligodendrocytes [97]. TRPM7 protein expression is pivotal for murine embryonal development [98, 99]. In adult tissue, TRPM7 function is essential for cell viability, migration, apoptosis, proliferation [89, 100-102] and maintaining magnesium ion (Mg^{2+}) homeostasis [103, 104]. Divalent cations, mainly Mg^{2+} and Ca^{2+} [89], but also trace metals [105] can flow through the pore of TRPM7 with the following permeation profile: Zn^{2+} ≈ Ni^{2+} >> Ba^{2+} > Co^{2+} > Mg^{2+} ≥ Mn^{2+} ≥ Sr^{2+} ≥ Cd^{2+} ≥ Ca^{2+} [105]. In murine TRPM7 channels, ion selectivity is determined by the presence of two conserved AA residues: the negatively charged E1047 and Y1049. Cryo-EM structures of murine TRPM7 channel domain in its closed state were released in 2018 [14]. Overall, the channel possesses the predicted fourfold symmetry with six TMDs, domain-swapping features, one N-terminal ARD, the conserved C-terminal TRP box and a CC known from other TRP channel structures [14]. The CC mediates channel subunit multimerization and trafficking of the channel [106].

Low levels of intracellular Mg^{2+} [89] and ROS [100, 107] potentiated TRPM7 currents. Naltriben was identified as potent, selective TRPM7 activator whose action did not depend on prior depletion of intracellular Mg^{2+} [108]. Reversible inhibition of the constitutively active TRPM7 channel [101] involves two distinct binding sites for intercellular Mg^{2+} and Mg-ATP [89, 102, 103, 109-111]. The Mg^{2+}-regulated inhibition appeared to rely on a decreased number of active channels and not on a diminished single-channel conductance [102, 110]. Further mechanisms of TRPM7 channel inhibition include low cytosolic pH [111], divalent cations (e.g. Ba^{2+}, Sr^{2+}, Zn^{2+} and Mn^{2+}) [112] and hydrolysis of membrane bound phosphatidylinositol-4,5-biphosphate (PIP$_2$) by phospholipase C (PLC) [113].

The α-kinase domain is located at the C-terminal side of TRPM7 and comprises about 300 AA residues [90]. Cleaving of TRPM7 at AA D1510 generates both the functional ion channel with increased activity

and the self-assembling kinase with phosphotransferase activity [114, 115]. The enzyme contains one ATP-, one Zn^{2+}- and two Mg^{2+}-binding sites [102]. Several autophosphorylation sites lay in the C-terminus [116, 117] and within the serine/threonine rich N-terminal domain of the kinase moiety [118]. The serine/threonine containing sequence enhances Mg^{2+}-dependent phosphorylation [119] of the substrates of the kinase (e.g. annexin A1 [120], myosin II heavy chain [121], PLCγ2 [122] and SMAD2 [123]) by facilitating their interaction [118]. Interestingly, mutations of some of the autophosphorylation sites (S1511 and S1567) did not affect the channel properties. While the channel activity is blocked by Mg^{2+}, the serine/threonine kinase function is enhanced by Mg^{2+}, unaltered by Ca^{2+} and blocked by Zn^{2+} [116].

2.2 Ca^{2+}– the ubiquitous secondary messenger

Activation of TRP channels can lead to elevation of $[Ca^{2+}]_i$ in the cell, where it serves as an important second messenger for a variety of processes [124]. Elevation of cytoplasmatic Ca^{2+} levels induces cellular responses which range from cell proliferation and growth to cell death by apoptosis [125] and also include exocytosis and muscle contraction [124, 126].

2.2.1 Calcium Signaling and its Regulation

The physiological cytoplasmic $[Ca^{2+}]$ is around 100 nM and upon stimulation increases to up to 1 μM [124]. Ca^{2+} entry to the cytoplasm occurs either from the extracellular space, where $[Ca^{2+}]$ is in the millimolar range, or from the endo/sarcoplasmic reticulum (ER/SR) with a $[Ca^{2+}]$ of 100 – 500 μM [124]. As continuous high cytoplasmic Ca^{2+} levels are toxic [124, 127], the second messenger is removed rapidly from the cytoplasm by Ca^{2+}-ATPases, Na^+/Ca^{2+} exchangers [128] and Ca^{2+} binding proteins for buffering of Ca^{2+} [129] in order to maintain Ca^{2+} homeostasis. This leads to an oscillation of Ca^{2+} levels [127, 129], which carry additional information, such as amplitude and frequency, to achieve more specific cellular responses [130]. To ensure that the universal second messenger evokes the correct signal in the cell, formation of microdomains restrict the signal spatially. Rapid changes in Ca^{2+} also prevent desensitization [130]. As mentioned in section 2.1.1 and 2.1.2, Ca^{2+} also has a dual effect on TRPA1 and TRPC6, as their channel activity is dependent on the intra- and/or extracellular $[Ca^{2+}]$ [83, 84].

2.2.2 Receptor- and Store-Operated Calcium Entry

Receptor-operated Ca^{2+} entry (ROCE) depends on agonist-induced activation of G protein-coupled receptors (GPCR) and the subsequent activation of PLC [77]. PLC hydrolyzes PIP_2 to generate DAG [131] and inositol triphosphate (IP_3) [132, 133]. As mentioned in section 2.1.2, DAG can serve as a direct activator of TRPC6 [131] to induce Ca^{2+} influx into the cells.
IP_3, the second product generated by PLC-mediated cleaving of PIP_2, is a key player in the initiation of store-operated Ca^{2+} entry (SOCE) [134, 135]. SOCE is a major pathway for Ca^{2+} influx in non-excitable cells [136] and was first described as capacitive Ca^{2+} entry by Putney in 1986 [135]. IP_3 binds to its receptor located in the ER membrane [134, 137] triggering release of Ca^{2+} from the intracellular Ca^{2+} stores [132, 133, 138], which is followed by influx of Ca^{2+} into the cytosol from the extracellular space. Ca^{2+} release-activated Ca^{2+} currents (I_{CRAC}), which are non-voltage dependent and selective [139], were identified as specific for SOCE [140]. Stromal interaction molecule 1 (STIM1) proteins sense the depletion of the $[Ca^{2+}]$ in the ER [141, 142], either in response to IP_3-mediated Ca^{2+} release or after application of Thapsigargin (Tg). Tg acts as a blocker of SR/ER Ca^{2+} ATPase pumps (SERCA) which are responsible for the refilling of ER Ca^{2+} levels [143]. The dissociation of Ca^{2+} from STIM1 causes a conformational change of the protein, which enables the STIM1 dimers to form oligomers and migrate towards the plasma membrane, where they form puncta [142, 144, 145] and recruit as well as interact with

plasma membrane-bound Orai channels through which the calcium entry occurs [146-148]. The formation of STIM1 puncta at ER-plasma membrane junctions is reversible and the STIM1 aggregates are dissolved after refilling of the ER Ca^{2+} stores [149]. Furthermore, a Ca^{2+}-dependent inactivation of SOCE can be observed after CRAC channel opening and Ca^{2+} influx [150]. SOCE contributes to a number of important cellular functions such as proliferation, apoptosis and transcription [139], e.g. by activation of nuclear factor of activated T cells (NFAT) [151]. Only Ca^{2+}-bound calmodulin is capable of activating calcineurin, which activates NFAT by cleaving N-terminal phosphates of its cytoplasmic region. This mechanism allows the transcription factor to translocate to the nucleus [152].

Prior to the discovery of Orai channels [146-148], TRPC channels were assumed to mediate Ca^{2+} entry after store depletion [66] and the discussion regarding the function of TRP channels in SOCE has yet to be resolved. Although TRP channels failed to match the electrophysical properties of I_{CRAC} currents [153-155], a contribution of TRPC channels to SOCE through interaction with STIM1/2 [156-158] and/or Orai1-3 proteins [159-162] was observed in several studies. Evidence pointing to an involvement of TRPA1 and TRPM7 channels in SOCE is sparse. TRPA1 was found to interact with STIM1, Orai1, TRPC1 and TRPC6 in co-immunoprecipitation experiments. TRPA1 inhibition strengthened STIM1-Orai1 association indicating that TRPA1 might be a negative regulator of SOCE [163]. TRPM7 kinase activity was shown to positively modulate SOCE [164-166].

2.3 Physiology, pathophysiology and TRP expression in the Respiratory Tract

The lungs are in constant contact with the environment facilitating gas exchange. Additional functions of the respiratory system include maintenance of the pH by releasing CO_2 from the body and host defense [167]. Airborne particles, microorganisms and toxins can cause tremendous damage in the lung. Due to their high expression in the lung, TRP channels might be druggable targets for treatment of lung diseases. The recent global SARS-COV-2 pandemic has highlighted the urgent need for lung research. TRPA1 is known to be a noxious sensor and can drive lung inflammation and cough [31, 39] and TRPA1 as well as TRPV1 signaling were proposed to contribute to the severity of COVID-19 symptoms. Desensitization of TRPA1 by consumption of TRPA1-activating aliments, such as broccoli and ginger, reduced the inflammation-induced symptoms [168]. The expression pattern of TRPC6 was altered in patients suffering from COVID-19-induced pneumonia [169] and the occurrence of pulmonary fibrosis is predicted to rise during COVID-19-triggered acute respiratory distress syndrome [170-172]. TRPM7 signaling is reported to be profibrotic (see chapter 2.3.3).

2.3.1 Structure and Cell Types of the Respiratory Tract

Anatomically, the respiratory system can be subdivided into the upper and the lower tract. The former includes the nasal cavity, the pharynx and the larynx. The latter consists of the trachea and the bronchial tree of the lungs [173]. The trachea branches into the two primary bronchi, which continue to separate into the lobar bronchi, the segmental bronchi, the bronchioles, the terminal bronchioles, the respiratory bronchioles and the alveolar ducts until they terminate in the alveolar sacs [174]. Functionally, there is a distinction between conducting and respiratory airways (see Fig. 3). The latter start within the respiratory bronchioles and the majority of the gas exchange occurs in the alveoli [175]. A mucous membrane lining the trachea and the bronchi captures and clears inhaled pathogens [173]. The pseudostratified epithelium contains mostly goblet cells, which secrete mucus, and ciliated cells, which move the mucus upwards. Further down in the bronchial tree, the mucous membrane transitions from a cuboidal epithelium to a simple squamous epithelium in the alveoli [173]. Long stretched alveolar epithelial type 1 (AT1)

cells, through which gas exchange occurs, cover 95 % of the alveolar surface [176]. AT2 cells are more numerous [177] and are responsible for surfactant protein secretion [178]. The only 0.2 – 0.5 µm thick barrier between alveolar space and capillaries enables efficient gas exchange [179]. Differences between the human and the murine respiratory tract include a reduced number of goblet cells and the lack of respiratory bronchioles in mice [174].
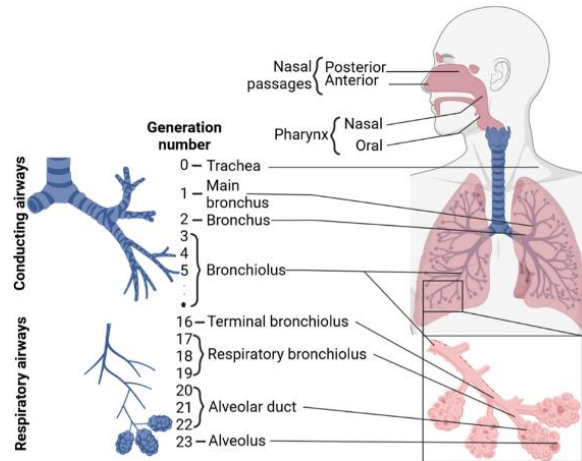
Figure 3: Schematic depiction of the anatomy of the human respiratory tract. Division of the human respiratory tract in conducting and respiratory tracts (created with BioRender after [180]).

2.3.2 Pulmonary Fibroblasts and the Extracellular Matrix

A major part of the lungs is comprised of connective tissue in between the airways. This interstitial space is mainly populated by fibroblasts, which secrete extracellular matrix (ECM) and interact with ECM constituents to maintain the integrity of the organ [175]. These mesenchymal cells are critical for embryonal development (reviewed in [181]), wound healing and tissue repair due to their various functions (e.g. secretion, maintenance and polarization of ECM components, wound contraction and migration) (reviewed in [182]). Pulmonary fibroblasts aid AT2 cells in proliferation, surfactant synthesis [183] and differentiation to AT1 cells [181]. Furthermore, fibroblasts also influence the innate immune system by macrophage polarization and cytokine synthesis, regulate the metabolism with production of lactate, pyruvate and lipids and are important for the maintenance of the mesenchymal lineage. Contraction of pulmonary fibroblasts supports breathing by stretching and recoiling the tissue [182].

In mammals, the entity of the ECM, termed "matrisome", comprises around 300 core ECM proteins and a number of associated factors, such as enzymes, growth-factors and interacting proteins [184, 185]. The large ECM proteins form an insoluble matrix, often with cross-links between the components [184, 185], thereby providing spatial information for the surrounding cells [186] (see Fig. 4). ECM proteins in the lung are found in the parenchyma and in the basement membranes, which are thin layers of ECM localized underneath epithelial and endothelial cell structures [186, 187]. ECM assembly and cell adhesion are mediated by glycoproteins. The integrity of the structural matrices is maintained by collagens [184], which are the most abundant molecules in the ECM [188]. Collagen I is responsible for tensile strength and collagen III provides lung flexibility [189]. Two important glycoprotein groups which mediate cell adhesion to the ECM via receptors (e.g. integrins) are laminin and fibronectin [184, 190, 191]. Fibronectin regulates cell migration (e.g. of fibroblasts towards an injury) and differentiation during development [192-194]. Laminins, in combination with additional ECM proteins, such as collagen IV, are part of the basement membranes [184, 195, 196]. Other ECM glycoproteins include elastin, tenascins and fibrinogen [184].

Proteoglycans are glycoproteins coupled to additional glycosaminoglycans, which are repeating disaccharide polymers containing negatively charged carboxyl and sulfate groups. By embedding water and divalent cations (e.g. Ca^{2+}) into the matrix, proteoglycans provide elasticity. Moreover, glycoproteins confer signals to proteoglycans allowing them to bind growth factors [197], which can be released from the ECM by proteolysis, rendering the ECM a kind of growth factor storage [198]. Matrix metalloproteinases (MMPs) contribute to ECM remodeling by degrading the connective tissue and are themselves inhibited by tissue inhibitors of metalloproteinases [189]. Plasma membrane bound plasminogen [199] is converted to plasmin by either urokinase or tissue plasminogen activator (u/tPA) [200, 201] and once activated, the serine protease can degrade fibronectin, collagen and fibrin [201-203]. Plasminogen activator inhibitor-1 (PAI-1), another factor released by myofibroblasts, acts as a major inhibitor of this fibrinolytic system by suppressing the u/tPAs [204].
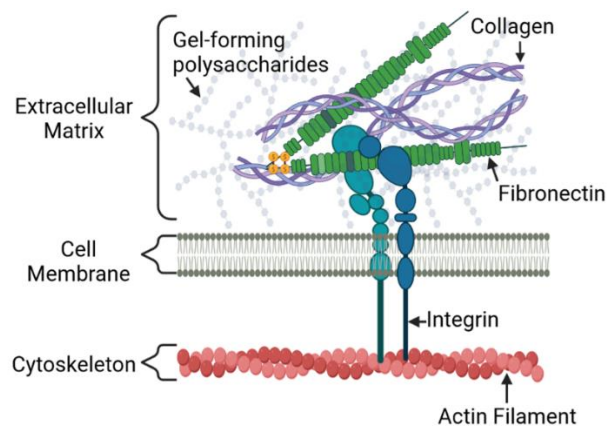
Figure 4: Schematic overview of the ECM. Collagens have a higher proportional expression in the lung than other ECM components [188, 205]. Integrins mediate ECM-cell-interactions via fibronectin and transfer mechanical stimuli from the ECM to the actin filaments in the cytoskeleton (Created with BioRender after [206]).

Homeostasis of ECM is important to maintain lung elasticity and alterations affect fibroblast behavior regarding tissue repair [186]. Following initial inflammation, resident fibroblasts [207] and bone marrow derived peripheral blood fibrocytes [208] invade wounded tissue in response to production of chemo attractants, such as platelet-derived growth factor (PDGF) and CXCL12, by epithelial and immune cells [207]. After adhesion to the injured site via integrins, the fibroblasts start proliferating and clear the wound from degraded proteins by secreting MMPs to prepare for new tissue formation [209, 210]. Other important secreted factors are TGF-β1, 2, 3 [211-213], with TGF-β1 as the key player in fibroblast to myofibroblast differentiation (FMD) [214-216]. Myofibroblasts express alpha smooth muscle actin (α-SMA) and actin stress fibers, which both contribute to cell contractility, and are important for wound closing and migration [217-220]. Furthermore, cell-cell and cell-matrix adherins can be found in myofibroblasts [221, 222] and myofibroblasts have an elevated turnover of ECM proteins compared to normal fibroblasts. After wound closure, myofibroblasts return to pre-injury levels by apoptosis [223, 224].

2.3.3 Pulmonary Fibrosis and TRP Channels

Pulmonary fibrosis (PF) can develop during acute lung injury, after radiation therapy (e.g. as cancer treatment) or due to unknown factors (idiopathic PF) [225]. It is widely accepted that PF develops in response to chronic microinjuries in the alveolar epithelium, which causes inflammatory responses, such as secretion of TGF-β1 from AT2 cells and alveolar macrophages. TGF-β1 signaling initiates fibroblast migration to the site of injury, proliferation of the cells as well as FMD (see Fig. 5). This process of wound healing becomes dysregulated due to unknown factors and myofibroblasts fail to undergo apoptosis in

PF. This leads to an exorbitant deposition of ECM and formation of myofibroblast foci within the lung parenchyma. The progression of the disease eventually leads to tissue stiffening and impaired gas exchange as the barrier between alveoli and capillaries thickens [226-230]. Hence, PF therapy remains a great challenge and patients rely on lung transplantation to ensure survival. Currently, two drugs, pirfenidone [231, 232] and nintedanib [233, 234], are approved for the treatment of PF and act to improve the patients' quality of live. Yet, both medications fail to cure the disease [235, 236]. However, taking all players known to be involved in fibrosis development into account would be far outside the scope of this work. Therefore, this section will focus on the role of TRP channels, pulmonary fibroblasts and Ca^{2+} in fibrosis.
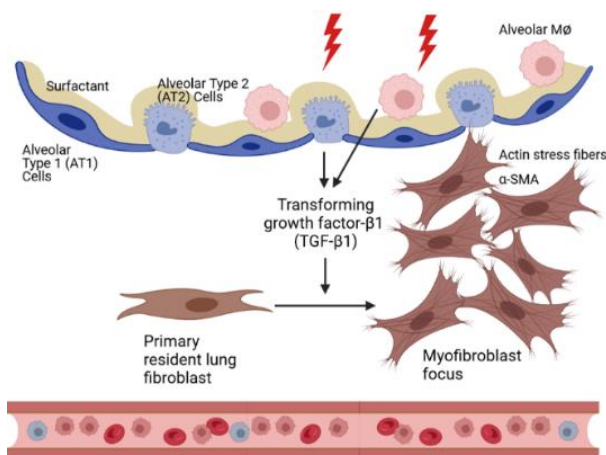
Figure 5: Schematic representation of accumulation of fibroblasts in the interstitial space during the development of PF. Myofibroblast clusters develop in response to TGF-β1-mediated signaling. Secretion of CXCL12 by injured alveolar epithelial cells leads to chemoattraction of CXCR4+ fibrocytes. PDGF release by activated alveolar epithelial cells induces local migration and proliferation of resident fibroblasts (Created with BioRender after [207]). See text and reference for more details.

The canonical TGF-β signaling pathway is considered to be pivotal for the pathophysiology of PF as it contributes to FMD and deposition of ECM [227, 228]. TGF-β1 binds to its receptor and induces phosphorylation of the C-terminal mad homology 2 (MH2) domain of SMAD2/3 [237]. This initiates SMAD2/3 translocation to the nucleus where these factors coordinate transcription of profibrotic genes such as PAI-1, collagens or fibronectin [238, 239].

Ca^{2+} influx was reported to be essential for the onset of lung fibrosis [240, 241] and fibroblast differentiation [242, 243]. TRPV4-mediated elevation of $[Ca^{2+}]_i$ crucially contributed to TGF-β1-triggered FMD and TRPV4$^{-/-}$ mice were protected from developing PF [240].

TRPC6$^{-/-}$ mice showed prolonged survival rates after exposure to bleomycin compared to WT mice. Moreover, TRPC6 is upregulated by TGF-β1 treatment in pulmonary, cardiac and dermal fibroblasts and also in vascular smooth muscle cells [4, 243, 244]. Although the function of TRPC6-calcineurin-NFAT signaling in pulmonary fibrosis is not well established, TRPC6 inhibition could be a promising strategy for the therapy of cardiac and renal fibrosis [245]. A large number of studies showed that inhibition or knockdown of TRPC6 ameliorated fibrotic remodeling in the kidneys [246-251] and the heart [245], while TRPC6 activation was shown to contribute to disease onset in kidneys [252, 253], the intestine [253, 254] and in the heart [255, 256]. So far, no connection between TRPC1 and pulmonary fibrosis has been reported. A possible involvement of TRPC1 in FMD was proposed because TRPC1 expression was upregulated in NIH/3T3 cells, a murine embryonic fibroblast cell line, after TGF-β1 treatment and KD or inhibition of the channel reduced TGF-β1-triggered fibroblast marker expression [257].

TRPM7 signaling also seems to drive fibrosis progression. Expression of this channel was upregulated in response to TGF-β1 in several cell types, including a fetal human lung fibroblast cell line (MRC5) [5], cardiac fibroblasts [242, 258, 259] and hepatic stellate cells [260, 261]. Furthermore, blocking or KD

of TRPM7 diminished TGF-β1-triggered activation and proliferation of cells as well as the upregulation of fibrosis markers, such as α-SMA, COL, FN1 and MMP-9, in cardiac fibroblasts and hepatic stellate cells [5, 242, 258, 259, 261, 262]. This interaction of TRPM7 and TGF-β1 is mediated via SMAD signaling and results in a synergism as the TRPM7 α-kinase moiety can phosphorylate SMAD2/3 proteins [258, 261]. Moreover, suppression of TRPM7 reduced development of cardiac fibrosis in rodent models [258, 263]. In addition to the canonical SMAD pathway, mitogen-activated protein kinase (MAPK) and phosphatidylinositol 3-kinase/ protein kinase B (PI3K/Akt) signaling were linked to TRPM7 function in fibrosis [5, 260, 262, 264]. In MRC5 cells, TGF-β1 simulation led to increased phosphorylation of Akt which was blocked by application of Gd^{3+} and 2-Aminoethoxydiphenylborane (2-APB), two TRPM7 antagonists [5]. H_2O_2-induced cardiac fibrosis was ameliorated by TRPM7 silencing, which also reduced Extracellular signal-regulated kinase (ERK1/2) activation [264]. Application of the non-specific TRPM7 antagonist carvacrol ameliorated the development of liver fibrosis by blocking the MAPK pathway as seen by reduced phosphorylation levels of ERK1/2, MAPK p38 and JNK1/2 [262]. siRNA-mediated silencing of TRPM7 decreased phosphorylation levels of ERK1/2 and Akt in hepatic stellate cells [261]. These results indicate that ERK1/2 phosphorylation might promote fibrosis progression.

However, several publications report a possible role of ERK1/2 proteins in the suppression of fibrosis progression. Inhibition of ERK1/2 and JNK in dermal fibroblasts was able to support FMD [265]. ERK1/2 signaling is necessary for the production of the anti-fibrotic cytokine IL-10 in immune cells [266] and ERK1/2 inhibition diminished the expression of IL-10 ([253], reviewed in [267]). Moreover, activation of TRPA1, which is reported to inhibit fibrosis development [268-272], led to ERK1/2 phosphorylation in HEK-293 cells as well as in small cell lung carcinoma cells [273]. Pirfenidone and steroids activated TRPA1, which led to attenuation of intestinal fibrosis [269]. TRPA1^{-/-} mice showed elevated levels of inflammation and fibrotic changes in a trinitrobenzene sulfonic acid (TNBS)-induced model of chronic colitis compared to WT animals. Administration of pirfenidone and steroids as well as of the herbal extract Daikenchuto reduced the effects of TNBS in WT but not in TRPA1^{-/-} mice [269, 271]. Li *et al*. showed in a rat model of cardiac fibrosis that activation of TRPA1 by cinnamaldehyde ameliorated the disease phenotype. In this model, TRPA1 acts by elevating autocrine calcitonin gene-related peptide, which in turn diminishes nuclear factor 'kappa-light-chain-enhancer' of activated B-cells (NFκB) signaling and thus fibroblast activation [270]. Recently, the protective effect of TRPA1 was also demonstrated in age-related cardiac fibrosis. TRPA1^{-/-} mice exhibited accelerated development of fibrotic changes compared to WT control mice [272]. In contrast, inhibition of TRPA1 reduced development of interstitial cardiac fibrosis in mice after transverse aortic constriction surgery [274].

2.4 Aim of the thesis

As outlined above, much is already known about multiple roles of TRP channels in primary lung fibroblasts and their involvement in the progression of pulmonary fibrosis. However, a few questions, for which my thesis aims to provide answers, remain:

(1) Does activation of TRPA1 channels in HLFs suppress TGF- β1-induced FMD and the progression of pulmonary fibrosis? Which signal transduction cascade is responsible for this inhibition?

(2) Do murine TRPC1/6[-/-] pmLFs show any changes in the expression patterns of STIM1/2 proteins and Oria1-3 channels?

(3) Are TRPM7 channels in HLFs involved in the progression of FMD and pulmonary fibrosis?

Along these lines, all three questions (paper 1 – 3) were answered in the following three publications with myself as co-author and first author.

3. Paper I

4.   Paper II

SCIENTIFIC REPORTS
natureresearch

Check for updates

OPEN

Store-operated Ca^{2+} entry in primary murine lung fibroblasts is independent of classical transient receptor potential (TRPC) channels and contributes to cell migration

Larissa Bendiks[1], Fabienne Geiger[1], Thomas Gudermann[1], Stefan Feske[2] & Alexander Dietrich[1] ✉

Stromal interaction molecules (STIM1, 2) are acting as sensors for Ca^{2+} in intracellular stores and activate Orai channels at the plasma membrane for store-operated Ca^{2+} entry (SOCE), while classical transient receptor potential (TRPC) channel mediate receptor-operated Ca^{2+} entry (ROCE). Several reports, however, indicate a role for TRPC in SOCE in certain cell types. Here, we analyzed Ca^{2+} influx and cell function in TRPC1/6-deficient (TRPC1/6$^{-/-}$) and STIM1/2- deficient (STIM1/2$^{\Delta pmLF}$) primary murine lung fibroblasts (pmLF). As expected, SOCE was decreased in STIM1/2- deficient pmLF and ROCE was decreased in TRPC1/6$^{-/-}$ pmLF compared to control cells. By contrast, SOCE was not significantly different in TRPC1/6$^{-/-}$ pmLF and ROCE was similar in STIM1/2-deficient pmLF compared to Wt cells. Most interestingly, cell proliferation, migration and nuclear localization of nuclear factor of activated T-cells (NFATc1 and c3) were decreased after ablation of STIM1/2 proteins in pmLF. In conclusion, TRPC1/6 channels are not involved in SOCE and STIM1/2 deficiency resulted in decreased cell proliferation and migration in pmLF.

Store-operated Ca^{2+} entry (SOCE) also named capacitive Ca^{2+} entry (CCE) was first described by J.W. Putney Jr. more than 30 years ago as depletion of intracellular Ca^{2+} stores which induces the opening of plasma membrane (PM) Ca^{2+} channels[1]. Since then, candidate proteins like classical transient receptor potential (TRPC) channels[2] and mechanisms, e.g. coupling of TRPC proteins to inositol 1-4-5 trisphosphate (IP3) receptor channels in the endoplasmic reticulum[3,4] for SOCE, were intensively discussed in the scientific community. In 2005 however, stromal interaction molecules (Stim in *Drosophila* and STIM1, STIM2 in humans) were identified as Ca^{2+} sensors in the ER directly regulating SOCE in two different large-scale screening approaches[5,6]. One year later, Ca^{2+} selective channels at the plasma membrane (Orai) were discovered[7–9], which were responsible for Ca^{2+} release activated Ca^{2+} (CRAC) currents originally described in mast cells[10]. A molecular model was developed to support the concept that upon ER Ca^{2+} depletion STIM proteins homo-multimerize and translocate to ER-PM junctions[11,12], where they recruit and gate Orai channels via direct interaction[13]. Ca^{2+} influx through Orai channels is important for cellular remodeling, e.g. in cardiovascular diseases[14], and mutations in these channels are responsible for multiple channelopathies[15]. Irrespective of these events, TRP channels trigger Ca^{2+} influx in response to extracellular stimuli or receptor activation (receptor-operated Ca^{2+} influx, ROCE) independently of STIM and Orai[16]. Some labs, however, reported that TRPC channels also interact with STIM proteins[17] and/or Orai channels[18]. Along these lines, TRPC channels like TRPC1 were invoked in SOCE in certain cells of salivary glands[19] and pancreatic acini[20], while in vascular smooth muscle cells TRPC1 channels work independently of SOCE[21]. The role of TRPC1 is even more confusing as the molecular architecture of native TRPC1 channels is still a matter of debate[22]. While all mammalian TRPC channels form homotetramers, the translocation of TRPC1 homotetramers to the plasma membrane and homomeric TRPC1 currents in native tissues were questioned[23].

[1]Walther Straub Institute of Pharmacology and Toxicology, Member of the German Center for Lung Research (DZL), Medical Faculty, LMU-Munich, Munich, Germany. [2]Department of Pathology, New York University School of Medicine, New York, NY, 10016, USA. ✉e-mail: alexander.dietrich@lrz.uni-muenchen.de

In heteromeric TRPC channels TRPC1 appears to work as an ion channel regulator rather than an ion channel per se, because it modifies currents of homotetrameric TRPC5[24] and reduces Ca^{2+} permeation of TRPC4/5/6/7 channels[25]. Therefore, the exact function of TRPC channels for SOCE or ROCE needs to be analyzed in each cell type independently.

In here, we set out to study the role of SOCE in primary murine lung fibroblasts (pmLF) using TRPC1/6- and STIM1/2-deficient fibroblasts in comparison to Wt control cells. SOCE was independent from TRPC1 and TRPC6 expression in pmLF but clearly dependent on STIM1/2 proteins. STIM1/2-deficiency reduced cell proliferation and migration as well as decreased nuclear levels of nuclear factor of activated T cells (NFATc1 and NFATc3) compared to control cells. Our data suggest an essential role of TRPC-independent SOCE in pmLF survival and cell migration.

Materials and Methods

Animals. *Stim1/2^{flox/flox}* mice were bred as previously described[26]. *Trpc1/6^{−/−}* mice were generated by crossing *Trpc1^{−/− 21}* and *TRPC6^{−/− 27}* mice. *Stim1/2^{flox/flox}* were crossed with *Trpc1/6^{−/−}* animals to gain *Stim1/2^{flox/flox}/Trpc1/6^{−/−}* mice. All mice were on a C57BL/6J background. All animal experiments were approved by the governmental authorities and guidelines of the European Union (EU) were followed for the care and use of animals.

Isolation and culture of primary murine lung fibroblasts. Primary murine lung fibroblasts (pmLF) were isolated as previously described for human lung fibroblasts[28]. Briefly, lungs of C57BL/6 mice were flushed through the right heart with sterile, cold PBS and excised. The lungs were dissected into pieces of 1–2 cm² in size and digested by 1 mg/ml of Collagenase I (Biochrom, Cambridge, UK) at 37 °C for 2 h. Digested lung pieces were filtered through a nylon filter (pore size 70 μm; BD Falcon, Franklin Lakes, NJ, USA) and centrifuged for 5 min. Subsequently, the pellet was re-suspended in DMEM/F12 fibroblast culture medium (Lonza, Basel, Switzerland) supplemented with 20% fetal bovine serum (Invitrogen, Carlsbad, USA) as well as penicillin/streptomycin (Lonza, Basel, Switzerland) and normocin (InvivoGen, San Diego, USA) before finally plated on 10 cm cell culture dishes. Medium was changed after 2 days and cells were split after reaching a confluence of 80–90%. Only pmLF from passage 3–4 were used for the studies.

Lentiviral infection of pmLF. PmLF from *Stim1/2^{flox/flox}* mice were infected by lentiviruses expressing Cre recombinase to obtain STIM1/2- deficient fibroblasts. Lentiviruses were produced as previously described[29] based on the protocol for the amplification of second generation lentiviruses from the Tronolab (tronolab.epfl.ch). Lenti-X 293T cells (Clontec/Takara, Mountain View, USA) grown in DMEM medium (Lonza, Basel, Switzerland) supplemented with 10% fetal bovine serum (Invitrogen, Carlsbad, USA) as well as penicillin/streptomycin (Lonza, Basel, Switzerland) were transfected with pWPXL (carrying the gene of interest), pMD2G (encoding VSV G envelope protein) and pSPAX (encoding HIV-1 Gag, Pol, Tat and Revprotein) by calcium phosphate transfection. Supernatant containing virus was collected for two days. Virus solution was concentrated by using Peg-it solution (SBI, Mountain View, USA) and the pellet was re-suspended in cold PBS, aliquoted and stored at −80 °C. Successful virus production was verified by LentiX Go-stix (Clontec/Takara, Mountain View, USA). PmLF of the second passage were seeded at 1.5×10^5 cells per well of a 6-well plate and infected by lentiviruses expressing Cre recombinase on the next day. Medium was changed the next morning and infected pmLF were used for experiments after 4–5 days. Excision of exons from *Stim1* and *Stim2* genes was monitored by genomic PCR.

Genomic PCR. Genotyping of *Trpc1/6^{−/−}* and *Stim1/2^{flox/flox}* mice as well as STIM1/2^{ΔpmLF} fibroblasts was done as described[21,26,27].

Ca²⁺ imaging of intracellular Ca²⁺. STIM1/2^{ΔpmLF}, TRPC1/6^{−/−}, and TRPC1/6^{−/−} STIM1/2^{ΔpmLF} as well as control cells (Wt and Wt infected Cre recombinase expressing lentiviruses) were grown on 25 mm coverslips and loaded with Fura-2-AM (2 μM, Sigma, Taufkirchen, Germany) in 0.1% BSA in HEPES/HBSS buffer at 37 °C for 30 min. Coverslips were washed with HEPES/HBSS buffer and placed on a microscope in a low-volume recording chamber. To measure receptor-operated Ca²⁺ entry (ROCE) endothelin-1 (4 μM, Merck, Darmstadt, Germany) was applied in HBSS buffer with (2 mM) Ca²⁺ or in nominal Ca²⁺ free (0.5 mM EGTA) buffer after adding Ca²⁺ (2 mM). Store-operated Ca²⁺ entry (SOCE) was analyzed after depletion of internal Ca²⁺ stores by 1 μM thapsigargin (Sigma, Taufkirchen, Germany) in Ca²⁺ free HBSS solution containing 0.5 mM EGTA by adding extracellular Ca²⁺ (2 mM)[30]. An increase in intracellular Ca²⁺ ([Ca²⁺]ᵢ) was recorded using a Polychrome V monochromator (Till Photonics, Martinsried, Germany) and a 14-bit EMCCD camera (iXON3 885, Andor, Belfast, UK) coupled to an inverted microscope (IX71with an UPlanSApo 20×/0.85 oil immersion objective, Olympus, Hamburg, Germany) at 340 and 380 nm as described[30].

Quantitative reverse transcription (qRT)–PCR analysis. Total RNA from primary lung fibroblasts was isolated using the Invitrap Spin Universal RNA Mini Kit (Stratec, Berlin, Germany) according to the manufacturer's protocol. First-strand cDNA was synthesized from the isolated total RNA using RevertAid RT containing reverse transcription polymerase (ThermoScientific, St. Leon-Rot, Germany) and random primer. MRNA expression of targeted genes in pmLF was analyzed by real time PCR as previously described[30]. Briefly, 10 pmol of each primer pair and 2 μl from the first strand synthesis were added to the reaction mixture consisting of 2x ABsolute QPCR SYBR Green Mix (ThermoScientific, St. Leon-Rot, Germany) and water. PCR was carried out in a light-cycler apparatus (Roche, Mannheim, Germany) using the following conditions: 15 min initial activation and 45 cycles of 12 s at 94 °C, 30 s at 50 °C, 30 s at 72 °C. Primer pairs (see Table 1) were used for the amplification of specific DNA-fragments from the first strand synthesis. Fluorescence intensities were recorded after an extension step at 72 °C after each cycle. Samples containing primer dimers were excluded by melting curve analysis and identification of the products were done by agarose gel electrophoresis. Crossing points were determined by

Target	Species	Forward primer (5′-3′)	Reverse primer (5′-3′)
STIM1	mouse	AAG CTT ATC AGC GTG GAG GA	CCT CAT CCA CAG TCC AGT TGT
STIM2	mouse	GAG GGC GCA GAG TGT GAG	TTT AGA GCC ATC CGG ACC T
Orai1	mouse	TAC TTA AGC CGC GCC AAG	ACT TCC ACC ATC GCT ACC A
Orai2	mouse	GGA CCT CAG CCC TCC TGT	GGG TAC TGG TAC TTG GTC TCC A
Orai3	mouse	CAC ATC TGC TCT GCT GTC G	GGT GGG TAT TCA TGA TCG TTC T
TRPC1	mouse	TGA ACT TAG TGC TGA CTT AAA GGA AC	CGG GCT AGC TCT TCA TAA TCA
TRPC3	mouse	TGG ATT GCA CCT TGT AGC AG	ACC CAG AAA GAT GAT GAA GGA G
TRPC4	mouse	GAT GAT ATT ACC GTG GGT CCT G	GAT TCC ACC AGT CAT GGA TGT
TRPC5	mouse	CTC TAC GCC ATC CGC AAG	TCA TCA GCG TGG GAA CCT
TRPC6	mouse	GCA GCT GTT CAG GAT GAA AAC	TTC AGC CCA TAT CAT GCC TA
TRPC7	mouse	AAT GGC GAT GTG AAC TTG C	CAG TTA GGG TGA GCA ACG AAC
β-actin	mouse	CTA AGG CCA ACC GTG AAA AG	ACC AGA GGC ATA CAG GGA CA

Table 1. Primer pairs used for amplification of quantitative RT-PCR fragments.

the software program provided by the manufacturer. Relative gene expression was quantified using the formula: $(2e(\text{Crossing point reference gene} - \text{Crossing point X})) \times 100 = \%$ of the reference gene expression of the housekeeping gene (β-actin).

Western blot analysis. Protein expression levels for STIM1 and STIM2 were determined by Western Blot analysis as previously described[30]. PmLF from cell culture dishes of 20 cm diameter were washed two times with cold PBS before 250 μl of lysis buffer (20 mM Tris-HCL, pH 7.5, 150 mM NaCl, 1% Nonidet P40, 0.5% sodium deoxycholate, 1% SDS, 5 mM EDTA) containing phosphatase und protease inhibitors (Roche, Mannheim, Germany) was applied for 60 min on ice. After centrifugation of the protein lysates at $5500 \times g$ for 30 min at 4 °C protein concentration was quantified using a BCA-Assay (Pierce, Thermo Fisher, Schwerte, Germany) according to the manufacturer's instructions. 6× Laemmli buffer (375 mM 4 × Tris/SDS buffer, pH 6.8, 48% glycerin, 6% SDS, 0,03% bromophenol blue and 9% β-mercaptoethanol) was added, the mixture incubated at 90 °C for 10 min and sonicated for 15 s. 10 μg protein of each sample was loaded on a 10% SDS gel. Protein separation was performed at room temperature using a current of 20 mA for 3–4 h. To transfer the proteins to a PVDF membrane a current of 20 mA was applied for 20 h at 4 °C. After transfer, the membrane was rinsed with 10 ml TBST for 5 min at room temperature. Transfer was checked using Ponceau solution (A2935 0500, AppliChem, Darmstadt, Germany). Blocking was performed for 1 h at room temperature using 10 ml blocking buffer (5% low fat milk in TBST). Each primary antibody was diluted in TBST containing 5% of blocking solution and applied over night at 4 °C. After washing with TBST three times for 10 min each, HRP-conjugated secondary antibody was applied for 2 h at room temperature. The membrane was washed with TBST three times, for 10 min each and incubated in SuperSignal West Femto chemiluminescent substrate (Thermo Scientific, Waltham, MA, USA). Chemiluminescence was detected by exposure of the filter in an Odyssey-Fc-unit (Licor, Lincoln, NE, USA). Used antibodies and dilutions: HRP-conjugated anti-β-actin antibody (Sigma A3854HRP, 1:10,000), anti-STIM1 (CellSignaling, #4916S, 1:1000), anti-STIM2 (CellSignaling, #4917S, 1:1000) and secondary anti-rabbit IgG peroxidase (POX)-antibody (Sigma A6154, 1:10000).

Viability assay. Viability assays were performed by using the WST-1 Reagent (Roche, Mannheim, Germany) according to the manufacturer's instructions. Tetrazolium salts like WST-1 are cleaved to colored formazan in viable cells, which can be measured by spectrophotometry. Cells were plated at a density of 2×10^4 cells per ml per well of a 24-well plate and incubated at 37 °C and 5% CO_2 overnight. WST-1 reagent was diluted 1:10 in pmLF medium before it was added to each well. After 3 hours of incubation absorbance of formazan was measured at a wavelength of 450 nm by spectrophotometry (Tecan, Switzerland). Cell free wells containing pmLF Medium plus WST-1 reagent served as background values.

Proliferation assay. DNA synthesis of lung fibroblasts was assessed using the Click-iT 5-ethynyl-2′-deoxyuridine (EdU) Imaging Kit (ThermoScientific, St. Leon-Rot, Germany). In brief, 1.5×10^5 pmLF per well of a 6 well plate were plated on coverslips overnight and were treated with 10 μM EdU for 3 hours on the next day. After washing cells with PBS and fixation in 3.7% formaldehyde for 10 min pmLF were treated according to the manufacturer's protocol as previously described[29]. EdU is a thymidine analogue which gets incorporated into DNA during active DNA synthesis, if added to the culture medium[31]. After incorporation the ethynyl group of EdU covalently couples to a small fluorescent azide in a copper-dependent click reaction, which can be detected under a fluorescence microscope. To detect all cell nuclei, an additional staining with Hoechst 33342 (Life Technologies, Darmstadt, Germany) was performed. Stained cells were visualized by confocal imaging (LSM 880, Carl Zeiss) and stained nuclei were analyzed by the ImageJ software.

Migration assay. Approximately 1.5×10^4 cells per insert were seeded on a 3 well silicone insert with a 500 μm cell-free gap (ibidi GmbH, Martinsried, Germany) and grown at 37 °C and 5% CO_2 overnight. Insert detachment created a defined cell-free gap. Images were taken 0, 4, 8, 12 and 24 h after releasing inserts. Migration was analyzed by measuring the remaining gap width by the ImageJ software in 3 pictures per time point and replicate.
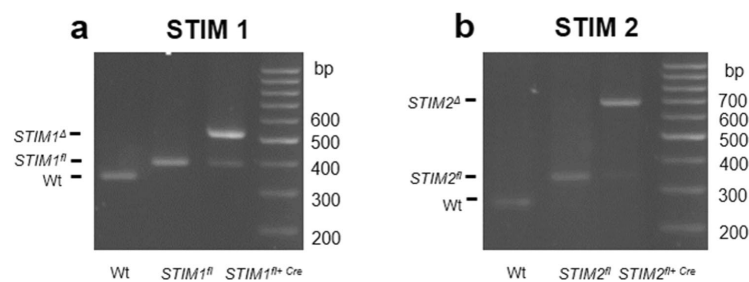
Figure 1. Representative images of PCR fragments obtained from genomic DNA of primary murine fibroblasts (pmLF) using gene specific primers separated by agarose gel electrophoresis (**a,b**). Wild-type (Wt), $Stim1/2^{flox/flox}$ ($Stim1^{fl}$, $Stim2^{fl}$) as well as $Stim1/2^{flox/flox}$ fibroblasts infected with lentiviruses expressing Cre recombinase ($Stim1^{fl+Cre}$, $Stim2^{fl+Cre}$) were analyzed. (**a**) DNA fragments amplified from Wt (Wt), $Stim1^{flox/flox}$ ($Stim1^{fl}$) or deleted $Stim1$ ($Stim1^{\Delta}$) alleles are marked. (**b**) DNA fragments amplified from Wt (Wt), $Stim2^{flox/flox}$ ($Stim2^{fl}$) or deleted $Stim2$ ($Stim2^{\Delta}$) alleles are marked.
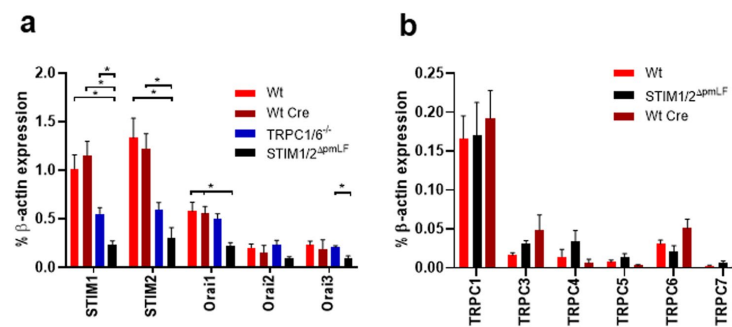
Figure 2. Quantification of STIM, Orai and TRPC mRNAs in primary murine lung fibroblasts (pmLF). Relative mRNA expression of STIM1 and STIM2 as well as Orai1-3 (**a**) or TRPC channels 1, 3–7 (**b**) in wild-type (Wt) pmLF, Wt cells infected with Cre recombinase expressing lentiviruses (Wt Cre), $STIM1/2^{fl/fl}$ fibroblasts infected with Cre recombinase expressing lentiviruses ($STIM1/2^{\Delta pmLF}$) and TRPC1/6- ($TRPC1/6^{-/-}$) deficient pmLF analyzed by quantitative RT-PCR. Columns show means +/− SEM (n > 3 mice, *P < 0.05, **P < 0.01, ***P < 0.001).

Isolation of nuclear fractions. Isolation of nuclear protein extracts from pmLF was performed with a Nuclear Extract Kit according to the manufacturer's instructions (Active Motif, 40010, La Hulpe, Belgium) as described[30]. In brief, cells were first washed with PBS containing phosphatase inhibitors. Cytoplasmic protein fractions were collected by adding hypotonic lysis buffer and detergent, causing leakage of cytoplasmic proteins into the supernatant. After centrifugation (14.000 × g for 30 s) nuclear protein fractions were obtained by re-suspending pellets in detergent-free lysis buffer containing protease inhibitors. NFAT proteins were analyzed by Western Blotting as described above with the following modifications: 20 μl of each protein sample was loaded on a 7.5% SDS gel. Transfer of proteins to PVDF membrane was performed by an applied current of 360 mA at 4 °C for 1 h and 15 min. Unspecific binding sites were blocked in 5%BSA in TBST for one hour prior to incubation with the first antibody incubation overnight. All other steps were performed as described before. Antibodies used: Anti NFATc1 (mouse, SantaCruz Biotechnology, sc-7294, 1:500), anti-NFATc3 (mouse, SantaCruz Biotechnology, sc-7294, 1:500), anti-mouse IgG HRP- linked antibody (CellSignaling, #7076, Danvers, USA) as secondary antibody. Anti Lamin B1 (rabbit, ThermoScientific, PA5-19468, 1:5000) and secondary anti-rabbit IgG peroxidase-linked antibodies (goat, Sigma A6154, 1:10000) served as loading control. Protein bands were normalized to loading controls and quantified by an Odyssey-Fc unit (Licor, Lincoln, USA).

Statistics. All statistical tests were performed using GraphPad Prism 7 (GraphPad Software, San Diego, USA). All Data were first tested for Gaussian distribution using the Shapiro-Wilk test. Gaussian distributed data were analyzed by t-tests or ordinary one-way ANOVA test. If Gaussian distribution was not assumed, nonparametric tests (Wilcoxon matched-pairs signed-rank test, Mann-Whitney U test or Kruskal-Wallis test) were used. Data are shown in means ± SEM. Significant differences are indicated by asterisks for P < 0.05 (*), 0.01 (**), 0.001 (***) and 0.0001 (****).
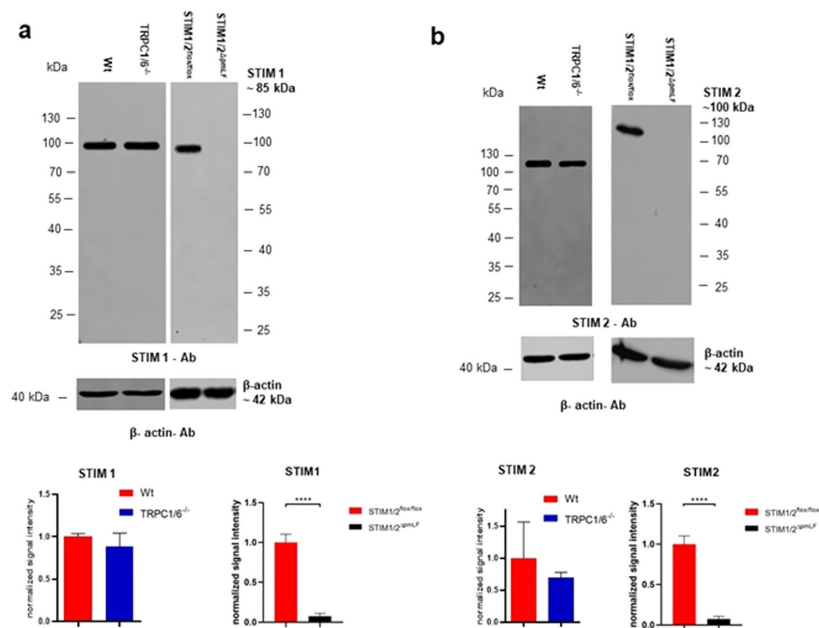
4

Figure 3. Quantification of STIM1 (**a**) and STIM2 (**b**) protein expression in cell lysates of of wildtype (Wt), TRPC1/6-deficient (TRPC1/6$^{-/-}$), and STIM1/2-deficient (STIM1/2$^{\Delta pmLF}$) primary murine lung fibroblasts (pmLF). Expression of β-actin was used as loading control. Signals were normalized and quantified by using the LICOR software. Columns show means +/− SEM (n = 3 mice). Representative images from STIM1 and STIM2 immunoblots. Asterisks mark significant differences (****P < 0.0001).

Results

Cre recombinase induced excision of exons in *Stim1* and *Stim2* genes in primary murine fibroblasts (pmLF) and resulting changes in mRNA and protein levels. To investigate the role of SOCE in pmLF we set out to delete exons in genes, which might be essential for SOCE. We first bred mice deficient for TRPC1 and TRPC6 to obtain *Trpc1/6*$^{-/-}$-double- deficient mice after a crossing over event on chromosome 9, where both genes are located. These mice are viable, fertile and have a normal life span. In clear contrast, STIM1/2 deficient mice die within a few weeks after birth[26]. To examine the effect of STIM deficiency in primary murine lung fibroblasts (pmLF), we therefore isolated these cells from mice with loxP flanked *Stim1* and *Stim2* genes[26] and infected them with recombinant lentiviruses expressing Cre-recombinase. By genomic PCR, we detected DNA fragments corresponding to the deleted *Stim1* and *Stim2* genes after lentiviral infection, respectively (Fig. 1a,b).

To test for any compensatory up- or down-regulation of STIM, Orai and TRPC1/6 mRNAs we quantified mRNA levels in STIM1/2 (STIM1/2$^{\Delta pmLF}$) and TRPC1/6-deficient (TRPC1/6$^{-/-}$) fibroblasts in comparison to wild-type (Wt) and Wt cells infected with recombinant lentiviruses expressing Cre recombinase (Wt Cre). No up-regulation but significantly lower levels of STIM1-2 as well as Orai1-3 mRNAs were observed in STIM1/2$^{\Delta pmLF}$ fibroblasts (Fig. 2a,b). In TRPC1/6-deficient pmLF, we detected significantly decreased levels of TRPC1 and TRPC6 mRNA as expected. TRPC5 mRNA levels, although very low, were also significantly reduced in TRPC1/6−/− pmLF (Fig. S1 in Supplementary Information).

In Western Blots STIM1 and STIM2 proteins were not detectable in STIM1/2$^{\Delta pmLF}$, but expressed in similar amounts in TRPC1/6$^{-/-}$ pmLF as in Wt cells (Fig. 3a,b).

Receptor-operated Ca^{2+} entry (ROCE) is decreased in TRPC1/6-deficient, but not significant different in STIM1/2-deficient fibroblasts. To quantify ROCE in primary murine lung fibroblasts (pmLF), endothelin 1 (Et-1) was used to activate Gq protein-coupled endothelin receptors. Stimulation of Phospholipases C-β by Gα$_q$-subunits resulted in cleavage of phosphatidylinositol 4,5-bisphosphate (PIP2) and generation of diacylglycerol (DAG), which activates TRPC6 channels[32]. ROCE was quantified by analyzing Ca^{2+} transients measured fluorometrically at wavelengths of 340 and 380 nm (Fig. 4a,b) and calculating areas under the curve (AUC) (Fig. 4c) after adding Et-1 to pmLF. Both values were significantly decreased in TRPC1/6-deficient but not in STIM1/2-deficient pmLF compared to control cells (Fig. 4a–c). We also performed recalcification experiments after application of Et-1 in Ca^{2+} free buffer (Fig. S2 in Supplementary Information). While there is no difference
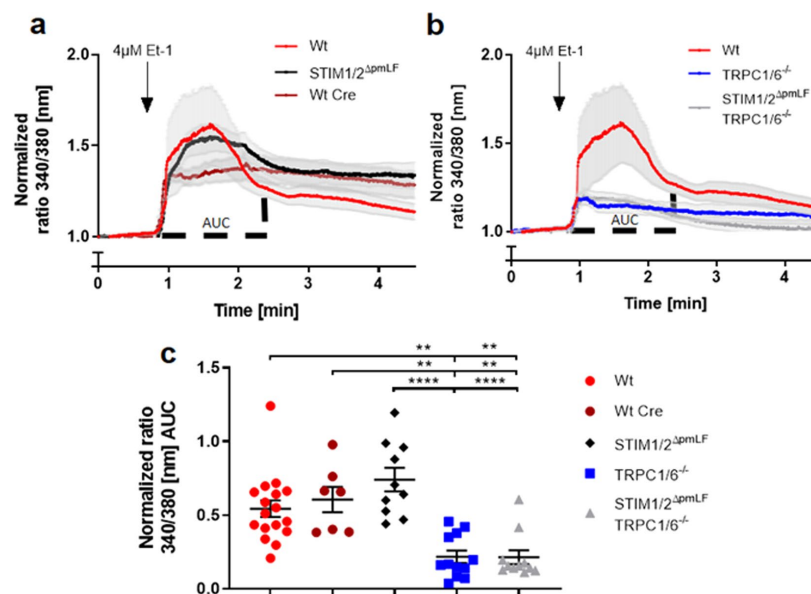
Paper II

Figure 4. Receptor-operated Ca^{2+} entry (ROCE) induced by application of endothelin-1 (Et-1) in TRPC1/6-(TRPC1/6$^{-/-}$) (**a,c**), STIM1/2− (STIM1/2$^{\Delta pmLF}$) (**b,c**) and STIM1/2−TRPC1/6− (TRPC1/6$^{-/-}$ STIM1/2$^{\Delta pmLF}$) deficient primary murine lung fibroblasts (pmLF) (**a,c**). Wild-type pmLF infected with recombinant lentiviruses expressing Cre recombinase (Wt Cre) served as controls. Fura-2-loaded pmLF were stimulated with 4 μM Et-1 in Ca^{2+} containing buffer to generate ROCE. Intracellular Ca^{2+} levels ($[Ca^{2+}]_i$) were quantified by analysis of fluorescence ratios at excitation wavelengths of 340 and 380 nm (ratio 340/380 nm) and normalized to initial values. Lines represent calculated means and light grey areas indicate standard error of the mean (SEM) of more than three independent experiments of at least three mice. Calculation of the areas under the curves (AUC) in Fig. 4a,b was used to quantify ROCE (**c**). One single dot represents the mean of at least 20 cells from one cell isolation. Asterisks mark significant differences from left to right (n > 3 mice, **P < 0.01, ***P < 0.001, ****P < 0.0001) between ratios of deficient cells compared to control cells.

in cytoplasmic Ca^{2+} levels after the release of Ca^{2+} from the internal stores following IP_3 production, Ca^{2+} influx from the extracellular medium is reduced in TRPC1/6$^{-/-}$ fibroblasts compared to Wt cells.

Store-operated Ca^{2+} entry (SOCE) is reduced in STIM1/2-deficient, but not in TRPC1/6-deficient primary murine lung fibroblasts (pmLF). SOCE was induced in pmLF by emptying internal Ca^{2+} stores after application of thapsigargin in Ca^{2+} free buffer containing the Ca^{2+} chelator EGTA and subsequent readdition of extracellular Ca^{2+}. While TRPC1/6-deficient fibroblasts showed no differences, SOCE in STIM1/2-deficient cells was significantly reduced comparing peak levels and areas under the curve (AUC) (Fig. 5a–c). Ablation of all four proteins STIM1/2 and TRPC1/6 did not further reduce SOCE. Therefore, SOCE is exclusively regulated by STIM1/2 proteins and Orai channels in primary murine fibroblasts and not dependent on TRPC1 and TRPC6.

STIM1/2 deficiency reduces cell proliferation, migration and nuclear localization of NFAT transcription factors in fibroblasts. To understand the general role of SOCE in cell function of pmLF, we quantified cell viability using a WST assay in STIM1/2- deficient fibroblasts in comparison to control cells. Cell viability was not impaired by STIM1/2 deficiency 5 to 8 days after infection with recombinant lentiviruses expressing Cre recombinase in comparison to infected and non-infected Wt pmLF (Fig. 6a). In contrast to these results. DNA synthesis as a measure of cell proliferation was significantly reduced in STIM1/2- deficient fibroblasts in comparison to Wt cells infected with recombinant lentiviruses expressing Cre recombinase (Fig. 6b,c).

To analyze SOCE on a molecular level in pmLF, we quantified nuclear levels of the Ca^{2+}-dependent transcription factor nuclear factor of activated T cells (NFAT). Both isoforms NFATc1 and NFATc3 were significantly reduced in nuclear extracts of STIM1/2- deficient pmLF compared to Wt pmLF infected with recombinant lentiviruses expressing Cre recombinase as control cells (Fig. 7).

An important function during repair processes by pmLF is cell migration. To ask whether SOCE may have a role in migration of pmLF, we quantified gap closure times of migrating STIM1/2- deficient and control pmLF. It took STIM1/2- deficient pmLF significantly longer to close a defined gap in a confluent cell layer compared to control cells (Wt and Wt Cre) (Fig. 8).
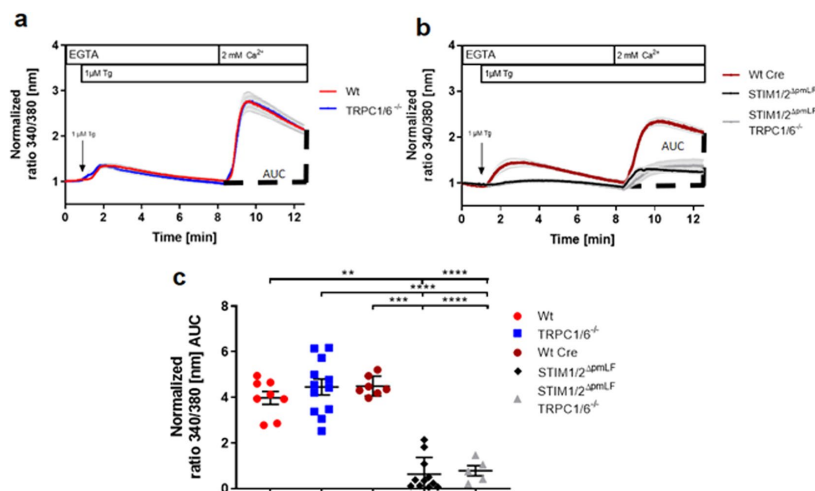
19

Paper II

Figure 5. Store-operated Ca²⁺ entry (SOCE) induced by application of thapsigargin in Ca²⁺-free buffer and subsequent readdition of extracellular Ca²⁺ in TRPC1/6− (TRPC1/6⁻/⁻) (**a,c**), STIM1/2− (STIM1/2^ΔpmLF) (**b,c**) and STIM1/2−TRPC1/6− (TRPC1/6⁻/⁻ STIM1/2^ΔpmLF) deficient primary murine pulmonary fibroblasts (pmLF) (**a,c**). (**a,b**) Wild-type fibroblasts infected with recombinant lentiviruses expressing Cre recombinase (Wt Cre) served as controls. Internal Ca²⁺ stores of fura-2-loaded pmLF were emptied by application of thapsigargin followed by recalcification. Intracellular Ca²⁺ levels ([Ca²⁺]ᵢ) were quantified by analysis of fluorescence ratios at excitation wavelengths of 340 and 380 nm (ratio 340/380 nm) and normalized to initial values. Lines represent calculated means and light grey areas indicate standard error of the mean (SEM) of more than three independent experiments of at least three mice. Calculation of the areas under the curves (AUC) in Fig. 6a,b was used to quantify SOCE (**c**). One single dot represents the mean of at least 20 cells from one cell isolation. Asterisks mark from left to right significant differences (*P < 0.05, **P < 0.01, ***P < 0.001, ****P < 0.0001) between ratios of deficient cells compared to control cells.
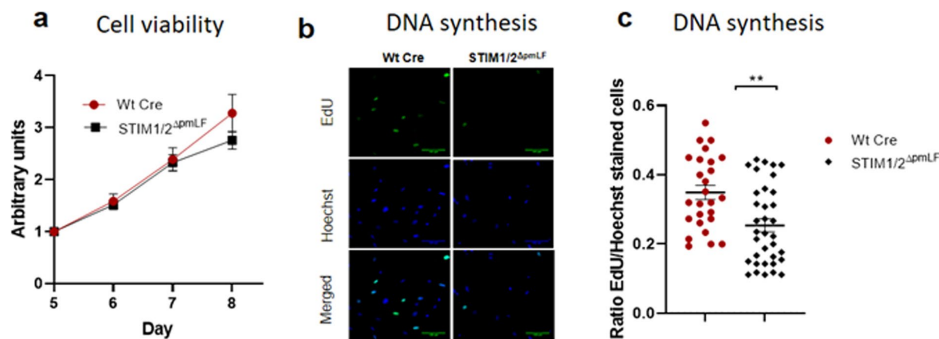
Figure 6. Cell viability (**a**) and DNA synthesis (**b,c**) quantified in STIM1/2- deficient primary murine lung fibroblasts (pmLF) compared to control cells. (**a**) Viability was analyzed in wild type pmLF infected with recombinant lentiviruses expressing Cre recombinase (Wt Cre) as well as STIM1/2- deficient pmLF using a WST-assay 5–8 days after infection. (**b**) Wild type pmLF infected with recombinant lentiviruses expressing Cre recombinase (Wt Cre) as well as STIM1/2- deficient pmLF were incubated with EdU (5-ethynyl-2′-deoxyuridine) for 4 hours and fixed cells were stained with cross- linked fluorescent azide. Nuclei staining was performed by Hoechst dye. (**c**) Individual values and means +/− SEM of EdU/Hoechst ratios were plotted . Asterisks mark significant differences (n > 3 mice, **P < 0.01) between ratios of STIM1/2-deficient cells compared to control cells.
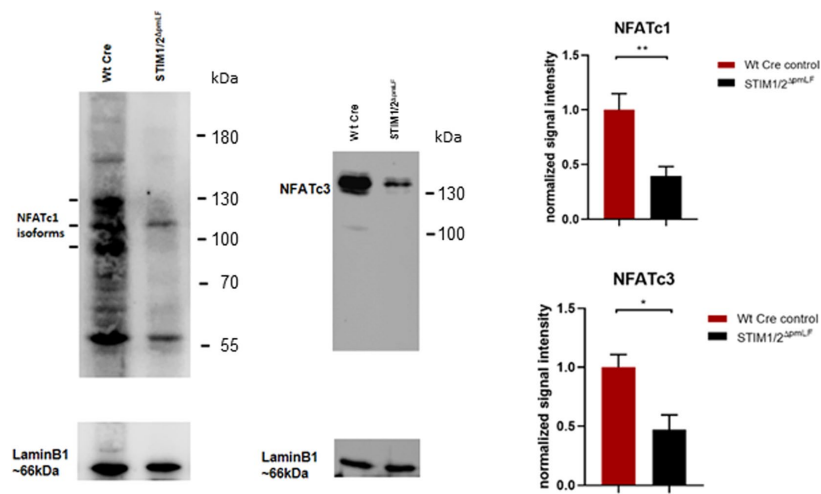
Figure 7. Quantification of nuclear NFATc levels in STIM1/2- deficient pmLF (STIM1/2$^{\Delta pmLF}$) and wild-type cells infected with recombinant lentiviruses expressing Cre recombinase as control cells (Wt Cre). Representative Western Blots showing NFATc1 (left panel) and NFATc3 (right panel) isoforms in nuclear extracts from STIM1/2$^{\Delta pmLF}$ and Wt Cre cells. Summary of quantitative analysis of nuclear NFAT levels of the c1 (upper bar graph) and c3 (lower bar graph) isoforms. Columns show calculated means +/− SEM. Asterisks mark significant differences (n > 3 mice, *P < 0.05, **P < 0.001) between ratios of STIM1/2$^{\Delta pmLF}$ cells compared to Wt Cre control cells.
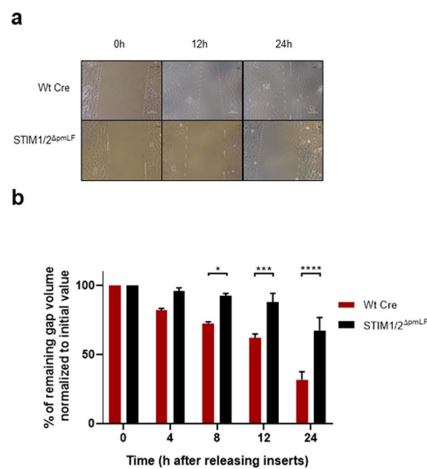
Figure 8. Migration of STIM1/2- deficient primary murine lung fibroblasts (pmLF) and control cells (**a,b**). (**a**) Images from a representative migration assay with STIM1/2- deficient pmLF compared to Wt cells infected with recombinant lentiviruses expressing Cre recombinase (Wt Cre) after removing inserts. (**b**) Summary of remaining gap values normalized to initial values quantified in migration assays of STIM1/2- deficient pmLF compared to Wt cells infected with recombinant lentiviruses expressing Cre recombinase (Wt Cre) after removing inserts at 0, 4, 8, 12 and 24 h. Data represent means ± SEM from 3 independent cell preparations of 5 mice each. Asterisks mark significant differences (*P < 0.05, **P < 0.01, ***P < 0.001, ****P < 0.0001) between ratios of STIM1/2-deficient cells compared to control cells.

Discussion

To dissect the molecular correlate of ROCE and SOCE in pmLF we deleted essential genes involved in one or presumably both processes in pmLF. In a former publication, we identified TRPC1 as the predominantly expressed TRPC channel in pmLF, while TRPC6 is up-regulated in TGF-β1 induced fibroblast to myofibroblast differentiation[30]. Three members of this TRPC family namely TRPC3, TRPC6 and TRPC7 are activated by diacylglycerol (DAG), which is produced after ligand binding to G protein-coupled receptors (GPCR) and subsequent cleavage of phosphatidylinositol 4,5-bisphosphate (PIP2) by phospholipase-C isozymes[32,33]. These so called DAG-sensitive channels are mainly expressed in brain, endothelial and smooth muscle cells of the vasculature and mediate ROCE (reviewed in[34]). Recent findings indicate that Na^+/H^+ exchanger regulatory factors dynamically determine the DAG sensitivity of TRPC4 and TRPC5 channels[35] and that TRPC1 proteins work as channel regulators in heteromeric complexes with all other six channels of the TRPC family[25]. Therefore, all TRPC channels are responsible for ROCE and global ablation of TRPC1 and TRPC6 proteins is sufficient to reduce intracellular Ca^{2+} levels during ROCE in pmLF from TRPC1/6- deficient mice (Fig. 4).

Activation of ubiquitously expressed Orai channels in the plasma membrane is exclusively dependent on the multimerization of the ER Ca^{2+} sensors STIM1 and 2 after detecting reduced Ca^{2+} levels after store depletion (summarized in[36]). As global deletion of STIM1 and 2 proteins induces early death in the corresponding gene-deficient mouse models[26], we choose a different approach and isolated pmLF from STIM1/2 floxed mouse models, which carry loxP sites downstream and upstream of exons essential for protein function. Infection of these cells with recombinant lentiviruses expressing Cre recombinase efficiently deletes floxed exons in both genes (Fig. 1) resulting in an almost complete absence of both proteins (Fig. 3). No compensatory up-regulation of mRNAs for Orai and TRPC channels (Fig. 2) was detected. On a protein level, TRPC1/6- deficient pmLF expressed similar amounts of STIM1/2 proteins (Fig. 3) in comparison to Wt cells and no changes in SOCE were observed (Fig. 5a). In contrast, complete ablation of STIM1/2 proteins in STIM1/2$^{\Delta pmLF}$ significantly reduced SOCE (Fig. 5b), but had no significant effect on ROCE induced by activation of endothelin receptors by endothelin 1 (Et-1) (Fig. 4b). ROCE, however, was significantly reduced in TRPC1/6- deficient cells (Fig. 4a) confirming the hypothesis that TRPC1 and -6 channels are responsible for receptor-dependent Ca^{2+} influx in these cells.

Several reports indicate TRPC3-mediated SOCE in pancreatic acini[37] and TRPC1-mediated SOCE in salivary gland cells[19], which may be due to STIM1/2[17,38,39] or Orai1/2/3[18,40,41] interactions with TRPC channels in these cells (reviewed in[42,43]). In pmLF however, we were not able to detect any difference in SOCE in TRPC1/6- deficient cells compared to control cells (Fig. 5a,c), while STIM1/2- deficient pmLF showed significantly decreased levels (Fig. 5b,c). Therefore, we conclude that SOCE and ROCE in pmLF are mediated by different entirely independent molecular correlates in pmLF as already described in transiently transfected HEK293 cells[16].

Next, we analyzed the role of SOCE in basal cell functions of pmLF. While metabolic activity indicative of cell viability was not changed in STIM1/2- deficient compared to lentivirus infected Wt cells (Fig. 6a), quantification of DNA synthesis as a marker for cell proliferation was decreased in STIM1/2- deficient cells compared to Wt cells infected with lentiviruses (Fig. 6b,c). The role of SOCE in cell proliferation has already been demonstrated in many other cell types (reviewed in[44]) and especially in cancer cells[45]. The nuclear translocation of NFATc transcription factors depends on increases in the intracellular Ca^{2+} concentration, which makes NFATc a preferred target for SOCE induced changes in cell function[46]. Accordingly, we identified lower levels of nuclear NFATc1 and 3 levels in STIM1/2- deficient pmLF compared to lentivirus infected Wt control cells emphasizing an important role of SOCE in Ca^{2+}-induced mRNA transcription of pmLF (Fig. 7). Similar results were obtained for NFATc3 in arterial smooth muscle cells[47]. We also quantified cell migration as an essential function of pmLF during repair processes in the lung and detected significant longer gap closure times in STIM1/2- deficient pmLF compared to lentivirus infected control cells (Fig. 8). The role of SOCE in cell migration was intensively studied in cancer cells (reviewed in[48]), where intracellular Ca^{2+} influx through STIM-Orai interaction affects focal adhesion turnover as a critical step in the migration mechanism[49]. A similar mechanism may be important in migration of pmLF and needs to be further analyzed.

In summary, we were able to show for the first time that SOCE, which is exclusively induced by STIM1/2 proteins in the ER of pmLF, is not dependent on TRPC1 and TRPC6, the predominantly expressed TRP channels in pmLF. Therefore, an interaction of STIM proteins and/or Orai channels with TRPC channels in these cells to mediate SOCE is unlikely. SOCE contributes to cell proliferation and migration as well as nuclear localization of nuclear factor of activated T-cells (NFATc1 and c3) in pmLF. Therefore, TRPC6 channels, which are also important for cellular functions of pmLF when differentiated to myofibroblasts by TGF-β1[30], work independently of STIM1/2 proteins and Orai channels in this cell type.

References

1. Putney, J. W. Jr. A model for receptor-regulated calcium entry. *Cell Calcium* **7**, 1–12, https://doi.org/10.1016/0143-4160(86)90026-6 (1986).
2. Zhu, X. *et al.* trp, a novel mammalian gene family essential for agonist-activated capacitative Ca2+ entry. *Cell* **85**, 661–671 (1996).
3. Kiselyov, K. *et al.* Functional interaction between InsP3 receptors and store-operated Htrp3 channels. *Nature* **396**, 478–482 (1998).
4. Boulay, G. *et al.* Modulation of Ca(2+) entry by polypeptides of the inositol 1,4,5-trisphosphate receptor (IP3R) that bind transient receptor potential (TRP): evidence for roles of TRP and IP3R in store depletion-activated Ca(2+) entry. *Proc Natl Acad Sci USA* **96**, 14955–14960 (1999).
5. Liou, J. *et al.* STIM is a Ca2+ sensor essential for Ca2+-store-depletion-triggered Ca2+ influx. *Curr Biol* **15**, 1235–1241 (2005).
6. Roos, J. *et al.* STIM1, an essential and conserved component of store-operated Ca2+ channel function. *J Cell Biol* **169**, 435–445, https://doi.org/10.1083/jcb.200502019 (2005).

7. Feske, S. *et al.* A mutation in Orai1 causes immune deficiency by abrogating CRAC channel function. *Nature* **441**, 179–185, https://doi.org/10.1038/nature04702 (2006).
8. Vig, M. *et al.* CRACM1 is a plasma membrane protein essential for store-operated Ca2+ entry. *Science* **312**, 1220–1223, https://doi.org/10.1126/science.1127883 (2006).
9. Yeromin, A. V. *et al.* Molecular identification of the CRAC channel by altered ion selectivity in a mutant of Orai. *Nature* **443**, 226–229, https://doi.org/10.1038/nature05108 (2006).
10. Hoth, M. & Penner, R. Depletion of intracellular calcium stores activates a calcium current in mast cells. *Nature* **355**, 353–356, https://doi.org/10.1038/355353a0 (1992).
11. Liou, J., Fivaz, M., Inoue, T. & Meyer, T. Live-cell imaging reveals sequential oligomerization and local plasma membrane targeting of stromal interaction molecule 1 after Ca2+ store depletion. *Proc Natl Acad Sci USA* **104**, 9301–9306, https://doi.org/10.1073/pnas.0702866104 (2007).
12. Barr, V. A. *et al.* Dynamic movement of the calcium sensor STIM1 and the calcium channel Orai1 in activated T-cells: puncta and distal caps. *Molecular biology of the cell* **19**, 2802–2817, https://doi.org/10.1091/mbc.E08-02-0146 (2008).
13. Luik, R. M., Wu, M. M., Buchanan, J. & Lewis, R. S. The elementary unit of store-operated Ca2+ entry: local activation of CRAC channels by STIM1 at ER-plasma membrane junctions. *J Cell Biol* **174**, 815–825, https://doi.org/10.1083/jcb.200604015 (2006).
14. Johnson, M. & Trebak, M. ORAI channels in cellular remodeling of cardiorespiratory disease. *Cell Calcium* **79**, 1–10, https://doi.org/10.1016/j.ceca.2019.01.005 (2019).
15. Feske, S. CRAC channels and disease - From human CRAC channelopathies and animal models to novel drugs. *Cell Calcium* **80**, 112–116, https://doi.org/10.1016/j.ceca.2019.03.004 (2019).
16. DeHaven, W. I. *et al.* TRPC channels function independently of STIM1 and Orai1. *J Physiol* **587**, 2275–2298, https://doi.org/10.1113/jphysiol.2009.170431 (2009).
17. Yuan, J. P., Zeng, W., Huang, G. N., Worley, P. F. & Muallem, S. STIM1 heteromultimerizes TRPC channels to determine their function as store-operated channels. *Nat Cell Biol* **9**, 636–645, https://doi.org/10.1038/ncb1590 (2007).
18. Liao, Y. *et al.* Orai proteins interact with TRPC channels and confer responsiveness to store depletion. *Proc Natl Acad Sci USA* **104**, 4682–4687, https://doi.org/10.1073/pnas.0611692104 (2007).
19. Liu, X. *et al.* Attenuation of store-operated Ca2+ current impairs salivary gland fluid secretion in TRPC1(−/−) mice. *Proc Natl Acad Sci USA* **104**, 17542–17547, https://doi.org/10.1073/pnas.0701254104 (2007).
20. Kim, M. S. *et al.* Native Store-operated Ca2+ Influx Requires the Channel Function of Orai1 and TRPC1. *J Biol Chem* **284**, 9733–9741, https://doi.org/10.1074/jbc.M808097200 (2009).
21. Dietrich, A. *et al.* Pressure-induced and store-operated cation influx in vascular smooth muscle cells is independent of TRPC1. *Pflugers Arch* **455**, 465–477, https://doi.org/10.1007/s00424-007-0314-3 (2007).
22. Dietrich, A., Fahlbusch, M. & Gudermann, T. Classical Transient Receptor Potential 1 (TRPC1): Channel or Channel Regulator? *Cells* **3**, 939–962, https://doi.org/10.3390/cells3040939 (2014).
23. Hofmann, T., Schaefer, M., Schultz, G. & Gudermann, T. Subunit composition of mammalian transient receptor potential channels in living cells. *Proc Natl Acad Sci USA* **99**, 7461–7466 (2002).
24. Strubing, C., Krapivinsky, G., Krapivinsky, L. & Clapham, D. E. TRPC1 and TRPC5 form a novel cation channel in mammalian brain. *Neuron* **29**, 645–655 (2001).
25. Storch, U., Forst, A. L., Philipp, M., Gudermann, T. & Mederos y Schnitzler, M. Transient receptor potential channel 1 (TRPC1) reduces calcium permeability in heteromeric channel complexes. *J Biol Chem* **287**, 3530–3540, https://doi.org/10.1074/jbc.M111.283218 (2012).
26. Oh-Hora, M. *et al.* Dual functions for the endoplasmic reticulum calcium sensors STIM1 and STIM2 in T cell activation and tolerance. *Nat Immunol* **9**, 432–443, https://doi.org/10.1038/ni1574 (2008).
27. Dietrich, A. *et al.* Increased vascular smooth muscle contractility in TRPC6−/− mice. *Mol Cell Biol* **25**, 6980–6989, https://doi.org/10.1128/MCB.25.16.6980-6989.2005 (2005).
28. Staab-Weijnitz, C. A. *et al.* FK506-Binding Protein 10, a Potential Novel Drug Target for Idiopathic Pulmonary Fibrosis. *American journal of respiratory and critical care medicine* **192**, 455–467, https://doi.org/10.1164/rccm.201412-2233OC (2015).
29. Kalwa, H. *et al.* Phospholipase C epsilon (PLCepsilon) induced TRPC6 activation: a common but redundant mechanism in primary podocytes. *J Cell Physiol* **230**, 1389–1399, https://doi.org/10.1002/jcp.24883 (2015).
30. Hofmann, K. *et al.* Classical transient receptor potential 6 (TRPC6) channels support myofibroblast differentiation and development of experimental pulmonary fibrosis. *Biochim Biophys Acta* **1863**, 560–568, https://doi.org/10.1016/j.bbadis.2016.12.002 (2017).
31. Buck, S. B. *et al.* Detection of S-phase cell cycle progression using 5-ethynyl-2′-deoxyuridine incorporation with click chemistry, an alternative to using 5-bromo-2′-deoxyuridine antibodies. *BioTechniques* **44**, 927–929, https://doi.org/10.2144/000112812 (2008).
32. Hofmann, T. *et al.* Direct activation of human TRPC6 and TRPC3 channels by diacylglycerol. *Nature* **397**, 259–263 (1999).
33. Okada, T. *et al.* Molecular and functional characterization of a novel mouse transient receptor potential protein homologue TRP7. Ca(2+)-permeable cation channel that is constitutively activated and enhanced by stimulation of G protein-coupled receptor. *J Biol Chem* **274**, 27359–27370 (1999).
34. Dietrich, A., Kalwa, H., Rost, B. R. & Gudermann, T. The diacylglycerol-sensitive TRPC3/6/7 subfamily of cation channels: functional characterization and physiological relevance. *Pflugers Arch* **451**, 72–80 (2005).
35. Storch, U. *et al.* Dynamic NHERF interaction with TRPC4/5 proteins is required for channel gating by diacylglycerol. *Proc Natl Acad Sci USA* **114**, E37–E46, https://doi.org/10.1073/pnas.1612263114 (2017).
36. Cahalan, M. D. STIMulating store-operated Ca(2+) entry. *Nat Cell Biol* **11**, 669–677, https://doi.org/10.1038/ncb0609-669 (2009).
37. Kim, M. S. *et al.* Deletion of TRPC3 in mice reduces store-operated Ca2+ influx and the severity of acute pancreatitis. *Gastroenterology* **137**, 1509–1517, https://doi.org/10.1053/j.gastro.2009.07.042 (2009).
38. Lee, K. P. *et al.* An endoplasmic reticulum/plasma membrane junction: STIM1/Orai1/TRPCs. *Febs Letters* **584**, 2022–2027, https://doi.org/10.1016/j.febslet.2009.11.078 (2010).
39. Lee, K. P., Yuan, J. P., So, I., Worley, P. F. & Muallem, S. STIM1-dependent and STIM1-independent Function of Transient Receptor Potential Canonical (TRPC) Channels Tunes Their Store-operated Mode. *Journal of Biological Chemistry* **285**, 38666–38673, https://doi.org/10.1074/jbc.M110.155036 (2010).
40. Liao, Y. *et al.* Functional interactions among Orai1, TRPCs, and STIM1 suggest a STIM-regulated heteromeric Orai/TRPC model for SOCE/Icrac channels. *Proc Natl Acad Sci USA* **105**, 2895–2900, https://doi.org/10.1073/pnas.0712288105 (2008).
41. Cheng, K. T., Liu, X., Ong, H. L. & Ambudkar, I. S. Functional requirement for Orai1 in store-operated TRPC1-STIM1 channels. *J Biol Chem* **283**, 12935–12940, https://doi.org/10.1074/jbc.C800008200 (2008).
42. Choi, S. *et al.* The TRPCs-STIM1-Orai interaction. *Handb Exp Pharmacol* **223**, 1035–1054, https://doi.org/10.1007/978-3-319-05161-1_13 (2014).
43. Liao, Y., Abramowitz, J. & Birnbaumer, L. The TRPC family of TRP channels: roles inferred (mostly) from knockout mice and relationship to ORAI proteins. *Handb Exp Pharmacol* **223**, 1055–1075, https://doi.org/10.1007/978-3-319-05161-1_14 (2014).
44. Pinto, M. C. *et al.* Calcium signaling and cell proliferation. *Cell Signal* **27**, 2139–2149, https://doi.org/10.1016/j.cellsig.2015.08.006 (2015).
45. Shuba, Y. M. Ca(2+) channel-forming ORAI proteins: cancer foes or cancer allies? *Exp Oncol* **41**, 200–206, https://doi.org/10.32471/exp-oncology.2312-8852.vol-41-no-3.13473 (2019).

23

46. Kar, P. *et al*. Dynamic assembly of a membrane signaling complex enables selective activation of NFAT by Orai1. *Curr Biol* **24**, 1361–1368, https://doi.org/10.1016/j.cub.2014.04.046 (2014).
47. Mancarella, S. *et al*. Targeted STIM deletion impairs calcium homeostasis, NFAT activation, and growth of smooth muscle. *FASEB J* **27**, 893–906, https://doi.org/10.1096/fj.12-215293 (2013).
48. Chen, Y. F., Lin, P. C., Yeh, Y. M., Chen, L. H. & Shen, M. R. Store-Operated Ca(2+) Entry in Tumor Progression: From Molecular Mechanisms to Clinical Implications. *Cancers (Basel)* **11**, https://doi.org/10.3390/cancers11070899 (2019).
49. Yang, S., Zhang, J. J. & Huang, X. Y. Orai1 and STIM1 are critical for breast tumor cell migration and metastasis. *Cancer Cell* **15**, 124–134, https://doi.org/10.1016/j.ccr.2008.12.019 (2009).

Acknowledgements

Author contributions

L.B., F.G. and A.D. performed the study and wrote the manuscript, S.F. and T.G. contributed to data interpretation; S.F. provided essential tools. All authors read and approved the final manuscript.

Competing interests

S.F. is a scientific cofounder of Calcimedica; the other authors declare no conflict of interest.

Additional information

Supplementary information is available for this paper at https://doi.org/10.1038/s41598-020-63677-2.

Correspondence and requests for materials should be addressed to A.D.

Reprints and permissions information is available at www.nature.com/reprints.

Publisher's note Springer Nature remains neutral with regard to jurisdictional claims in published maps and institutional affiliations.

24

Store-operated Ca^{2+} entry in primary murine lung fibroblasts is independent of classical transient receptor channels and contributes to cell migration

Larissa Bendiks[1], Thomas Gudermann[1], Stefan Feske[2] & Alexander Dietrich[1*]

[1] Walther Straub Institute of Pharmacology and Toxicology, Member of the German Center for Lung Research (DZL), Medical Faculty, LMU-Munich, Munich Germany
[2] Department of Pathology, New York University School of Medicine, New York, NY, 10016, USA.
* email: alexander.dietrich@lrz.uni-muenchen.de

Supplementary Information

Contents

Figure S1: : Relative mRNA amounts of TRPC channels (TRPC1, 3–6) in WT and TRPC6−/− PMLFs analyzed by quantitative RT-PCR

Figure S2: Receptor-operated Ca^{2+} entry (ROCE) induced by application of endothelin-1 (Et-1) in Ca^{2+} free medium and after recalcification in TRPC1/6- (TRPC1/6$^{-/-}$) deficient primary murine lung fibroblasts (pmLF).
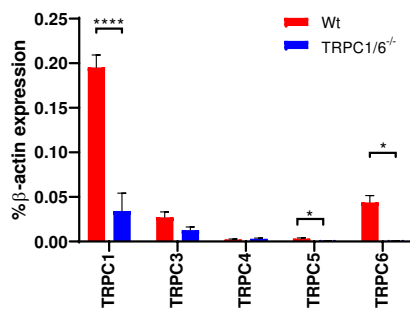
Supplementary Figure 1: Relative mRNA amounts of TRPC channels (TRPC1, 3–6) in WT and TRPC6−/− PMLFs analyzed by quantitative RT-PCR (WT, n = 5 mice; TRPC6−/− n = 5 mice).
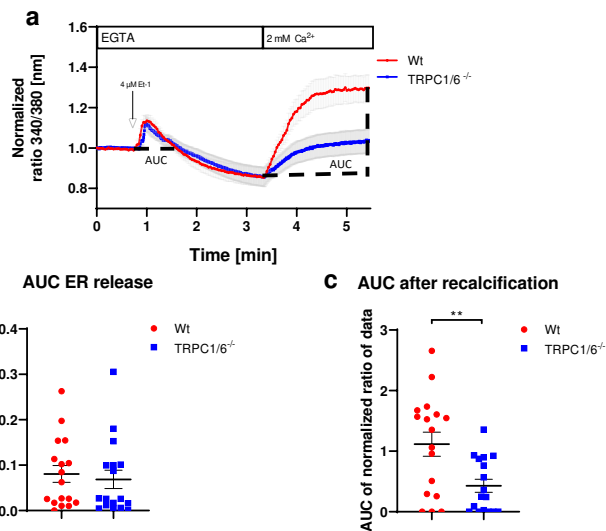
Supplementary Figure 2: Receptor-operated Ca²⁺ entry (ROCE) induced by application of endothelin-1 (Et-1) in Ca²⁺ free medium and after recalcification in TRPC1/6-(TRPC1/6⁻/⁻) deficient primary murine lung fibroblasts (pmLF). Wild-type (Wt) pmLF served as controls. Fura-2-loaded pmLF were stimulated with 4 µM Et-1 in Ca²⁺ free, EGTA (1.5 mM) containing buffer to empty ER Ca²⁺ stores and Ca²⁺ (2mM) was added to generate ROCE (**a**). Intracellular Ca 2+ levels ([Ca2+]i) were quantified by analysis of fluorescence ratios at excitation wavelengths of 340 and 380 nm (ratio 340/380 nm) and normalized to initial values. Lines represent calculated means and light grey areas indicate standard error of the mean (SEM) of more than three independent experiments of at least three mice. Calculation of the areas under the curves (AUC) in a was used to quantify ROCE (c). One single dot represents the mean of at least 20 cells from one cell isolation. Asterisks mark significant differences from left to right (n = 5 mice, ** P < 0.01) between ratios of deficient cells compared to control cells.

5.   Paper III

MOLECULAR TOXICOLOGY

Check for updates

TRPM7 restrains plasmin activity and promotes transforming growth factor-β1 signaling in primary human lung fibroblasts

Sarah Zeitlmayr[1] · Susanna Zierler[1,2] · Claudia A. Staab-Weijnitz[3] · Alexander Dietrich[1] · Fabienne Geiger[1] · F. David Horgen[4] · Thomas Gudermann[1] · Andreas Breit[1]

Abstract

Sustained exposure of the lung to various environmental or occupational toxins may eventually lead to pulmonary fibrosis, a devastating disease with no cure. Pulmonary fibrosis is characterized by excessive deposition of extracellular matrix (ECM) proteins such as fibronectin and collagens. The peptidase plasmin degrades the ECM, but protein levels of the plasmin activator inhibitor-1 (PAI-1) are increased in fibrotic lung tissue, thereby dampening plasmin activity. Transforming growth factor-β1 (TGF-β1)-induced activation of SMAD transcription factors promotes ECM deposition by enhancing collagen, fibronectin and PAI-1 levels in pulmonary fibroblasts. Hence, counteracting TGF-β1-induced signaling is a promising approach for the therapy of pulmonary fibrosis. Transient receptor potential cation channel subfamily M Member 7 (TRPM7) supports TGF-β1-promoted SMAD signaling in T-lymphocytes and the progression of fibrosis in kidney and heart. Thus, we investigated possible effects of TRPM7 on plasmin activity, ECM levels and TGF-β1 signaling in primary human pulmonary fibroblasts (pHPF). We found that two structurally unrelated TRPM7 blockers enhanced plasmin activity and reduced fibronectin or PAI-1 protein levels in pHPF under basal conditions. Further, TRPM7 blockade strongly inhibited fibronectin and collagen deposition induced by sustained TGF-β1 stimulation. In line with these data, inhibition of TRPM7 activity diminished TGF-β1-triggered phosphorylation of SMAD-2, SMAD-3/4-dependent reporter activation and PAI-1 mRNA levels. Overall, we uncover TRPM7 as a novel supporter of TGF-β1 signaling in pHPF and propose TRPM7 blockers as new candidates to control excessive ECM levels under pathophysiological conditions conducive to pulmonary fibrosis.

Keywords Pulmonary fibrosis · Primary human lung fibroblasts · TGF-β1 · TRPM7 · Plasmin

Abbreviations

ECM	Extracellular matrix
FMT	Fibroblast-to-myofibroblast transition
Plg	Plasminogen
PA	Plasminogen activator
PAI-1	Plasminogen activator inhibitor-1
pHPF	Primary human lung fibroblasts
α-SMA	α-Smooth muscle actin
SRB	Sulforhodamine B
TGF-β1	Transforming growth factor-β1
TRP	Transient receptor potential
TRPM7	Transient receptor potential cation channel subfamily M Member 7

✉ Andreas Breit
andreas.breit@lrz.uni-muenchen.de

1   Walther Straub Institute of Pharmacology and Toxicology, Medical Faculty, LMU Munich, Goethestrasse 33, 80336 Munich, Germany

2   Faculty of Medicine, Johannes Kepler University, Life Science Park, Huemerstraße 3-5, 4020 Linz, Austria

3   Institute of Lung Health and Immunity and Comprehensive Pneumology Center, Helmholtz Zentrum München GmbH, Member of the German Center for Lung Research, Max-Lebsche-Platz 31, 81377 Munich, Germany

4   Department of Natural Sciences, Hawaii Pacific University, Kaneohe, HI 96744, USA

Introduction

Pulmonary fibrosis caused by chronic lung injury is characterized by affluent deposition of ECM leading to stiffness of lung tissue and reduced gas exchange (Kristensen et al. 2014). The prevalence per 10,000 individuals of the population ranges from 0.57 to 4.51 in Asia–Pacific countries, 0.33 to 2.51 in Europe, and 2.40 to 2.98 in North America (Maher et al. 2021). As no effective therapy apart from lung

∅ Springer

transplantation is available yet, prognoses for individuals diagnosed with pulmonary fibrosis is poor and the median survival of patients with idiopathic pulmonary fibrosis is only 3–5 years. Estimated mortality rates are 64.3 deaths per million in men and 58.4 deaths per million in women (Ryerson and Kolb 2018). A wide range of environmental and occupational inhalation hazards like beryllium, nylon flock, polyvinyl chloride, carbon nanotubes, asbestos or silica are known to engender pulmonary fibrosis (Boag et al. 1999; Cordasco et al. 1980; Dong and Ma 2016; Mossman and Churg 1998; Newman et al. 1996; Vehmas et al. 2012; Yoshida et al. 2011). Likewise cigarette smoke and cancer chemo- or radiotherapy have also been linked to this devastating disease (Giuranno et al. 2019; Morse and Rosas 2014; Sleijfer 2001). Noteworthy, in light of the ongoing Covid-19 pandemic, it is a matter of debate as to whether pulmonary fibrosis treatment might ameliorate the development of severe Covid-19 cases and that pulmonary fibrosis might occur as a long-term consequence of the Covid-19 acute respiratory distress syndrome (George et al. 2020; Ojo et al. 2020; Vasarmidi et al. 2020). Therefore, the incidence of pulmonary fibrosis is expected to further increase in the years to come and thus, the demand for effective therapy options will continue to rise.

Pulmonary fibroblasts are recognized as the major source of extracellular ECM proteins like collagens and fibronectin (Pardo and Selman 2016; Peyser et al. 2019). Innate immune cells such as macrophages and platelets release TGF-β1 and thereby induce migration of activated fibroblasts to the injured lung epithelium (Jiang et al. 2014). Initially, this process leads to beneficial ECM secretion and wound healing (Wilson and Wynn 2009). However, sustained activation of fibroblasts by TGF-β1 results in fibroblast-to-myofibroblast transition (FMT) characterized by expression of α-smooth muscle actin (α-SMA) and overproduction of collagens and fibronectin (Habiel and Hogaboam 2017; Lekkerkerker et al. 2012). Hence, TGF-β1-promoted FMT is key in the development and progression of pulmonary fibrosis and cellular mechanisms that regulate ECM production or secretion from fibroblasts became the focus of pulmonary research (Lin et al. 2020).

The fibrinolytic system is a major regulator of the ECM and composed of the proteolytic enzyme plasmin, its precursor plasminogen (Plg) and plasminogen activators (PA) (Deryugina and Quigley 2012). There are two types of PA: urokinase (uPA) and tissue type PA. In wounded tissues plasmin is primarily generated by uPA (Andreasen et al. 2000). Most components of the plasmin system are secreted proteins that act extracellularly. Plg and uPA, however, are bound to the plasma membrane by cognate receptors: PlgR and uPAR (Felez et al. 1991; Miles et al. 1991; Plow et al. 1986, 2012). Thus, active plasmin can be generated either in the extracellular fluid or in close association to the cell

membrane (Deryugina and Quigley 2012; Irigoyen et al. 1999). Plasmin has been shown to degrade major components of the ECM such as collagens and fibronectin, suggesting that stimulation of plasmin activity is a promising strategy for the treatment of pulmonary fibrosis (Deryugina and Quigley 2012; Papp et al. 1987; Pins et al. 2000). Activity of PAs is counterbalanced by the product of the *SERPINE1* gene: the plasminogen activator inhibitor type 1 (PAI-1). PAI-1 is also secreted from pHPF and reported to inhibit soluble and cell-associated PA activity (Bharadwaj et al. 2021). Overexpression of *SERPINE1* and concomitant decreased plasmin activity is strongly associated with pulmonary fibrosis (Ghosh and Vaughan 2012; Huang et al. 2012; Lin et al. 2020; Shioya et al. 2018; Zhang et al. 2012).

TGF-β1 activates transmembrane receptors of the serine/threonine kinase receptor family, which phosphorylate SMAD proteins and trigger their translocation into the nucleus where they induce SMAD-responsive genes in pulmonary fibroblasts (Heldin and Moustakas 2016). This process enhances ECM deposition via two pathways. First, SMADs directly induce transcription of fibronectin/collagens and thus promote ECM production (Vindevoghel et al. 1998; Zhao et al. 2002). Second, SMADs inhibit ECM degradation by activation of the *SERPINE1* gene and concomitant reduction of plasmin activity (Hua et al. 1999; Song et al. 1998). Thus, TGF-β1 is a key player in the propagation of pulmonary fibrosis and inhibition of TGF-β1 signaling in pulmonary fibroblasts is a promising therapeutic strategy (Fernandez and Eickelberg 2012; Gu et al. 2007; Phan et al. 2005; Saito et al. 2018a, b; Song et al. 1998; Walker et al. 2019). Of note, mitigating TGF-β1-dependent ECM production may be useful to prevent fibrosis or progression at early stages. Additionally, increasing plasmin activity may degrade preformed ECM and thus eventually lead to tissue repair at late stages of the disease (Staab-Weijnitz 2021).

The superfamily of mammalian transient receptor potential (TRP) channels represents a multifunctional group of proteins that consists of 27 members in humans (Wu et al. 2010). In recent years, TRP proteins have attracted much interest as potential drug targets for a wide range of pathological conditions (Koivisto et al. 2022). TRPM7 is a bifunctional protein comprising a cation channel and a serine/threonine kinase moiety which are covalently linked (Monteilh-Zoller et al. 2003; Nadler et al. 2001; Nadolni and Zierler 2018; Ryazanova et al. 2004). TRPM7 is ubiquitously expressed and involved in fundamental cellular processes such as cell survival, proliferation, apoptosis and migration (Fleig and Chubanov 2014; Paravicini et al. 2012). In MRC5 cells, a fetal human lung fibroblast cell line, down-regulation of the TRPM7 protein was shown to decrease TGF-β1-induced collagen and α-SMA synthesis (Yu et al. 2013). However, the molecular and cellular underpinnings of these effects have remained elusive and possible effects

of TRPM7 activity on the plasmin system have not been addressed yet. Likewise, it is still unknown whether TRPM7 blockers are able to decrease ECM and/or α-SMA protein levels in pHPF. Interestingly, TRPM7 kinase directly phosphorylates SMAD-2 and enhances acute TGF-β1-induced SMAD-2 activation in isolated T-lymphocytes, offering a potential explanation for the positive effects of TRPM7 on TGF-β1-induced collagen expression observed in MRC5 cells (Romagnani et al. 2017). Furthermore, TRPM7 promotes the development of heart and kidney fibrosis, pointing to a possible role of TRPM7 in signaling pathways leading to fibrotic processes (Du et al. 2010; Rios et al. 2020; Suzuki et al. 2020).

Based on the current literature, we postulated that small-molecule TRPM7 blockers may represent new pulmonary fibrosis therapeutics. To this end, we aimed at identifying a mechanistic link between TRPM7, TGF-β1 and the plasmin system in pHPF. We directly measured plasmin activity using a specific fluorogenic substrate for plasmin and analyzed the effects of two unrelated TRPM7 blockers on untreated and TGF-β1-treated pHPF. We determined protein levels of PAI-1, α-SMA, collagen and fibronectin by Western-blot analysis and Sircol™ assays under identical conditions. Finally, we monitored the effects of TRPM7 blockade on TGF-β1-induced SMAD signaling and *SERPINE1,* fibronectin (*FN1*) and alpha-1 type I collagen (*Col1A1*) mRNA expression.

Materials and methods

Chemicals and antibodies

N-[(1*R*)-1,2,3,4-Tetrahydro-1-naphthalenyl]-1*H*-benzimidazol-2-amine hydrochloride (NS-8593), apamin, human transforming growth factor (TGF-β1; T7039), plasminogen, α2-antiplasmin and D-Val-Leu-Lys-7-amido-4-methylcoumarin were all from SigmaAldrich. Waixenicin A was isolated as described previously (Zierler et al. 2011). For protein detection specific antibodies against PAI-1 (abcam, ab66705), fibronectin (abcam, ab2413), smooth muscle actin (abcam, ab5694), collagen-1 (abcam, ab34710), p-SMAD-2 (cell signaling, clone 138D4, #3108), SMAD-3 (cell signaling, clone C67H9, #9523), SMAD-2 (cell signaling, clone D43B4, #5339), SDHA (abcam, ab14715) and histone H3 (abcam, ab1791) were used.

Cell culture

pHPF were purchased from PromoCell (C-12360) and cultured using fibroblast growth medium II provided by the manufacturer. Data obtained with cells from two different donors were combined (a 79 and a 44-year-old female).

Cells were used between passage 2 and 10. In Fig. 2d and Suppl. Fig. S1, data obtained with pHPF from Lonza (CC-2512) are shown. These cells were also cultured in fibroblast growth medium II provided by the manufacturer and derived from a male donor 37 years of age.

Stimulation procedure

Data shown in Figs. 1–5 were obtained after stimulation of the cells for 24 h in the presence of 5% FCS. In Figs. 6–10, cells were stimulated for 48 h with 0.5% FCS. TGF-β1 treatment of pHPF for 48 h with reduced FCS levels has been established to induce FMT (Malmstrom et al. 2004; Staab-Weijnitz et al. 2015; Thannickal et al. 2003). NS-8593 was dissolved in DMSO (50 mM final), waixenicin A (1 mM) in ethanol and plasminogen (25 mg/ml final) in glycerol. Thus, in each experiment appropriate carrier controls were used. Apamin and TGF-β1 were dissolved in water.

Plasmin activity

D-Val-Leu-Lys-7-amido-4-methylcoumarin (D-Val-Leu-Lys-AMC) was used as a plasmin substrate (Gyzander and Teger-Nilsson 1980; Kato et al. 1980; Li et al. 2018; Schuliga et al. 2011; Wu et al. 2019). D-Val-Leu-Lys-AMC is a selective fluorogenic substrate for plasmin and enzymatic activity is quantified by release of the free AMC fluorophore, which is excited at 360–380 nm and emits light at 440–460 nm. In detail, ~5,000 pHPF were seeded per cavity of a 96-well plate 24 h before the experiment. Cells were stimulated or not with 50 µl medium for the indicated periods of time. Because active plasmin remains first associated to the cell surface and is then subsequently secreted (Deryugina and Quigley 2012), we measured plasmin activity in two cell fractions. To detect secreted plasmin activity, 10 µl of the supernatant was transferred to a new 96-well plate and added to 90 µl Tris/HCl (20 mM, pH 7.4) containing 55 µM of D-Val-Leu-Lys-AMC. For detection of cell and cell-associated plasmin activity, the remaining cell culture medium was aspirated and 50 µL Tris/HCl (20 mM, pH 7.4) with 50 µM D-Val-Leu-Lys-AMC directly added to the cells. After 3 h incubation at 37 °C, fluorescence was measured using a FLUOstar® Omega plate reader. To normalize fluorescence signals to the total protein amount, a second 96-well plate was prepared, treated equally and protein amount monitored by sulforhodamine B (SRB) colorimetric assay (Vichai and Kirtikara 2006). SRB signals were calibrated to the cell number. Plasmin activity was determined as the ratio of the RLU values of the D-Val-Leu-Lys-AMC detection and the OD values of the SRB measurement.
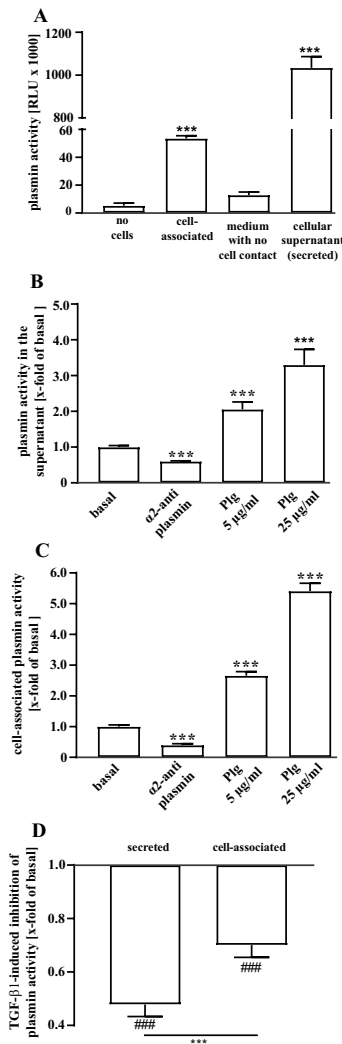
Fig. 1 Detection of plasmin activity in living pHPF by D-Val-Leu-Lys-AMC. **a** D-Val-Leu-Lys-AMC (50 μM) was incubated with unstimulated pHPF, without any cells or with fresh medium for 3 h at 37 °C and secreted and cell-associated fluorescence measured. Bars represent SEM of RLU, $n=10$. **b** secreted and **c** cell-associated plasmin activity was measured after incubating the cells with Plg (5 or 25 μg/ml) for 24 h at 37 °C. α_2-antiplasmin (500 nM) was co-administrated with D-Val-Leu-Lys-AMC. Bars represent SEM of RLU, $n=4$. **d** Plasmin activity was measured after stimulation of the cells with TGF-β1 (2 ng/ml) for 24 h. Bars represent SEM of x-fold of basal values, $n=10$. Statistical analysis was performed using one-way ANOVA (**a**–**c**) followed by Tukey's post-test or one- and two-sample t test (in **c**) using the GraphPad prism software 9.1. Asterisks indicate in **a** significant differences to "no cells", in **b** and **c** to basal and in **d** between the cellular fractions. Hash signs indicate significant differences to 1.0
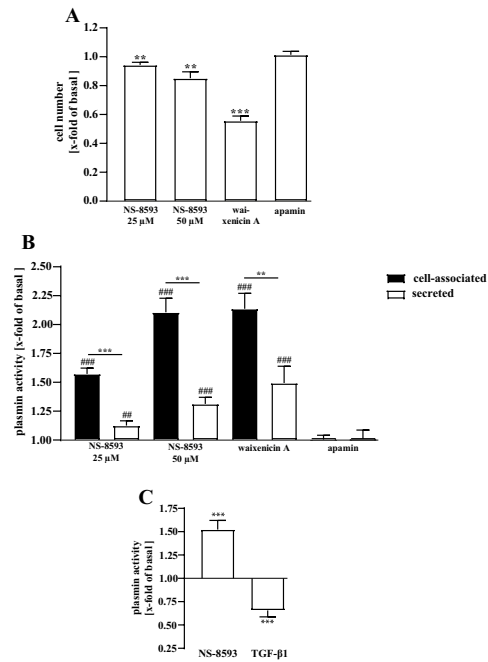
Fig. 2 Detection of plasmin activity in living pHPF. **a** pHPF were stimulated with NS-8593 (25 or 50 μM), with waixenicin A (10 μM) or apamin (100 nM) for 24 h and cell numbers determined using SRB. For NS-8593 corresponding DMSO and for waixenicin A ethanol controls were used. Bars represent SEM of x-fold of basal (DMSO or ethanol) values, $n=4$–6. **b** pHPF were stimulated with NS-8593 (25 or 50 μM), with waixenicin A (10 μM) or apamin (100 nM) for 24 h and cell-associated and secreted plasmin activity determined. For NS-8593 corresponding DMSO and for waixenicin A ethanol control were used. Bars represent SEM of x-fold of basal values, $n=4$–6. **c** Cell-associated plasmin activity was measured after stimulation of the cells with TGF-β1 (2 ng/ml) or NS-8593 (25 μM) for 24 h. Bars represent SEM of x-fold of basal values, $n=4$. In **b**, data obtained with two distinct donors provided from PromoCell (C-12360) and in **c**, from one donor provided by Lonza (CC-2512) are shown. Statistical analysis was performed using one-sample t test or one-way ANOVA followed by Tukey´s post-test using the Graph-Pad prism software 9.1. Asterisks indicate in **b** significant differences between the cellular fractions and in **a** and **c** to 1.0. In **b** hash signs indicate significant differences to 1.0

TRPM7 down-regulation with siRNA

To down-regulate *TRPM7* expression, two pre-designed siR-NAs from Ambion (AM16708: ID103360 and ID104677) were incorporated into pHPF by Lipofectamine RNAiMAX Transfection Reagent (#13778100, Thermo Fisher), and data compared to cells transfected with a control siRNA (AM4611). For each cavity of a 96-well plate, 1 pmol siRNA

was mixed with 0.3 µl lipofectamine in Opti-MEM medium (#31985062, Thermo Fisher). After 30 min at RT, 10 µl were added to the bottom of the well. ~ 10,000 cells were added to the siRNA/lipofectamine mixture in growth medium (90 µl). After 3 days in culture, cells were stimulated and plasmin activity measured as described above. As a control, 100,000 cells were seeded on one cavity of a 6-well plate and total RNA extracted after 3 days. TRPM7 mRNA was analyzed as described under *mRNA detection by qRT-PCR*.

Protein detection by Western blotting

Cells were seeded on 6-well plates (~ 100,000/well), cultured for one day and stimulated for the indicated periods of time. To detect expression of secreted proteins, supernatants were transferred to fresh tubes and lysed with Laemmli buffer (fourfold). The corresponding cell fraction was lysed by directly adding Laemmli buffer (onefold) to the 6-well plates. Lysates were subjected to SDS-PAGE (10%) and proteins transferred to nitrocellulose (Amersham Protran™ 0.45 µm, #10600002) by western blotting. After adding the primary antibody over night at 4 °C, blots were washed and incubated with the corresponding HRP-conjugated secondary antibody (anti-rabbit 1:4000, anti-mouse 1:2000) for 1 h at RT. After intensive washing immune reactivity was detected by monitoring the ECL-dependent light emission with a chemiluminescence detection system (Peqlab, Germany). Resulting signals were quantified by densitometry (ImageJ) and ratios of the protein of interest and the loading control calculated.

Detection of soluble collagen

~ 500,000 cells were seeded on 10-cm dishes 24 h before stimulation of the cells. Afterwards collagen levels were determined using the Sircol™ soluble collagen assay from biocolor in accordance with the manufacturer´s protocol.

Firefly luciferase reporter gene assay

To monitor SMAD activation, the pCAGA-luc reporter construct containing the SMAD-3/4 sensitive part of the human *SERPINE1* promotor was used (Dennler et al. 1998). Activation of YAP/TAZ was monitored by the 8xGTIIC-luciferase plasmid (#34615) obtained from addgene (Dupont et al. 2011). Plasmids were transfected into pHPF via electroporation using the Neon® transfection system from Invitrogen according to the manufacturer´s protocol. Briefly, for each electroporation step, ~ 250,000 cells together with 5 µg of the corresponding plasmid cDNA were challenged 3 times with 1650 V for 10 ms. Cells were immediately placed on 96-well plates (~ 20,000 cell per well) and cultured for 24 h. After stimulation, cells were lysed in 50 µl of lysis buffer (25 mM

Tris/HCl pH 7.4, 4 mM EGTA, 8 mM $MgCl_2$, 1 mM DTT and 1% Triton-X-100) and a volume of 40 µl transferred to white-bottomed, 96-well plates. Luciferase activity was measured after automatically injecting a luciferase substrate (20 µl) from Promega (E1500) using a FLUOstar® Omega plate reader.

mRNA detection by qRT-PCR

~ 150,000 cells were seeded per cavity of a 6-well plate. After 24 h cells were stimulated or not for the time indicated and stimulation terminated by rapid cooling on ice. Total RNA was isolated using the Trizol® reagent (Invitrogen, Darmstadt, Germany) according to the manufacturer´s instructions. First strand synthesis was carried out with oligo(dT)$_{18}$ primer using 1 µg of total RNA and the RevertAid™ H Minus First Strand cDNA Synthesis Kit (Fermentas, Sankt-Leon Roth, Germany). qRT-PCR was done using the LightCycler® 480 SybrGreen I Master Mix kappa (Roche, Mannheim, Germany). Exon-spanning primer pairs were used at a final concentration of 1 µM each. Final assay volume was 20 µl and first strand synthesis reaction was diluted 1:20 or 1:50. A LightCycler® 480 II (Roche) was used with the following conditions: initial denaturation for 2 min at 94 °C, 55 cycles of 94 °C for 10 s, 55 °C for 10 s and 72 °C for 10 s. Primer design was performed using the ProbeFinder (version 2.53) provided on the website of Roche Life Science. Crossing points (Cp) were determined by the software supplied with the LightCycler® 480 and data analysed by the ΔΔCp method ($2^{-((\text{gene}–ACTB)_{\text{TGF-}\beta1/\text{TRPM7 siRNA}} - (\text{gene}–ACTB))_{\text{basal/control siRNA}}}$). Primer sequences were as follows: *SERPIN1*-forward: 5′-AAGGCACCTCT-GAGAAC TTCA-3′, *SERPIN1*-reverse: 5′-CCCAGGACTAGGCAG GTG-3′, *ACTB*-forward: 5′-CTAAGGCCAACCGTGAAA AG-3′, *ACTB*-reverse: 5′-ACCAGAGGCATACAGGGA CA-3′, *TRPM7*-forward: 5′-TTGACATTGCCAAAAATC ATGT-3′, *TRPM7*-reverse: 5′-CTTGTCCAAGG-ATCCAA CC-3′, *FN1*-forward: 5′-CCGACCAGAAGTTTGGGT TCT-3′, *FN1*-reverse: 5′-CAATGC-GGTACATGACCC CT-3′, *COL1A1*-forward: 5′-TACAGAACGGCCTCAGGT ACAA-3′, *COL1A1*-reverse: 5′-ACAGATCACGTCATC GCACA-AC-3′.

Quantification and statistical analysis

Values represent the mean ± SEM of three to eight independent experiments. Statistical analysis was performed using one- or two-sample student's *t* test, one-way or two-way ANOVA followed by Tukey's post-test using the GraphPad prism software 9.1. Shapiro–Wilk tests were performed to ensure normal distribution of the data sets. One symbol indicates a *p*-value of ≤ 0.05, two of ≤ 0.01 and three of ≤ 0.001.

Results

TRPM7 blockers enhance constitutive plasmin activity of pHPF

Despite the importance of the plasmin system for the development of pulmonary fibrosis, plasmin activity has not been systematically investigated directly in pHPF. Hence, we first aimed at establishing a protocol that allows reliable measurements of plasmin activity in cultured pHPF. We used D-Val-Leu-Lys-AMC as a plasmin substrate (Gyzander and Teger-Nilsson 1980; Kato et al. 1980; Li et al. 2018; Wu et al. 2019). D-Val-Leu-Lys-AMC is a selective fluorogenic substrate for plasmin, and enzymatic activity is quantified by the release of the free AMC fluorophore. Indeed, when D-Val-Leu-Lys-AMC was incubated either with an aliquot of pHPF supernatant (secreted) or directly with cells (cell-associated), fluorescence signals were profoundly increased compared to the same amount of substrate, which had not been in contact with any cell fraction (Fig. 1a). Further, medium, which had never been in contact with cells, showed no significant fluorescence increase, indicating that plasmin activity in the secreted fraction was indeed produced by pHPF (Fig. 1a). To test whether this increase in fluorescence could be attributed to plasmin activity, we analyzed effects of the plasmin inhibitor α2-antiplasmin or the plasmin precursor Plg (Moroi and Aoki 1976). As indicated in Fig. 1b, c, the plasmin inhibitor significantly decreased fluorescence signals generated by D-Val-Leu-Lys-AMC and Plg enhanced these signals in the secreted and the cell-associated fraction. Thus, in both fractions there was a clear-cut correlation between D-Val-Leu-Lys-AMC-based fluorescence and plasmin activity. Based on the enhancing effects of TGF-β1 on PAI-1 protein levels, it is expected that TGF-β1 decreases plasmin activity (Horowitz et al. 2008; Schuliga et al. 2011; Song et al. 1998). Thus, to finally validate whether this assay would be able to monitor the dynamic regulation of plasmin activity in pHPF, we treated cells for 24 h with TGF-β1. In previous studies using airway smooth muscle cells or IMR-90 fibroblasts, exogenous Plg was added to increase basal plasmin activity and thus to detect the inhibitory effects of TGF-β1 (Horowitz et al. 2008; Schuliga et al. 2011). As we found very robust basal signals without adding exogenous Plg to pHPF (Fig. 1a), we did not use additional Plg. As expected, TGF-β1 reduced D-Val-Leu-Lys-AMC-dependent fluorescence to 0.48 ± 0.04 fold of basal in the secreted and to 0.7 ± 0.05 in the cell-associated fraction (Fig. 1d), indicating that this protocol reliably monitors plasmin activity of living pHPF.

NS-8593 has been identified as a small-molecule TRPM7 blocker (Chubanov and Gudermann 2020). Due to the fundamental role of TRPM7 in cell homeostasis, prolonged inhibition of TRPM7 activity has been proposed to induce some cell death under certain circumstances (Chubanov et al. 2012). Thus, we first tested how pHPF treatment with 25 or 50 μM of NS-8593 for 24 h affects cell numbers. As shown in Fig. 2a, 25 μM of the TRPM7 blocker reduced the number of pHPF to 0.94 ± 0.02 fold of basal and 50 μM to 0.85 ± 0.04. Thus, overall cytotoxicity of NS-8593 was rather moderate. Next, we asked whether there is a possible link between TRPM7 and plasmin activity. To this end, we treated cells with both NS-8593 concentrations for 24 h, measured plasmin activity in both fractions and normalized the data to the cell number. An increase in plasmin activity of 2.1 ± 0.6 fold of basal was found in the cell-associated and of 1.3 ± 0.6 in the secreted fraction for 50 μM and of 1.6 ± 0.3 and 1.2 ± 0.2, respectively, for 25 μM NS-8593 (Fig. 2b). NS-8593 blocks TRPM7 but also SK potassium (KCa2.1–2.3) channels (Chubanov et al. 2012). Therefore, we used the selective KCa2.1–2.3 blocker apamin as a control (Lamy et al. 2010). Apamin had no effects at all on plasmin activity (Fig. 2b), strongly suggesting that TRPM7 and not KCa2.1–2.3 channels affect the plasmin system in pHPF. To support this notion, we used a second structurally unrelated TRPM7 blocker. Waixenicin A, a xenicane diterpenoid from the Hawaiian soft coral *Sarcothelia edmondsoni* has also been reported to block TRPM7 activity (Zierler et al. 2011). 10 μM waixenicin A reduced the number of pHPF to 0.56 ± 0.03 fold of basal, indicating significant higher cytotoxicity of waixenicin A compared to NS-8593 (Fig. 2a). However, Waixenicin A increased, when normalized to the cell number, cell-associated plasmin activity to 2.2 ± 0.1 and secreted activity to 1.5 ± 0.2 fold of basal (Fig. 2b). Thus, it appeared that TRPM7 activity restrains plasmin activity in pHPF. Accordingly, two structurally unrelated TRPM7 blockers reverse this process and enhance plasmin activity.

Data presented so far were obtained using pHPF derived from two distinct donors provided by the same supplier. We next used cells from a third donor and an independent second provider, to clarify whether the observed effects of TRPM7 blockade represent a common feature of cultured pHPF. As shown in Fig. 2c, a significant increase in plasmin activity $(1.5 \pm 0.1$ of basal) induced by NS-8593 (25 μM) was also detectable with cells from the third donor, indicating that the functional link between TRPM7 blockers and plasmin activity is not dependent on the origin of fibroblasts. In line with this notion, TGF-β1-induced reduction in plasmin activity was also very similar in all cell pools (Figs. 1a, 2c). Finally, we aimed at defining the target of NS-8593 in pHPF. To this end, we introduced human TRPM7-specific siRNAs into pHPF and compared resulting cell numbers and TRPM7 mRNA levels to cells transfected with a control siRNA. As
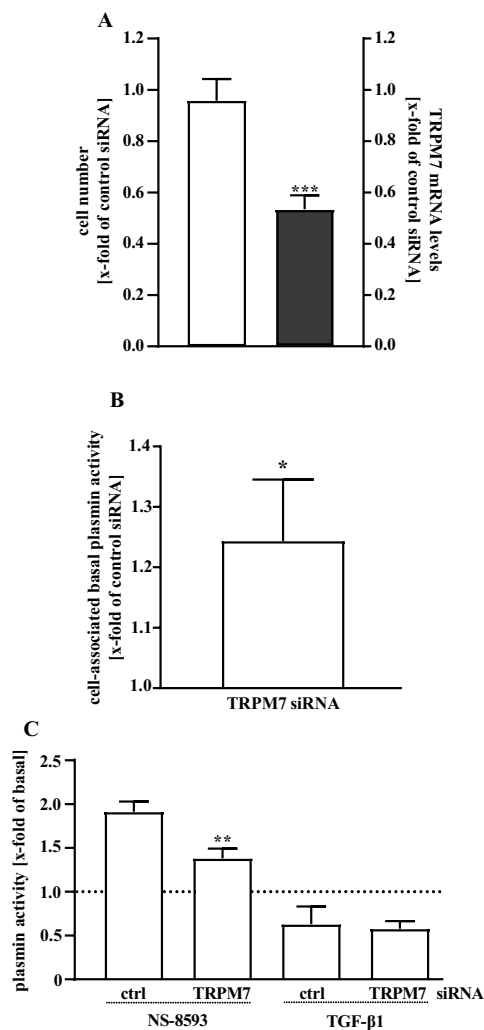
A

B

C

Fig. 3 Detection of plasmin activity in living pHPF. pHPF were transfected with a pool of two distinct siRNAs against TRPM7 or a random control siRNA. In **a** 72 h post transfection of TRPM7 specific or control siRNAs cell numbers were determined using SRB (left *y*-axes) or TRPM7 mRNA detected by qRT-PCR (right *y*-axes). In **b** plasmin activity of unstimulated cells was determined. Bars represent SEM of x-fold of the control siRNA, $n = 4$. **c** 48 h post transfection pHPF were stimulated with TGF-β (2 ng/ml) or NS-8593 (25 µM) for 24 h and secreted (TGF-β1) or cell-associated (NS-8593) plasmin activity determined. Bars represent SEM of x-fold of basal values, $n = 4$. Statistical analysis was performed using one-sample *t* test or one-way ANOVA followed by Tukey s post-test using the GraphPad prism software 9.1. Asterisks indicate in **a** and **b** significant differences to 1.0 and in **c** between control and TRPM7 siRNA

shown in Fig. 3a, TRPM7 siRNAs did not significantly affect cell numbers of pHPF but decreased TRPM7 mRNA levels to 0.53 ± 0.05 fold of basal TRPM7 levels detected in the presence of the control siRNA. TRPM7 siRNA-induced reduction of TRPM7 mRNA was accompanied with slightly increased basal plasmin activity (Fig. 3b), further substantiating the notion that TRPM7 restrains plasmin activity in pHPF. Furthermore, effects of NS-8593 but not of TGF-β1 on plasmin activity were significantly reduced in cells transfected with TRPM7 specific siRNAs (Fig. 3c), reinforcing the concept that the TRPM7 protein is the cellular target that links NS-8593 to the plasmin system.

TRPM7 blockers decrease PAI-1 and fibronectin protein levels in pHPF

Dynamic regulation of the *SERPINE1* gene leads to altered PAI-1 protein levels and is a common plasmin activity regulating mechanism in pHPF (Ghosh and Vaughan 2012). Thus, we postulated that enhanced plasmin activity following TRPM7 blockade might be associated with reduced PAI-1 protein levels. Western-blot data shown in Fig. 4 clearly indicate that incubation of pHPF with NS-8593 (25 µM) or waixenicin A (10 µM) for 24 h inhibited basal PAI-1 levels in the cell-associated and secreted fraction. Next, we tested whether levels of fibrosis-relevant ECM proteins such as fibronectin correlate with the observed increase in plasmin activity ensuing TRPM7 blockade. Both blockers significantly reduced fibronectin levels in the cell-associated fraction (Fig. 5a, b). Hence, we identified TRPM7 blockers as new experimental tools for the regulation of plasmin activity and fibronectin levels of untreated, inactive pHPF.

TRPM7 blockade inhibits TGF-β1-induced fibroblast-to-myofibroblast transition

TGF-β1-treated, activated pHPF undergo a transition to myofibroblasts characterized by increased protein levels of α-SMA and PAI-1. Further, myofibroblasts secrete high amounts of ECM proteins such as collagens and fibronectin (Habiel and Hogaboam 2017; Lekkerkerker et al. 2012). When cultured pHPF were stimulated with TGF-β1 for 48 h under reduced serum concentrations (0.5%), the entire set of FMT markers was detectable. α-SMA levels increased within the cells (Fig. 6a) and the amount of PAI-1, fibronectin and collagen-1 proteins robustly rose in the cell-associated and secreted fraction (Fig. 6b–d). Next, we wondered whether TRPM7 blockade would counteract FMT. Thus, we left pHPF untreated or challenged them with NS-8593 (25 µM) or TGF-β1 alone or with both ligands for 48 h. The TRPM7 blocker significantly reduced α-SMA levels in untreated and TGF-β1-treated cells (Fig. 7a), suggesting that TRPM7 inhibition prevents FMT. In line with this notion,
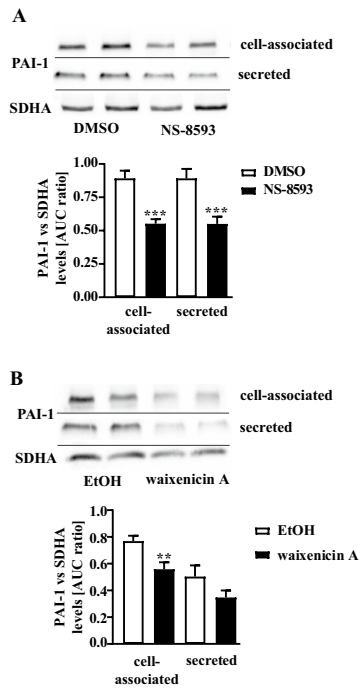
🙋 Springer

A

PAI-1 — cell-associated
— secreted

SDHA

DMSO   NS-8593

B

PAI-1 — cell-associated
— secreted

SDHA

EtOH   waixenicin A

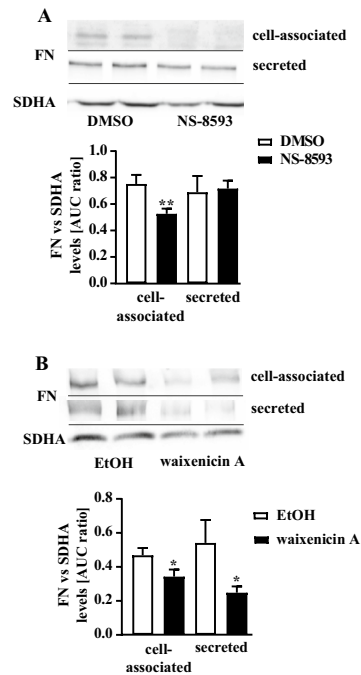**Fig. 4** Detection of PAI-1 protein levels in pHPF. **a** cells were stimulated with NS-8593 (25 µM) and **b** with waixenicin A (10 µM) for 24 h and protein amount of PAI-1 or SDHA (loading control) determined. SDHA control of the cellular fraction was also used for the secreted fraction. Blots of the cellular fraction were cut in half and the upper part used for detection of PAI-1 and the lower part for SDHA. Resulting signals were quantified by densitometry and AUC ratios between PAI-1 and SDHA calculated. One set of representative blots is shown. Bars represent SEM of % AUC ratios, $n=4$. Statistical analysis was performed using one-way ANOVA followed by Tukey's post-test using the GraphPad prism software 9.1. Asterisks indicate significant differences between basal (DMSO or EtOH) and the TRPM7 blocker

A

FN — cell-associated
— secreted

SDHA

DMSO   NS-8593

B

FN — cell-associated
— secreted

SDHA

EtOH   waixenicin A

Fig. 5 Detection of fibronectin (FN) protein levels in pHPF. **a** cells were stimulated with NS-8593 (25 µM) and **b** with waixenicin A (10 µM) for 24 h and protein amount of FN or SDHA (loading control) determined. SDHA control of the cellular fraction was also used for the secreted fraction. Blots of the cellular fraction were cut in half and the upper part used for detection of FN and the lower part for SDHA. Resulting signals were quantified by densitometry and AUC ratios between FN and SDHA calculated. One set of representative blots is shown. Bars represent SEM of % AUC ratios, $n=3$. Statistical analysis was performed using one-way ANOVA followed by Tukey's post-test using the GraphPad prism software 9.1. Asterisks indicate significant differences between basal (DMSO or EtOH) and the TRPM7 blocker

NS-8593 reduced basal and TGF-β1-promoted fibronectin levels in the cell-associated fraction (Fig. 7b) and strongly reduced the amount of collagen-1 in both fractions under basal conditions (Fig. 7c). However, in TGF-β1-treated cells no significant effect of NS-8593 on collagen-1 secretion was observed, despite a strong tendency of the TRPM7 blocker to inhibit TGF-β1-induced collagen-1 levels in the supernatant. Hence, we used a second approach (Sircol™ soluble collagen assay) to detect collagens in pHPF cultures. Data obtained with the Sircol™ assay revealed highly significant inhibition of TGF-β1-induced collagen secretion after TRPM7 blockade (Fig. 7d). Next, we analyzed whether the effects of NS-8593 on TGF-β1 might also occur on the level

of the plasmin system. When basal *SERPINE1* expression was analyzed in the cell-associated and secreted fraction by Western blot, no secreted PAI-1 protein was detectable (Fig. 8a). Cell-associated basal PAI-1 levels were significantly inhibited after TRPM7 blockade by ~70% (Fig. 8a). TGF-β1-treatment increased PAI-1 levels in the cell-associated and the secreted fraction and co-administration of NS-8593 significantly reduced the amount of PAI-1 protein in the secreted fraction (Fig. 8a). When plasmin activity was monitored, NS-8593 alone enhanced cell-associated enzymatic activity to 2.5 ± 0.2 fold of basal and secreted activity to 1.3 ± 0.1 fold (Fig. 8b). Co-application of NS-8593 elevated TGF-β1-mediated inhibition of plasmin activity in the

Fig. 6 Detection of FMT markers in pHPF treated with TGF-β1. pHPF were stimulated with TGF-β1 (2 ng/ml) for 48 h. Protein amount of α-SMA in **a,** of PAI-1 in **b,** of FN in **c** and of collagen-1 (Coll-1) in **d** was determined in the cell-associated and secreted fraction by western blotting. SDHA control of the cellular fraction was also used for the secreted fraction. Blots of the cellular fraction were cut in half and the upper part used for detection of α-SMA, PAI-1, FN or Coll-1 and the lower part for SDHA. Resulting signals were quantified by densitometry and AUC ratios of α-SMA, PAI-1, FN or Coll-1 and SDHA calculated. One set of representative blots is shown. Bars represent SEM of % AUC ratios, $n = 3$–5. Statistical analysis was performed using one-way ANOVA followed by Tukey's post-test using the GraphPad prism software 9.1. Asterisks indicate significant differences between basal and TGF-β1
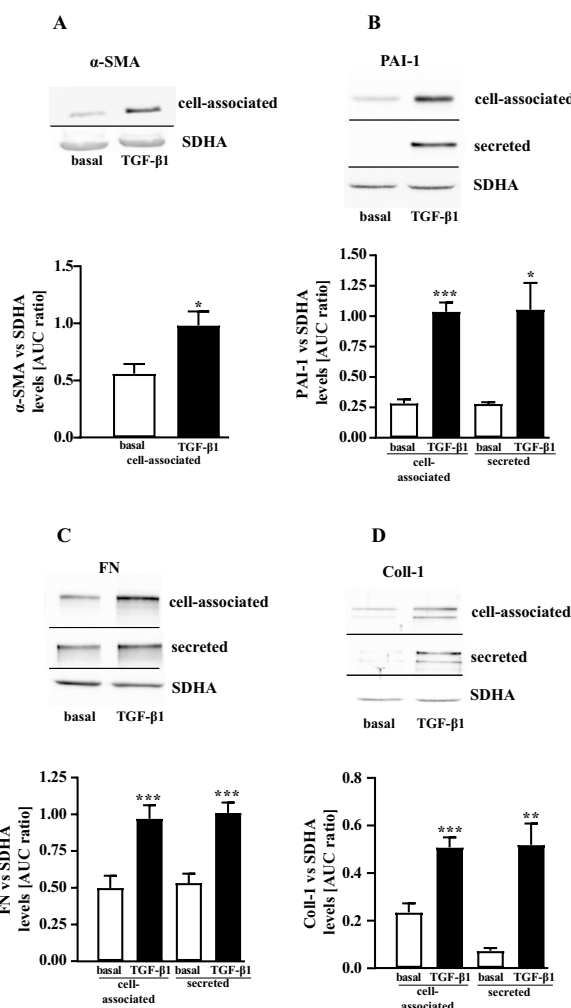
secreted fraction from 0.15 ± 0.03 fold of basal to 0.32 ± 0.06 (Fig. 8c). Thus, TRPM7 blockade also affected the plasmin system in TGF-β1-treated, activated pHPF.

TRPM7 blockade inhibits TGF-β1-induced SMAD signaling in pHPF

Phosphorylation of the transcription factor SMAD-2 is crucial for TGF-β1-promoted FMT (Kawarada et al. 2016). Accordingly, treatment of pHPF with TGF-β1 for 48 h induced SMAD-2 phosphorylation (Fig. 9a). In line with its inhibitory effects on TGF-β1-induced FMT, NS-8593 almost completely abolished TGF-β1-promoted phosphorylation of SMAD-2 (Fig. 9a), whereas total SMAD-2 protein levels were unaffected (Fig. 9b). Previous studies revealed that sustained stimulation of MRC5 cells or pHPF with TGF-β1 reduced total protein levels of SMAD-3 (Breton et al. 2018; Staab-Weijnitz et al. 2015). Accordingly, we observed a profound reduction of SMAD-3 levels after TGF-β1 stimulation of pHPF (Fig. 9c). Interestingly, NS-8593 also significantly diminished SMAD-3 levels (Fig. 9c), indicative of hitherto unappreciated positive effects of TRPM7 activity on total SMAD-3 protein levels. Overall, these data indicate functional interactions between TRPM7 activity and

Fig. 7 Detection of FMT markers in pHPF co-treated with TGF-β ▶ and NS-8593. pHPF were stimulated with TGF-β1 (2 ng/ml) or NS-8593 (25 μM) for 48 h alone or together with both ligands. Protein amount of α-SMA in **a,** of FN in **b** and of collagen-1 (Coll-1) in **c** was determined in the cell-associated and secreted fraction by western blotting. SDHA control of the cellular fraction was also used for the secreted fraction. Blots of the cellular fraction were cut in half and the upper part used for detection of α-SMA, FN or Coll-1 and the lower part for SDHA. Resulting signals were quantified by densitometry and AUC ratios of α-SMA, FN or Coll-1 and SDHA calculated. One set of representative blots is shown. Bars represent SEM of % AUC ratios (NS-8593) or x-fold of basal values (TGF-β1), $n = 3–5$. In **d**, pHPF were stimulated with TGF-β1 (2 ng/ml) alone or together with NS-8593 (25 μM) for 48 h and secreted collagen levels determined by Sircol™ soluble collagen assay. Bars represent SEM of OD_{555} values, $n = 5$. Statistical analysis was performed using one-way ANOVA followed by Tukey's post-test using the GraphPad prism software 9.1. Asterisks indicate significant differences between DMSO and NS-8593

TGF-β1-induced SMAD signaling in pHPF. To analyze whether these interactions affect expression of the *SER-PINE1* gene, we took advantage of a previously established reporter gene construct containing the SMAD-3/4 sensitive part of the *SERPINE1* promotor (Dennler et al. 1998). As shown in Fig. 9d, NS-8593 strongly inhibited TGF-β1-induced SMAD-dependent reporter activation. TGF-β1 does not only signal via SMAD proteins but also via SMAD-independent activation of transcription factors of the YAP/TAZ family (Miranda et al. 2017). Of note, inhibitory actions of TRPM7 blockade on TGF-β1 signaling were not observed when TGF-β1-induced activation of a YAP/TAZ sensitive reporter was analyzed (Fig. 9e). Finally, we analyzed whether NS-8593-mediated blockade of TGF-β1-induced SMAD signaling is sufficient to inhibit promoter activity of SMAD-dependent genes by monitoring mRNA expression of the *FN1*, the *COL1A1* and the *SERPINE1* gene after 24 and 48 h. TGF-β1 induced expression of all three genes at both time points, but whereas *FN1* and *COL1A1* mRNA levels rose linearly, *SERPINE1* expression peaked after 24 h and sunk afterwards (Fig. 10). Of note, co-treatment with NS-8593 significantly inhibited TGF-β1-induced *SERPINE1* expression at both time points (Fig. 10a) but had no inhibitory effect on *FN1* or *COL1A1* expression (Fig. 10b, c), indicating that absence of TRPM7 activity weakened rather selectively TGF-β1-promoted activation of the *SERPINE1* gene.

Discussion

Excessive ECM deposition in the lung eventually leads to pulmonary fibrosis and death. TGF-β1-induced SMAD activation enhances ECM deposition by increasing its production and reducing its degradation (Fernandez and Eickelberg 2012; Gu et al. 2007; Phan et al. 2005; Saito et al. 2018a, b; Song et al. 1998; Walker et al. 2019). This process is beneficial for wound healing, but prolongation eventually leads to pathophysiological conditions such as pulmonary fibrosis. Here, we report that activity of the TRPM7 protein supports TGF-β1-promoted ECM
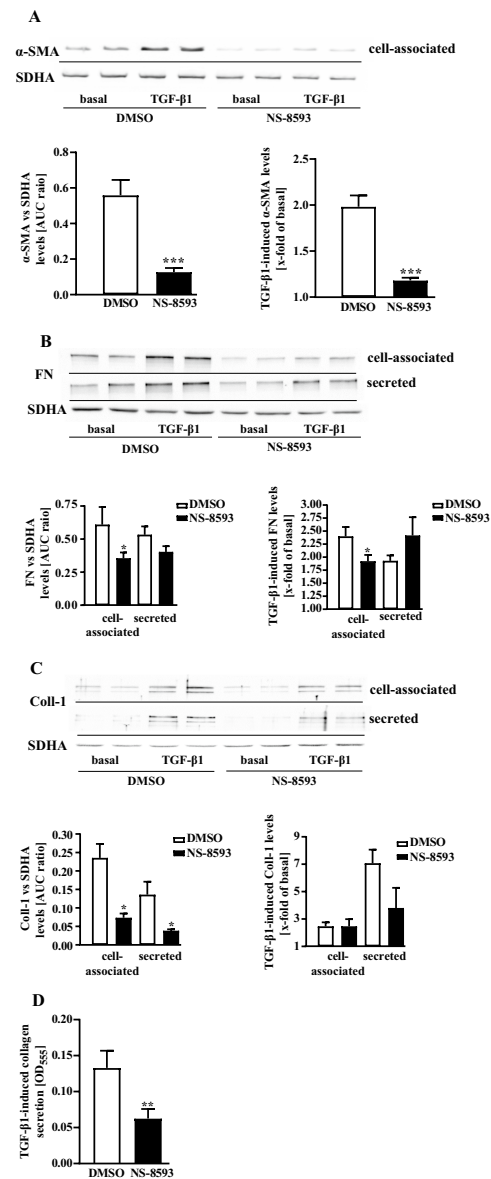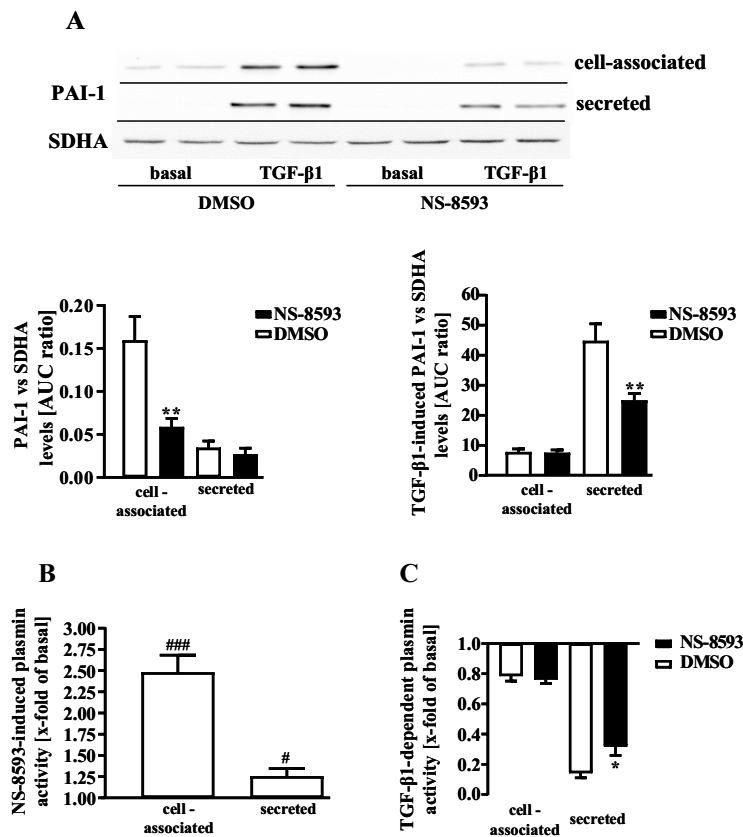
Paper III

A

Fig. 8 Detection of PAI-1 protein levels and plasmin activity in pHPF co-treated with TGF-β1 and NS-8593. **a** pHPF were stimulated with TGF-β1 (2 ng/ml) or NS-8593 (25 μM) for 48 h alone or together with both ligands. Protein amount of PAI-1 in the cell-associated and secreted fraction was determined by western blotting. SDHA control of the cellular fraction was also used for the secreted fraction. Blots of the cellular fraction were cut in half and the upper part used for detection of PAI-1 and the lower part for SDHA. Resulting signals were quantified by densitometry and AUC ratios of PAI-1 and SDHA calculated. One set of representative blots is shown. Bars represent SEM of PAI-1/SDHA expression ratios, $n = 3–5$. Asterisks indicate significant differences between DMSO and NS-8593, hash signs between basal and TGF-β1. In **b**, pHPF were stimulated with NS-8593 (25 μM) alone and in **c** only with TGF-β1 (2 ng/ml) or together with NS-8593 (25 μM) for 48 h and plasmin activity determined. In **b**, bars represent SEM of x-fold of basal (DMSO), $n = 5$. In **c**, bars represent SEM of x-fold of basal values, $n = 5$. Statistical analysis was performed using one-sample t test or one-way ANOVA followed by Tukey's post-test using the GraphPad prism software 9.1. In **a**, asterisks indicate significant differences between DMSO and NS-8593 in the absence of TGF-β and hash signs in the presence of TGF-β. In **b**, hash signs indicate significant differences to 1.0. In **c**, asterisks indicate significant differences between DMSO and NS-8593

deposition on the level of SMAD dependent transcription, *SERPINE-1* expression, plasmin activation and ECM production in pHPF. To the best of our knowledge, this is the first report of a TRP channel involved in the modulation of plasmin activity. Hence, we propose TRPM7 blockers as new tools to modify plasmin activity in pHPF.

Plg and PA act in solution or cell associated when bound to their cognate cell surface receptors (Deryugina and Quigley 2012; Hoyer-Hansen and Lund 2007; Hu et al. 2007; Milenkovic et al. 2017). Therefore, we analyzed the plasmin system in the cell associated and secreted fraction of pHPF. The total amount of secreted basal plasmin activity
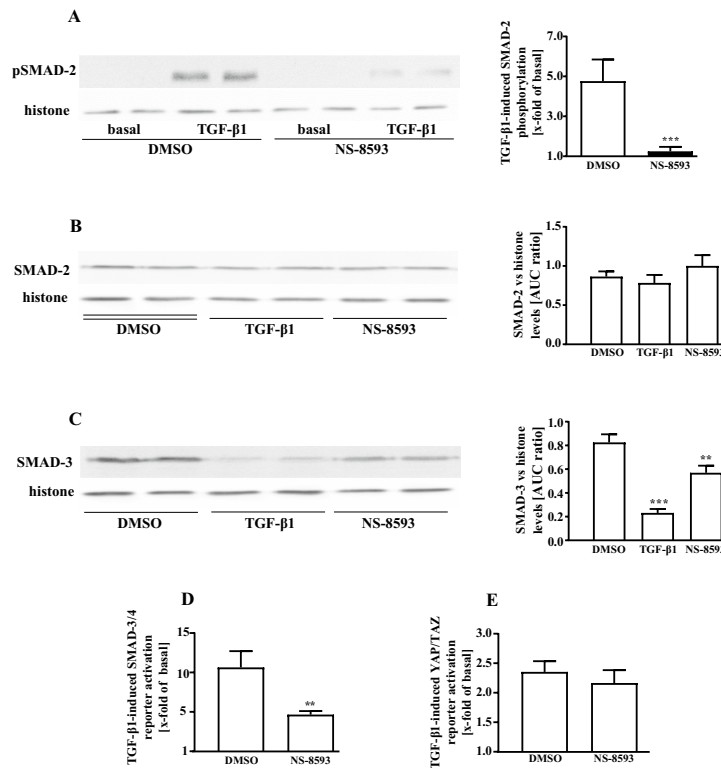
Springer

A

pSMAD-2

histone

basal　　TGF-β1　　basal　　TGF-β1
　　DMSO　　　　　　NS-8593

B

SMAD-2

histone

DMSO　　　　TGF-β1　　NS-8593

C

SMAD-3

histone

DMSO　　　　TGF-β1　　NS-8593

D

E

Fig. 9 NS-8593 inhibits TGF-β1-induced SMAD activation in pHPF. pHPF were stimulated with TGF-β1 (2 ng/ml) or NS-8593 (25 μM) for 48 h alone or together with both ligands. In **a**, the amount of pSMAD-2, in **b** of total SMAD-2 and in **c** of total SMAD-3 was determined by western blotting. Histone detection served as a loading control. Blots were cut in half and the upper part used for detection of pSMAD-2, SMAD-2 or SMAD-3 and the lower part for histone. Resulting signals were quantified by densitometry and AUC ratios of pSMAD-2, SMAD-2 or SMAD-3 and histone calculated. One set of representative blots is shown. Bars represent SEM of % AUC ratios, $n = 3–8$. In **d**, pHPF were electroporated with the pCAGA-luc reporter and in **e** with the 8xGTIIC-luciferase plasmid. After 24 h, cells were stimulated with TGF-β1 (2 ng/ml) alone or together with NS-8593 (25 μM) for 48 h and then luciferase activity determined. Bars represent SEM of x-fold over basal values, $n = 5$. Statistical analysis was performed using one-way ANOVA followed by Tukey's post-test using the GraphPad prism software 9.1. Asterisks indicate significant differences to DMSO

was ~ 20 times higher compared to the cell-associated fraction. However, it should be noted that the volume of the supernatant (50 μl) by far exceeds the volume of the cellular fraction (~ 0.05–0.1 μl). Hence, when plasmin is released into the supernatant there is a strong dilution effect and the actual plasmin concentration might be even higher in the cell-associated fraction. Despite the outstanding role of TGF-β1-mediated inhibition of plasmin activity for ECM deposition, to the best of our knowledge, direct effects of TGF-β1 on plasmin activity in pHPF have not yet been analyzed. As expected, we found that TGF-β1 decreased plasmin activity in both fractions of pHPF, but stronger in the secreted fraction. Strong effects of TGF-β on secreted

plasmin activity are in line with previous studies using other cell models (Horowitz et al. 2008; Schuliga et al. 2011). In contrast to these studies, no exogenous Plg was required to assess the effects of TGF-β1 on plasmin in pHPF, suggesting rather high endogenous Plg levels in these cells. Under these conditions, two unrelated TRPM7 blockers enhanced plasmin activity of pHPF, indicating that TRPM7 activity restrains plasmin activity in pulmonary fibroblasts. In contrast to TGF-β1, NS-8593 elevated plasmin activity largely in the cell-associated fraction. One obvious explanation for this phenomenon could be that activation and inhibition of the plasmin system follows distinct kinetics. Further, effects of NS-8593 on plasmin activity most likely depend on basal
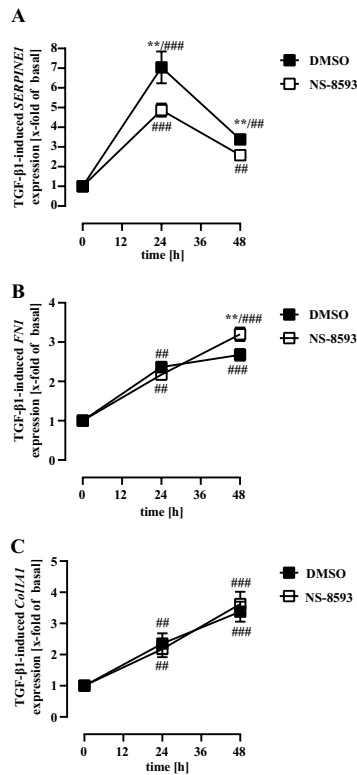
Fig. 10 NS-8593 inhibits TGF-β1-induced *SERPINE1* but not *FN1* or *Col1A1* mRNA expression in pHPF. pHPF were stimulated with TGF-β1 (2 ng/ml) for 24 or 48 h alone or together with NS-8593 (25 µM). In **a**, *SERPINE1*, in **b** *FN1* and in **c** *Col1A1* mRNA was determined by qRT-PCR. Data are represented as SEM of x-fold of basal values, $n=4$. Statistical analysis was performed using two-way ANOVA followed by Tukey's post-test using the GraphPad prism software 9.1. Asterisks indicate significant differences to DMSO, hash signs to time point zero

PAI-1 levels. As basal cell-associated PAI-1 levels in pHPF were significantly higher than those secreted, it appears reasonable that inhibitory actions on basal PAI-1 levels affected cell-associated plasmin activity stronger than secreted. Finally, the enhancing effects of TGF-β1 on PAI-1 levels were much stronger than the oppressive effects of NS-8593. Smaller changes of basal PAI-1 levels by NS-8593 might not affect PA activity in the supernatant due to the abovementioned dilution effects. However, despite these differential actions, NS-8593 clearly affected TGF-β1-promoted inhibition of the plasmin system. Of note, PAI-1 proteins that are induced and secreted by TGF-β1 have to be produced first

in the cell-associated fraction. Hence, inhibitory actions of NS-8593 on the cellular pool of PAI-1 proteins, should consequently lead to reduced TGF-β1-induced PAI-1 secretion. In line with this notion, co-administration of NS-8593 and TGF-β1 significantly reduced cell-associated and secreted PAI-1 levels and enhanced secreted plasmin activity. Furthermore, NS-8593 counteracted TGF-β1-induced production of fibronectin and collagens. Hence, TRPM7 blockade not only has the potential to enhance plasmin activity and thus to degrade ECM in native pHPF, but also in fibroblasts continuously exposed to TGF-β1.

We found a causal relationship between TRPM7 and plasmin activity after 24 and 48 of channel blockade. Inhibition of TRPM7 activity for 4 h did not affect plasmin activity (data not shown), indicating that acute TRPM7 inhibition is not linked to the plasmin system. Thus, we favor the hypothesis that TRPM7 activity affects plasmin indirectly via modulating gene expression in pHPF. Because TRPM7 blockade decreased TGF-β1-induced SMAD but not YAP/TAZ activation, it is reasonable to assume that SMAD-dependent genes are involved. The *SERPINE1* gene is a SMAD-dependent gene of utmost importance for pulmonary fibrosis (Hua et al. 1999; Song et al. 1998). TRPM7 blockade reduced TGF-β1-induced SMAD-2 phosphorylation, SMAD-3/4 reporter activation and *SERPINE1* expression on the mRNA and protein level. Hence, we provide a substantial body of evidence indicating that TRPM7 supports the SMAD pathway and thereby affects plasmin activity and thus ECM levels via regulation of PAI-1 protein levels. Of note, collagens and fibronectin are also encoded by SMAD-dependent genes (Vindevoghel et al. 1998; Zhao et al. 2002). Thus, lower ECM levels after TRPM7 blockade could also be caused by reduced transcription of these genes. However, TRPM7 blocker did not reduce TGF-β1-induced *FN1* or *Col1A1* mRNA levels. Hence, TRPM7 supports TGF-β1-promoted ECM deposition most likely by depressing plasmin-mediated degradation. These actions might be relevant in late stages of pulmonary fibrosis. Enhanced plasmin activity due to TRPM7 blockade might degrade already deposited ECM, eventually leading to tissue repair or even restoration. Of note, NS-8593 application to mice prevented and ameliorated kidney fibrosis, indicating the effectiveness of TRPM7 blocker in vivo (Suzuki et al. 2020).

At this point, we can only speculate about possible mechanism leading to rather selective effects of TRPM7 on TGF-β1-induced SERPINE1 expression. It appeared that TGF-β1 elevated SERPINE1 mRNA levels with different kinetics compared to *FN1* and *Col1A1,* indicative for distinct mode of actions by the cytokine on SMAD-dependent promoters. Although all three promoters have a regulatory binding site for SMADs in common, they also differ in binding sites for other transcription factors. In line with this notion, TRPM7 blockade selectively affected TGF-β1 signaling leading to

🙋 Springer

SMAD but not to YAP/TAZ activation. Such fine-tuned effects of TRPM7 on TGF-β1 could lead to selective reduction of SERPINE-1 mRNA by TRPM7 blockers. However, it will be an interesting task for future studies to decipher why inhibition of TGF-β1-promoted SMAD activity by TRPM7 blocker affects the *SERPINE1* but not the *FN1* or *Col1A1* promoter.

TRPM7 is a bifunctional protein with an ion channel moiety and a kinase function. The TRPM7 pore is permeable for Mg^{2+}, Ca^{2+} and Zn^{2+} ions and the α-kinase domain phosphorylates serine/threonine residues of the TRPM7 protein itself or of other cellular substrates (Koivisto et al. 2022; Monteilh-Zoller et al. 2003; Nadler et al. 2001; Nadolni and Zierler 2018; Ryazanova et al. 2004). Both TRPM7 functions could potentially affect SMAD-dependent gene expression. As no specific TRPM7 blocker is available that would target either the channel or the kinase activity independently from each other, we cannot discriminate between both activities by employing pharmacological tools. Lysine at position 1646 is essential for TRPM7 kinase activity but not for ion channel function (Kaitsuka et al. 2014; Ryazanova et al. 2014). Thus, genetically modified mice models (TRPM7-K1646R mice) have been introduced, in which the TRPM7 wild-type protein was replaced by a lysine 1646 arginine point mutant (Kaitsuka et al. 2014; Romagnani et al. 2017). TRPM7-K1646R mice appeared as useful tools to discriminate TRPM7 kinase from ion channel function in vivo and in vitro. Noteworthy, SMAD-2 is a direct substrate of the TRPM7 kinase and after 10 min of TGF-β1 stimulation SMAD-2 phosphorylation was reduced in isolated T-lymphocytes from TRPM7-K1646R mice compared to wild-type littermates, indicating that TRPM7 kinase activity supports TGF-β1-induced SMAD stimulation in these cells (Romagnani et al. 2017). Hence, we aimed at using isolated pulmonary fibroblasts from TRPM7-K1646R mice, in to analyze a role of the TRPM7 kinase in the regulation of SMAD and plasmin activity in lung fibroblasts. In this process, we soon realized that TRPM7 blockade did not affect TGF-β-induced SMAD-3/4-dependent reporter activation in wild-type mouse fibroblasts (Fig. S1a), indicating species-specific differences in the functional interactions between TRPM7 and the TGF-β system in lung fibroblasts. Furthermore, in contrast to the data obtained with pHPF, TGF-β did not decrease SMAD-3 expression in lung fibroblasts from mice (Fig. S1b), indicating species-specific differences of the TGF-β system independent from TRPM7. Because of these significant species-specific differences of the TGF-β system in pulmonary fibroblasts, we refrained to use mice models to analyze interactions between TRPM7 and TGF-β. Thus, although we provide significant evidence that TRPM7 blockade affects TGF-β signaling at multiple levels in pHPF, at this point, due to the lack of suitable tools, it remains unclear which TRPM7 function is involved.

Conclusion

The peptidase plasmin plays a central role in the pathophysiology of pulmonary fibrosis, a fatal disease with essentially no treatment. Plasmin activity elevating processes in pHPF very likely ameliorate pulmonary fibrosis. We report that TRPM7 blockers enhance plasmin activity in untreated and TGF-β-treated pHPF. Further, TRPM7 blockade limited SMAD activation and reduced PAI-1, collagen and fibronectin levels. Thus, we identify a so far unappreciated role for the TRPM7 as a positive modulator of the plasmin system in pulmonary fibroblasts and propose TRPM7 blockers as new promising tools to treat pulmonary fibrosis.

Declarations

**Conflict of interest** The authors declare no conflict of interest.

References

Andreasen PA, Egelund R, Petersen HH (2000) The plasminogen activation system in tumor growth, invasion, and metastasis. Cell Mol Life Sci 57(1):25–40. https://doi.org/10.1007/s000180050497

Bharadwaj AG, Holloway RW, Miller VA, Waisman DM (2021) Plasmin and plasminogen system in the tumor microenvironment: implications for cancer diagnosis, prognosis, and therapy. Cancers (basel). https://doi.org/10.3390/cancers13081838

Boag AH, Colby TV, Fraire AE et al (1999) The pathology of interstitial lung disease in nylon flock workers. Am J Surg Pathol 23(12):1539–1545. https://doi.org/10.1097/00000478-199912000-00012

Breton JD, Heydet D, Starrs LM, Veldre T, Ghildyal R (2018) Molecular changes during TGFbeta-mediated lung fibroblast-myofibroblast differentiation: implication for glucocorticoid resistance. Physiol Rep 6(7):e13669. https://doi.org/10.14814/phy2.13669

Chubanov V, Gudermann T (2020) Mapping TRPM7 function by NS8593. Int J Mol Sci. https://doi.org/10.3390/ijms21197017

Chubanov V, Mederos y Schnitzler M, Meissner M et al (2012) Natural and synthetic modulators of SK (K(ca)2) potassium channels inhibit magnesium-dependent activity of the kinase-coupled cation channel TRPM7. Br J Pharmacol 166(4):1357–1376. https://doi.org/10.1111/j.1476-5381.2012.01855.x

Cordasco EM, Demeter SL, Kerkay J et al (1980) Pulmonary manifestations of vinyl and polyvinyl chloride (interstitial lung disease). Newer Aspects Chest 78(6):828–834. https://doi.org/10.1378/chest.78.6.828

Dennler S, Itoh S, Vivien D, ten Dijke P, Huet S, Gauthier JM (1998) Direct binding of Smad3 and Smad4 to critical TGF beta-inducible elements in the promoter of human plasminogen activator inhibitor-type 1 gene. EMBO J 17(11):3091–3100. https://doi.org/10.1093/emboj/17.11.3091

Deryugina EI, Quigley JP (2012) Cell surface remodeling by plasmin: a new function for an old enzyme. J Biomed Biotechnol 2012:564259. https://doi.org/10.1155/2012/564259

Dong J, Ma Q (2016) Myofibroblasts and lung fibrosis induced by carbon nanotube exposure. Part Fibre Toxicol 13(1):60. https://doi.org/10.1186/s12989-016-0172-2

Du J, Xie J, Zhang Z et al (2010) TRPM7-mediated Ca2+ signals confer fibrogenesis in human atrial fibrillation. Circ Res 106(5):992–1003. https://doi.org/10.1161/CIRCRESAHA.109.206771

Dupont S, Morsut L, Aragona M et al (2011) Role of YAP/TAZ in mechanotransduction. Nature 474(7350):179–183. https://doi.org/10.1038/nature10137

Felez J, Chanquia CJ, Levin EG, Miles LA, Plow EF (1991) Binding of tissue plasminogen activator to human monocytes and monocytoid cells. Blood 78(9):2318–2327

Fernandez IE, Eickelberg O (2012) The impact of TGF-beta on lung fibrosis: from targeting to biomarkers. Proc Am Thorac Soc 9(3):111–116. https://doi.org/10.1513/pats.201203-023AW

Fleig A, Chubanov V (2014) Trpm7. Handb Exp Pharmacol 222:521–546. https://doi.org/10.1007/978-3-642-54215-2_21

George PM, Wells AU, Jenkins RG (2020) Pulmonary fibrosis and COVID-19: the potential role for antifibrotic therapy. Lancet Respir Med 8(8):807–815. https://doi.org/10.1016/S2213-2600(20)30225-3

Ghosh AK, Vaughan DE (2012) PAI-1 in tissue fibrosis. J Cell Physiol 227(2):493–507. https://doi.org/10.1002/jcp.22783

Giuranno L, Ient J, De Ruysscher D, Vooijs MA (2019) Radiation-induced lung injury (RILI). Front Oncol 9:877. https://doi.org/10.3389/fonc.2019.00877

Gu L, Zhu YJ, Yang X, Guo ZJ, Xu WB, Tian XL (2007) Effect of TGF-beta/Smad signaling pathway on lung myofibroblast differentiation. Acta Pharmacol Sin 28(3):382–391. https://doi.org/10.1111/j.1745-7254.2007.00468.x

Gyzander E, Teger-Nilsson AC (1980) Activity of the alpha 2-macroglobulin-plasmin complex on the plasmin specific substrate H-D-Val-Leu-Lys-p-nitroanilide. Thromb Res 19(1–2):165–175. https://doi.org/10.1016/0049-3848(80)90416-8

Habiel DM, Hogaboam CM (2017) Heterogeneity of fibroblasts and myofibroblasts in pulmonary fibrosis. Curr Pathobiol Rep 5(2):101–110. https://doi.org/10.1007/s40139-017-0134-x

Heldin CH, Moustakas A (2016) Signaling receptors for TGF-beta family members. Cold Spring Harb Perspect Biol. https://doi.org/10.1101/cshperspect.a022053

Horowitz JC, Rogers DS, Simon RH, Sisson TH, Thannickal VJ (2008) Plasminogen activation induced pericellular fibronectin proteolysis promotes fibroblast apoptosis. Am J Respir Cell Mol Biol 38(1):78–87. https://doi.org/10.1165/rcmb.2007-0174OC

Hoyer-Hansen G, Lund IK (2007) Urokinase receptor variants in tissue and body fluids. Adv Clin Chem 44:65–102

Hu K, Wu C, Mars WM, Liu Y (2007) Tissue-type plasminogen activator promotes murine myofibroblast activation through LDL receptor-related protein 1-mediated integrin signaling. J Clin Invest 117(12):3821–3832. https://doi.org/10.1172/JCI32301

Hua X, Miller ZA, Wu G, Shi Y, Lodish HF (1999) Specificity in transforming growth factor beta-induced transcription of the plasminogen activator inhibitor-1 gene: interactions of promoter DNA, transcription factor muE3, and Smad proteins. Proc Natl Acad Sci USA 96(23):13130–13135. https://doi.org/10.1073/pnas.96.23.13130

Huang WT, Vayalil PK, Miyata T, Hagood J, Liu RM (2012) Therapeutic value of small molecule inhibitor to plasminogen activator inhibitor-1 for lung fibrosis. Am J Respir Cell Mol Biol 46(1):87–95. https://doi.org/10.1165/rcmb.2011-0139OC

Irigoyen JP, Munoz-Canoves P, Montero L, Koziczak M, Nagamine Y (1999) The plasminogen activator system: biology and regulation. Cell Mol Life Sci 56(1–2):104–132. https://doi.org/10.1007/pl00000615

Jiang F, Liu GS, Dusting GJ, Chan EC (2014) NADPH oxidase-dependent redox signaling in TGF-beta-mediated fibrotic responses. Redox Biol 2:267–272. https://doi.org/10.1016/j.redox.2014.01.012

Kaitsuka T, Katagiri C, Beesetty P et al (2014) Inactivation of TRPM7 kinase activity does not impair its channel function in mice. Sci Rep 4:5718. https://doi.org/10.1038/srep05718

Kato H, Adachi N, Ohno Y, Iwanaga S, Takada K, Sakakibara S (1980) New fluorogenic peptide substrates for plasmin. J Biochem 88(1):183–190

Kawarada Y, Inoue Y, Kawasaki F et al (2016) TGF-beta induces p53/Smads complex formation in the PAI-1 promoter to activate transcription. Sci Rep 6:35483. https://doi.org/10.1038/srep35483

Koivisto AP, Belvisi MG, Gaudet R, Szallasi A (2022) Advances in TRP channel drug discovery: from target validation to clinical studies. Nat Rev Drug Discov 21(1):41–59. https://doi.org/10.1038/s41573-021-00268-4

Kristensen JH, Karsdal MA, Genovese F et al (2014) The role of extracellular matrix quality in pulmonary fibrosis. Respiration 88(6):487–499. https://doi.org/10.1159/000368163

Lamy C, Goodchild SJ, Weatherall KL et al (2010) Allosteric block of KCa2 channels by apamin. J Biol Chem 285(35):27067–27077. https://doi.org/10.1074/jbc.M110.110072

Lekkerkerker AN, Aarbiou J, van Es T, Janssen RA (2012) Cellular players in lung fibrosis. Curr Pharm Des 18(27):4093–4102. https://doi.org/10.2174/138161212802430396

Li M, Zhou J, Jin W, Li X, Zhang Y (2018) Danhong injection combined with t-PA improves thrombolytic therapy in focal embolic stroke. Front Pharmacol 9:308. https://doi.org/10.3389/fphar.2018.00308

Lin H, Xu L, Yu S, Hong W, Huang M, Xu P (2020) Therapeutics targeting the fibrinolytic system. Exp Mol Med 52(3):367–379. https://doi.org/10.1038/s12276-020-0397-x

Maher TM, Bendstrup E, Dron L et al (2021) Global incidence and prevalence of idiopathic pulmonary fibrosis. Respir Res 22(1):197. https://doi.org/10.1186/s12931-021-01791-z

Malmstrom J, Lindberg H, Lindberg C et al (2004) Transforming growth factor-beta 1 specifically induce proteins involved in

🖄 Springer

41

the myofibroblast contractile apparatus. Mol Cell Proteomics 3(5):466–477. https://doi.org/10.1074/mcp.M300108-MCP200

Milenkovic J, Milojkovic M, Jevtovic Stoimenov T, Djindjic B, Miljkovic E (2017) Mechanisms of plasminogen activator inhibitor 1 action in stromal remodeling and related diseases. Biomed Pap Med Fac Univ Palacky Olomouc Czech Repub 161(4):339–347. https://doi.org/10.5507/bp.2017.046

Miles LA, Dahlberg CM, Plescia J, Felez J, Kato K, Plow EF (1991) Role of cell-surface lysines in plasminogen binding to cells: identification of alpha-enolase as a candidate plasminogen receptor. Biochemistry 30(6):1682–1691. https://doi.org/10.1021/bi00220a034

Miranda MZ, Bialik JF, Speight P et al (2017) TGF-beta1 regulates the expression and transcriptional activity of TAZ protein via a Smad3-independent, myocardin-related transcription factor-mediated mechanism. J Biol Chem 292(36):14902–14920. https://doi.org/10.1074/jbc.M117.780502

Monteilh-Zoller MK, Hermosura MC, Nadler MJ, Scharenberg AM, Penner R, Fleig A (2003) TRPM7 provides an ion channel mechanism for cellular entry of trace metal ions. J Gen Physiol 121(1):49–60. https://doi.org/10.1085/jgp.20028740

Moroi M, Aoki N (1976) Isolation and characterization of alpha2-plasmin inhibitor from human plasma. A novel proteinase inhibitor which inhibits activator-induced clot lysis. J Biol Chem 251(19):5956–5965

Morse D, Rosas IO (2014) Tobacco smoke-induced lung fibrosis and emphysema. Annu Rev Physiol 76:493–513. https://doi.org/10.1146/annurev-physiol-021113-170411

Mossman BT, Churg A (1998) Mechanisms in the pathogenesis of asbestosis and silicosis. Am J Respir Crit Care Med 157(5 Pt 1):1666–1680. https://doi.org/10.1164/ajrccm.157.5.9707141

Nadler MJ, Hermosura MC, Inabe K et al (2001) LTRPC7 is a Mg.ATP-regulated divalent cation channel required for cell viability. Nature 411(6837):590–595. https://doi.org/10.1038/35079092

Nadolni W, Zierler S (2018) The channel-kinase TRPM7 as novel regulator of immune system homeostasis. Cells. https://doi.org/10.3390/cells7080109

Newman LS, Lloyd J, Daniloff E (1996) The natural history of beryllium sensitization and chronic beryllium disease. Environ Health Perspect 104(Suppl 5):937–943. https://doi.org/10.1289/ehp.96104s5937

Ojo AS, Balogun SA, Williams OT, Ojo OS (2020) Pulmonary fibrosis in COVID-19 survivors: predictive factors and risk reduction strategies. Pulm Med 2020:6175964. https://doi.org/10.1155/2020/6175964

Papp B, Kovacs T, Lerant I, Nagy Z, Machovich R (1987) Conditions of formation of the heparin-fibronectin-collagen complex and the effect of plasmin. Biochim Biophys Acta 925(3):241–247. https://doi.org/10.1016/0304-4165(87)90188-7

Paravicini TM, Chubanov V, Gudermann T (2012) TRPM7: a unique channel involved in magnesium homeostasis. Int J Biochem Cell Biol 44(8):1381–1384. https://doi.org/10.1016/j.biocel.2012.05.010

Pardo A, Selman M (2016) Lung fibroblasts, aging, and idiopathic pulmonary fibrosis. Ann Am Thorac Soc 13(Suppl 5):S417–S421. https://doi.org/10.1513/AnnalsATS.201605-341AW

Peyser R, MacDonnell S, Gao Y et al (2019) Defining the activated fibroblast population in lung fibrosis using single-cell sequencing. Am J Respir Cell Mol Biol 61(1):74–85. https://doi.org/10.1165/rcmb.2018-0313OC

Phan TT, Lim IJ, Aalami O et al (2005) Smad3 signalling plays an important role in keloid pathogenesis via epithelial-mesenchymal interactions. J Pathol 207(2):232–242. https://doi.org/10.1002/path.1826

Pins GD, Collins-Pavao ME, Van De Water L, Yarmush ML, Morgan JR (2000) Plasmin triggers rapid contraction and degradation of fibroblast-populated collagen lattices. J Invest Dermatol 114(4):647–653. https://doi.org/10.1046/j.1523-1747.2000.00858.x

Plow EF, Doeuvre L, Das R (2012) So many plasminogen receptors: why? J Biomed Biotechnol 2012:141806. https://doi.org/10.1155/2012/141806

Plow EF, Freaney DE, Plescia J, Miles LA (1986) The plasminogen system and cell surfaces: evidence for plasminogen and urokinase receptors on the same cell type. J Cell Biol 103(6 Pt 1):2411–2420. https://doi.org/10.1083/jcb.103.6.2411

Rios FJ, Zou ZG, Harvey AP et al (2020) Chanzyme TRPM7 protects against cardiovascular inflammation and fibrosis. Cardiovasc Res 116(3):721–735. https://doi.org/10.1093/cvr/cvz164

Romagnani A, Vettore V, Rezzonico-Jost T et al (2017) TRPM7 kinase activity is essential for T cell colonization and alloreactivity in the gut. Nat Commun 8(1):1917. https://doi.org/10.1038/s41467-017-01960-z

Ryazanova LV, Dorovkov MV, Ansari A, Ryazanov AG (2004) Characterization of the protein kinase activity of TRPM7/ChaK1, a protein kinase fused to the transient receptor potential ion channel. J Biol Chem 279(5):3708–3716. https://doi.org/10.1074/jbc.M308820200

Ryazanova LV, Hu Z, Suzuki S, Chubanov V, Fleig A, Ryazanov AG (2014) Elucidating the role of the TRPM7 alpha-kinase: TRPM7 kinase inactivation leads to magnesium deprivation resistance phenotype in mice. Sci Rep 4:7599. https://doi.org/10.1038/srep07599

Ryerson CJ, Kolb M (2018) The increasing mortality of idiopathic pulmonary fibrosis: fact or fallacy? Eur Respir J. https://doi.org/10.1183/13993003.02420-2017

Saito A, Horie M, Micke P, Nagase T (2018a) The role of TGF-beta signaling in lung cancer associated with idiopathic pulmonary fibrosis. Int J Mol Sci. https://doi.org/10.3390/ijms19113611

Saito A, Horie M, Nagase T (2018b) TGF-beta signaling in lung health and disease. Int J Mol Sci. https://doi.org/10.3390/ijms19082460

Schuliga M, Harris T, Stewart AG (2011) Plasminogen activation by airway smooth muscle is regulated by type I collagen. Am J Respir Cell Mol Biol 44(6):831–839. https://doi.org/10.1165/rcmb.2009-0469OC

Shioya S, Masuda T, Senoo T et al (2018) Plasminogen activator inhibitor-1 serves an important role in radiation-induced pulmonary fibrosis. Exp Ther Med 16(4):3070–3076. https://doi.org/10.3892/etm.2018.6550

Sleijfer S (2001) Bleomycin-induced pneumonitis. Chest 120(2):617–624. https://doi.org/10.1378/chest.120.2.617

Song CZ, Siok TE, Gelehrter TD (1998) Smad4/DPC4 and Smad3 mediate transforming growth factor-beta (TGF-beta) signaling through direct binding to a novel TGF-beta-responsive element in the human plasminogen activator inhibitor-1 promoter. J Biol Chem 273(45):29287–29290. https://doi.org/10.1074/jbc.273.45.29287

Staab-Weijnitz CA (2021) Fighting the fiber: targeting collagen in lung fibrosis. Am J Respir Cell Mol Biol. https://doi.org/10.1165/rcmb.2021-0342TR

Staab-Weijnitz CA, Fernandez IE, Knuppel L et al (2015) FK506-Binding protein 10, a potential novel drug target for idiopathic pulmonary fibrosis. Am J Respir Crit Care Med 192(4):455–467. https://doi.org/10.1164/rccm.201412-2233OC

Suzuki S, Penner R, Fleig A (2020) TRPM7 contributes to progressive nephropathy. Sci Rep 10(1):2333. https://doi.org/10.1038/s41598-020-59355-y

Thannickal VJ, Lee DY, White ES et al (2003) Myofibroblast differentiation by transforming growth factor-beta1 is dependent on cell adhesion and integrin signaling via focal adhesion kinase.

J Biol Chem 278(14):12384–12389. https://doi.org/10.1074/jbc.M208544200

Vasarmidi E, Tsitoura E, Spandidos DA, Tzanakis N, Antoniou KM (2020) Pulmonary fibrosis in the aftermath of the COVID-19 era (Review). Exp Ther Med 20(3):2557–2560. https://doi.org/10.3892/etm.2020.8980

Vehmas T, Pallasaho P, Oksa P (2012) Lung and pleural fibrosis in asbestos-exposed workers: a risk factor for pneumonia mortality. Epidemiol Infect 140(11):1987–1992. https://doi.org/10.1017/S0950268811002810

Vichai V, Kirtikara K (2006) Sulforhodamine B colorimetric assay for cytotoxicity screening. Nat Protoc 1(3):1112–1116. https://doi.org/10.1038/nprot.2006.179

Vindevoghel L, Kon A, Lechleider RJ, Uitto J, Roberts AB, Mauviel A (1998) Smad-dependent transcriptional activation of human type VII collagen gene (COL7A1) promoter by transforming growth factor-beta. J Biol Chem 273(21):13053–13057. https://doi.org/10.1074/jbc.273.21.13053

Walker EJ, Heydet D, Veldre T, Ghildyal R (2019) Transcriptomic changes during TGF-beta-mediated differentiation of airway fibroblasts to myofibroblasts. Sci Rep 9(1):20377. https://doi.org/10.1038/s41598-019-56955-1

Wilson MS, Wynn TA (2009) Pulmonary fibrosis: pathogenesis, etiology and regulation. Mucosal Immunol 2(2):103–121. https://doi.org/10.1038/mi.2008.85

Wu LJ, Sweet TB, Clapham DE (2010) International Union of Basic and Clinical Pharmacology. LXXVI. Current progress in the mammalian TRP ion channel family. Pharmacol Rev 62(3):381–404. https://doi.org/10.1124/pr.110.002725

Wu SR, Lin CH, Shih HP et al (2019) HAI-2 as a novel inhibitor of plasmin represses lung cancer cell invasion and metastasis. Br J Cancer 120(5):499–511. https://doi.org/10.1038/s41416-019-0400-2

Yoshida T, Ohnuma A, Horiuchi H, Harada T (2011) Pulmonary fibrosis in response to environmental cues and molecular targets involved in its pathogenesis. J Toxicol Pathol 24(1):9–24. https://doi.org/10.1293/tox.24.9

Yu M, Huang C, Huang Y, Wu X, Li X, Li J (2013) Inhibition of TRPM7 channels prevents proliferation and differentiation of human lung fibroblasts. Inflamm Res 62(11):961–970. https://doi.org/10.1007/s00011-013-0653-9

Zhang YP, Li WB, Wang WL et al (2012) siRNA against plasminogen activator inhibitor-1 ameliorates bleomycin-induced lung fibrosis in rats. Acta Pharmacol Sin 33(7):897–908. https://doi.org/10.1038/aps.2012.39

Zhao J, Shi W, Wang YL et al (2002) Smad3 deficiency attenuates bleomycin-induced pulmonary fibrosis in mice. Am J Physiol Lung Cell Mol Physiol 282(3):L585–L593. https://doi.org/10.1152/ajplung.00151.2001

Zierler S, Yao G, Zhang Z et al (2011) Waixenicin A inhibits cell proliferation through magnesium-dependent block of transient receptor potential melastatin 7 (TRPM7) channels. J Biol Chem 286(45):39328–39335. https://doi.org/10.1074/jbc.M111.264341

🖄 Springer
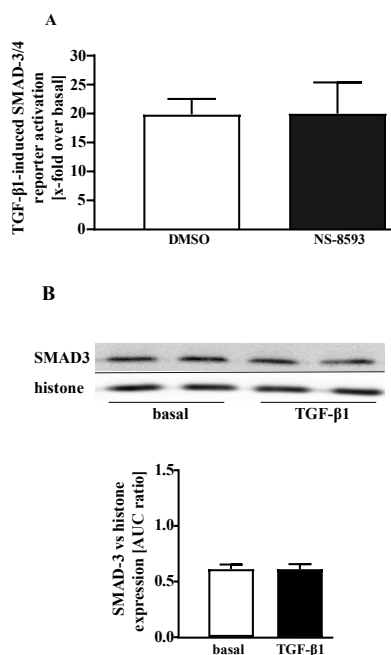
Suppl. Fig. S1 TGF-β signaling in primary pulmonary mouse fibroblasts is distinct from pHPF. Primary pulmonary mouse fibroblasts were isolated as previously described (Staab-Weijnitz et la., Am J Respir Crit Care Med. 2015 Aug 15; 192 (4): 455-67) and electroporated with the pCAGA-luc reporter. After 24 h, cells were stimulated with TGF (2 ng/ml) alone or together with NS-8593 (25 µM) for 48 h and then luciferase activity was determined. Bars represent SEM of x-fold over basal values, n = 3. In **b**, the amount of total SMAD-3 was determined by western-blotting. Histone detection served as a loading control. Blots were cut in half and the upper part used for detection of SMAD-3 and the lower part for histone. Resulting signals were quantified by densitometry and AUC ratios of SMAD-3 and histone calculated. One set of representative blots is shown. Bars represent SEM of % AUC ratios, n = 10.

Suppl. Figure 1

6.   References

1.   Geiger F, Zeitlmayr S, Staab-Weijnitz CA, Rajan S, Breit A, Gudermann T, et al. An Inhibitory Function of TRPA1 Channels in TGF-β1-driven Fibroblast to Myofibroblast Differentiation. American Journal of Respiratory Cell and Molecular Biology. 2023; In press. https://doi.org/10.1165/rcmb.2022-0159OC.

2.   Bendiks L, Geiger F, Gudermann T, Feske S, Dietrich A. Store-operated Ca2+ entry in primary murine lung fibroblasts is independent of classical transient receptor potential (TRPC) channels and contributes to cell migration. Scientific Reports. 2020;10(1):6812. https://doi.org/10.1038/s41598-020-63677-2.

3.   Zeitlmayr S, Zierler S, Staab-Weijnitz CA, Dietrich A, Geiger F, Horgen FD, et al. TRPM7 restrains plasmin activity and promotes transforming growth factor-β1 signaling in primary human lung fibroblasts. Archives of Toxicology. 2022;96(10):2767-83. https://doi.org/10.1007/s00204-022-03342-x.

4.   Hofmann K, Fiedler S, Vierkotten S, Weber J, Klee S, Jia J, et al. Classical transient receptor potential 6 (TRPC6) channels support myofibroblast differentiation and development of experimental pulmonary fibrosis. Biochimica et Biophysica Acta (BBA) - Molecular Basis of Disease. 2017;1863(2):560-8. https://doi.org/10.1016/j.bbadis.2016.12.002.

5.   Yu M, Huang C, Huang Y, Wu X, Li X, Li J. Inhibition of TRPM7 channels prevents proliferation and differentiation of human lung fibroblasts. Inflammation Research. 2013;62(11):961-70. https://doi.org/10.1007/s00011-013-0653-9.

6.   Cosens DJ, Manning A. Abnormal Electroretinogram from a Drosophila Mutant. Nature. 1969;224(5216):285-7. https://doi.org/10.1038/224285a0.

7.   Nilius B, Szallasi A. Transient receptor potential channels as drug targets: from the science of basic research to the art of medicine. Pharmacol Rev. 2014;66(3):676-814. https://doi.org/10.1124/pr.113.008268.

8.   Wes PD, Chevesich J, Jeromin A, Rosenberg C, Stetten G, Montell C. TRPC1, a human homolog of a Drosophila store-operated channel. Proc Natl Acad Sci U S A. 1995;92(21):9652-6. https://doi.org/10.1073/pnas.92.21.9652.

9.   Dietrich A. Transient Receptor Potential (TRP) Channels in Health and Disease. Cells. 2019;8(5):413. https://doi.org/10.3390/cells8050413.

10.   Achanta S, Jordt S-E. Transient receptor potential channels in pulmonary chemical injuries and as countermeasure targets. Ann N Y Acad Sci. 2020;1480(1):73-103. https://doi.org/10.1111/nyas.14472.

11.   Clapham DE. TRP channels as cellular sensors. Nature. 2003;426(6966):517-24. https://doi.org/10.1038/nature02196.

12.   Venkatachalam K, Montell C. TRP Channels. Annual Review of Biochemistry. 2007;76(1):387-417. https://doi.org/10.1146/annurev.biochem.75.103004.142819.

13.   Xie J, Sun B, Du J, Yang W, Chen H-C, Overton JD, et al. Phosphatidylinositol 4,5-bisphosphate (PIP2) controls magnesium gatekeeper TRPM6 activity. Scientific Reports. 2011;1(1):146. https://doi.org/10.1038/srep00146.

14.   Duan J, Li Z, Li J, Hulse RE, Santa-Cruz A, Valinsky WC, et al. Structure of the mammalian TRPM7, a magnesium channel required during embryonic development. Proceedings of the National Academy of Sciences. 2018;115(35):E8201-E10. https://doi.org/10.1073/pnas.1810719115.

15.   Clapham DE, Runnels LW, Strübing C. The trp ion channel family. Nature Reviews Neuroscience. 2001;2(6):387-96. https://doi.org/10.1038/35077544.

16.   Lipski J, Park TIH, Li D, Lee SCW, Trevarton AJ, Chung KKH, et al. Involvement of TRP-like channels in the acute ischemic response of hippocampal CA1 neurons in brain slices. Brain Research. 2006;1077(1):187-99. https://doi.org/10.1016/j.brainres.2006.01.016.

17.   Owsianik G, Talavera K, Voets T, Nilius B. PERMEATION AND SELECTIVITY OF TRP CHANNELS. Annual Review of Physiology. 2006;68(1):685-717. https://doi.org/10.1146/annurev.physiol.68.040204.101406.

18.   Launay P, Fleig A, Perraud A-L, Scharenberg AM, Penner R, Kinet J-P. TRPM4 Is a Ca2+-Activated Nonselective Cation Channel Mediating Cell Membrane Depolarization. Cell. 2002;109(3):397-407. https://doi.org/10.1016/S0092-8674(02)00719-5.

19.   Hofmann T, Chubanov V, Gudermann T, Montell C. TRPM5 Is a Voltage-Modulated and Ca2+-Activated Monovalent Selective Cation Channel. Current Biology. 2003;13(13):1153-8. https://doi.org/10.1016/S0960-9822(03)00431-7.

20.   Vennekens R, Hoenderop JGJ, Prenen J, Stuiver M, Willems PHGM, Droogmans G, et al. Permeation and Gating Properties of the Novel Epithelial Ca2+ Channel *. Journal of Biological Chemistry. 2000;275(6):3963-9. https://doi.org/10.1074/jbc.275.6.3963.

21.   Yue L, Peng J-B, Hediger MA, Clapham DE. CaT1 manifests the pore properties of the calcium-release-activated calcium channel. Nature. 2001;410(6829):705-9. https://doi.org/10.1038/35070596.

22.   NCBI. TRPA1 (Homo sapiens) [Webpage]. National Center for Biotechnology Information; [updated Dec-18-2022; cited Dec-19-2022]. Available from: https://www.ncbi.nlm.nih.gov/gene?cmd=retrieve&dopt=default&rn=1&list_uids=8989.

23.   NCBI. Trpa1 (Mus muculus) [Webpage]. National Center for Biotechnology Information; [updated Dec-13-2022; cited Dec-19-2022]. Available from: https://www.ncbi.nlm.nih.gov/gene/277328.

24.   Chen J, Kym PR. TRPA1: the species difference. Journal of General Physiology. 2009;133(6):623-5. https://doi.org/10.1085/jgp.200910246.

References

25. Story GM, Peier AM, Reeve AJ, Eid SR, Mosbacher J, Hricik TR, et al. ANKTM1, a TRP-like Channel Expressed in Nociceptive Neurons, Is Activated by Cold Temperatures. Cell. 2003;112(6):819-29. https://doi.org/10.1016/S0092-8674(03)00158-2.

26. Wang YY, Chang RB, Waters HN, McKemy DD, Liman ER. The Nociceptor Ion Channel TRPA1 Is Potentiated and Inactivated by Permeating Calcium Ions*. Journal of Biological Chemistry. 2008;283(47):32691-703. https://doi.org/10.1074/jbc.M803568200.

27. Bobkov YV, Corey EA, Ache BW. The pore properties of human nociceptor channel TRPA1 evaluated in single channel recordings. Biochimica et Biophysica Acta (BBA) - Biomembranes. 2011;1808(4):1120-8. https://doi.org/10.1016/j.bbamem.2010.12.024.

28. Jaquemar D, Schenker T, Trueb B. An ankyrin-like protein with transmembrane domains is specifically lost after oncogenic transformation of human fibroblasts. J Biol Chem. 1999;274(11):7325-33. https://doi.org/10.1074/jbc.274.11.7325.

29. Jordt S-E, Bautista DM, Chuang H-h, McKemy DD, Zygmunt PM, Högestätt ED, et al. Mustard oils and cannabinoids excite sensory nerve fibres through the TRP channel ANKTM1. Nature. 2004;427(6971):260-5. https://doi.org/10.1038/nature02282.

30. Nagata K, Duggan A, Kumar G, García-Añoveros J. Nociceptor and Hair Cell Transducer Properties of TRPA1, a Channel for Pain and Hearing. The Journal of Neuroscience. 2005;25(16):4052-61. https://doi.org/10.1523/jneurosci.0013-05.2005.

31. Bessac BF, Jordt S-E. Breathtaking TRP Channels: TRPA1 and TRPV1 in Airway Chemosensation and Reflex Control. Physiology. 2008;23(6):360-70. https://doi.org/10.1152/physiol.00026.2008.

32. Groneberg DA, Niimi A, Dinh QT, Cosio B, Hew M, Fischer A, et al. Increased Expression of Transient Receptor Potential Vanilloid-1 in Airway Nerves of Chronic Cough. American Journal of Respiratory and Critical Care Medicine. 2004;170(12):1276-80. https://doi.org/10.1164/rccm.200402-174OC.

33. Andrè E, Campi B, Materazzi S, Trevisani M, Amadesi S, Massi D, et al. Cigarette smoke–induced neurogenic inflammation is mediated by α,β-unsaturated aldehydes and the TRPA1 receptor in rodents. The Journal of Clinical Investigation. 2008;118(7):2574-82. https://doi.org/10.1172/JCI34886.

34. Wilson SR, Gerhold KA, Bifolck-Fisher A, Liu Q, Patel KN, Dong X, et al. TRPA1 is required for histamine-independent, Mas-related G protein–coupled receptor–mediated itch. Nature Neuroscience. 2011;14(5):595-602. https://doi.org/10.1038/nn.2789.

35. Wilson SR, Nelson AM, Batia L, Morita T, Estandian D, Owens DM, et al. The Ion Channel TRPA1 Is Required for Chronic Itch. The Journal of Neuroscience. 2013;33(22):9283-94. https://doi.org/10.1523/jneurosci.5318-12.2013.

36. Dai Y, Wang S, Tominaga M, Yamamoto S, Fukuoka T, Higashi T, et al. Sensitization of TRPA1 by PAR2 contributes to the sensation of inflammatory pain. The Journal of Clinical Investigation. 2007;117(7):1979-87. https://doi.org/10.1172/JCI30951.

37. Bang S, Kim KY, Yoo S, Kim YG, Hwang SW. Transient receptor potential A1 mediates acetaldehyde-evoked pain sensation. European Journal of Neuroscience. 2007;26(9):2516-23. https://doi.org/10.1111/j.1460-9568.2007.05882.x.

38. Bautista DM, Jordt S-E, Nikai T, Tsuruda PR, Read AJ, Poblete J, et al. TRPA1 Mediates the Inflammatory Actions of Environmental Irritants and Proalgesic Agents. Cell. 2006;124(6):1269-82. https://doi.org/10.1016/j.cell.2006.02.023.

39. Talavera K, Startek JB, Alvarez-Collazo J, Boonen B, Alpizar YA, Sanchez A, et al. Mammalian Transient Receptor Potential TRPA1 Channels: From Structure to Disease. Physiological Reviews. 2020;100(2):725-803. https://doi.org/10.1152/physrev.00005.2019.

40. Paulsen CE, Armache J-P, Gao Y, Cheng Y, Julius D. Structure of the TRPA1 ion channel suggests regulatory mechanisms. Nature. 2015;520(7548):511-7. https://doi.org/10.1038/nature14367.

41. Cvetkov TL, Huynh KW, Cohen MR, Moiseenkova-Bell VY. Molecular Architecture and Subunit Organization of TRPA1 Ion Channel Revealed by Electron Microscopy Journal of Biological Chemistry. 2011;286(44):38168-76. https://doi.org/10.1074/jbc.M111.288993.

42. Zhao J, Lin King JV, Paulsen CE, Cheng Y, Julius D. Irritant-evoked activation and calcium modulation of the TRPA1 receptor. Nature. 2020;585(7823):141-5. https://doi.org/10.1038/s41586-020-2480-9.

43. Cordero-Morales JF, Gracheva EO, Julius D. Cytoplasmic ankyrin repeats of transient receptor potential A1 (TRPA1) dictate sensitivity to thermal and chemical stimuli. Proceedings of the National Academy of Sciences. 2011;108(46):E1184-E91. https://doi.org/10.1073/pnas.1114124108.

44. Jabba S, Goyal R, Sosa-Pagán Jason O, Moldenhauer H, Wu J, Kalmeta B, et al. Directionality of Temperature Activation in Mouse TRPA1 Ion Channel Can Be Inverted by Single-Point Mutations in Ankyrin Repeat Six. Neuron. 2014;82(5):1017-31. https://doi.org/10.1016/j.neuron.2014.04.016.

45. Hinman A, Chuang H-H, Bautista DM, Julius D. TRP channel activation by reversible covalent modification. Proceedings of the National Academy of Sciences of the United States of America. 2006;103(51):19564-8. https://doi.org/10.1073/pnas.0609598103.

46. Suo Y, Wang Z, Zubcevic L, Hsu AL, He Q, Borgnia MJ, et al. Structural Insights into Electrophile Irritant Sensing by the Human TRPA1 Channel. Neuron. 2020;105(5):882-94.e5. https://doi.org/10.1016/j.neuron.2019.11.023.

47. Bautista DM, Movahed P, Hinman A, Axelsson HE, Sterner O, Högestätt ED, et al. Pungent products from garlic activate the sensory ion channel TRPA1. Proceedings of the National Academy of Sciences. 2005;102(34):12248-52. https://doi.org/10.1073/pnas.0505356102.

References

48. Bandell M, Story GM, Hwang SW, Viswanath V, Eid SR, Petrus MJ, et al. Noxious cold ion channel TRPA1 is activated by pungent compounds and bradykinin. Neuron. 2004;41(6):849-57. https://doi.org/10.1016/s0896-6273(04)00150-3.

49. Macpherson LJ, Dubin AE, Evans MJ, Marr F, Schultz PG, Cravatt BF, et al. Noxious compounds activate TRPA1 ion channels through covalent modification of cysteines. Nature. 2007;445(7127):541-5. https://doi.org/10.1038/nature05544.

50. Bahia PK, Parks TA, Stanford KR, Mitchell DA, Varma S, Stevens SM, Jr., et al. The exceptionally high reactivity of Cys 621 is critical for electrophilic activation of the sensory nerve ion channel TRPA1. Journal of General Physiology. 2016;147(6):451-65. https://doi.org/10.1085/jgp.201611581.

51. Kremeyer B, Lopera F, Cox JJ, Momin A, Rugiero F, Marsh S, et al. A Gain-of-Function Mutation in TRPA1 Causes Familial Episodic Pain Syndrome. Neuron. 2010;66(5):671-80. https://doi.org/10.1016/j.neuron.2010.04.030.

52. Zíma V, Witschas K, Hynkova A, Zímová L, Barvík I, Vlachova V. Structural modeling and patch-clamp analysis of pain-related mutation TRPA1-N855S reveal inter-subunit salt bridges stabilizing the channel open state. Neuropharmacology. 2015;93:294-307. https://doi.org/10.1016/j.neuropharm.2015.02.018.

53. Zurborg S, Yurgionas B, Jira JA, Caspani O, Heppenstall PA. Direct activation of the ion channel TRPA1 by Ca2+. Nature Neuroscience. 2007;10(3):277-9. https://doi.org/10.1038/nn1843.

54. Doerner JF, Gisselmann G, Hatt H, Wetzel CH. Transient Receptor Potential Channel A1 Is Directly Gated by Calcium Ions *. Journal of Biological Chemistry. 2007;282(18):13180-9. https://doi.org/10.1074/jbc.M607849200.

55. Fajardo O, Meseguer V, Belmonte C, Viana F. TRPA1 Channels Mediate Cold Temperature Sensing in Mammalian Vagal Sensory Neurons: Pharmacological and Genetic Evidence. The Journal of Neuroscience. 2008;28(31):7863-75. https://doi.org/10.1523/jneurosci.1696-08.2008.

56. Karashima Y, Talavera K, Everaerts W, Janssens A, Kwan KY, Vennekens R, et al. TRPA1 acts as a cold sensor in vitro and in vivo. Proceedings of the National Academy of Sciences. 2009;106(4):1273-8. https://doi.org/10.1073/pnas.0808487106.

57. Zygmunt PM, Högestätt ED. TRPA1. In: Nilius B, Flockerzi V, editors. Mammalian Transient Receptor Potential (TRP) Cation Channels: Volume I. Berlin, Heidelberg: Springer Berlin Heidelberg; 2014. p. 583-630.

58. Moparthi L, Sinica V, Moparthi VK, Kreir M, Vignane T, Filipovic MR, et al. The human TRPA1 intrinsic cold and heat sensitivity involves separate channel structures beyond the N-ARD domain. Nature Communications. 2022;13(1):6113. https://doi.org/10.1038/s41467-022-33876-8.

59. Kwan KY, Glazer JM, Corey DP, Rice FL, Stucky CL. TRPA1 modulates mechanotransduction in cutaneous sensory neurons. J Neurosci. 2009;29(15):4808-19. https://doi.org/10.1523/jneurosci.5380-08.2009.

60. da Costa DSM, Meotti FC, Andrade EL, Leal PC, Motta EM, Calixto JB. The involvement of the transient receptor potential A1 (TRPA1) in the maintenance of mechanical and cold hyperalgesia in persistent inflammation. PAIN®. 2010;148(3):431-7. https://doi.org/10.1016/j.pain.2009.12.002.

61. Kerstein PC, del Camino D, Moran MM, Stucky CL. Pharmacological blockade of TRPA1 inhibits mechanical firing in nociceptors. Molecular Pain. 2009;5(1):19. https://doi.org/10.1186/1744-8069-5-19.

62. Hofmann T, Schaefer M, Schultz G, Gudermann T. Subunit composition of mammalian transient receptor potential channels in living cells. Proceedings of the National Academy of Sciences. 2002;99(11):7461-6. https://doi.org/10.1073/pnas.102596199.

63. Vazquez G, Wedel BJ, Aziz O, Trebak M, Putney JW. The mammalian TRPC cation channels. Biochimica et Biophysica Acta (BBA) - Molecular Cell Research. 2004;1742(1):21-36. https://doi.org/10.1016/j.bbamcr.2004.08.015.

64. Dietrich A, Fahlbusch M, Gudermann T. Classical Transient Receptor Potential 1 (TRPC1): Channel or Channel Regulator? Cells. 2014;3(4):939-62. https://doi.org/10.3390/cells3040939.

65. Storch U, Forst A-L, Philipp M, Gudermann T, Mederos y Schnitzler M. Transient Receptor Potential Channel 1 (TRPC1) Reduces Calcium Permeability in Heteromeric Channel Complexes. Journal of Biological Chemistry. 2012;287(5):3530-40. https://doi.org/10.1074/jbc.M111.283218.

66. Zhu X, Chu PB, Peyton M, Birnbaumer L. Molecular cloning of a widely expressed human homologue for the Drosophila trp gene. FEBS Letters. 1995;373(3):193-8. https://doi.org/10.1016/0014-5793(95)01038-G.

67. Boulay G, Zhu X, Peyton M, Jiang M, Hurst R, Stefani E, et al. Cloning and Expression of a Novel Mammalian Homolog ofDrosophila Transient Receptor Potential (Trp) Involved in Calcium Entry Secondary to Activation of Receptors Coupled by the Gq Class of G Protein*. Journal of Biological Chemistry. 1997;272(47):29672-80. https://doi.org/10.1074/jbc.272.47.29672.

68. Hofmann T, Obukhov AG, Schaefer M, Harteneck C, Gudermann T, Schultz G. Direct activation of human TRPC6 and TRPC3 channels by diacylglycerol. Nature. 1999;397(6716):259-63. https://doi.org/10.1038/16711.

69. NCBI. TRPC1 (Homo sapiens) [Webpage]. National Center for Biotechnology Information; [updated Dec-08-2022; cited Dec-20-2022]. Available from: https://www.ncbi.nlm.nih.gov/gene/7220.

70. NCBI. Trpc1 (Mus musculus) [Webpage]. National Center for Biotechnology Information; [updated Dec-08-2022; cited Dec-20-2022]. Available from: https://www.ncbi.nlm.nih.gov/gene/22063.

71. Nesin V, Tsiokas L. TRPC1. In: Nilius B, Flockerzi V, editors. Mammalian Transient Receptor Potential (TRP) Cation Channels: Volume I. Berlin, Heidelberg: Springer Berlin Heidelberg; 2014. p. 15-51.

72. GeneCards. TRPC1 [Webpage]. [updated Nov-09-2022; cited Dec-20]. Available from: https://www.genecards.org/cgi-bin/carddisp.pl?gene=TRPC1.

References

73. Dohke Y, Oh YS, Ambudkar IS, Turner RJ. Biogenesis and Topology of the Transient Receptor Potential Ca2+ Channel TRPC1 *. Journal of Biological Chemistry. 2004;279(13):12242-8. https://doi.org/10.1074/jbc.M312456200.

74. D'Esposito M, Strazzullo M, Cuccurese M, Spalluto C, Rocchi M, D'Urso M, et al. Identification and assignment of the human transient receptor potential channel 6 gene TRPC6 to chromosome 11q21→q22. Cytogenetic and Genome Research. 1998;83(1-2):46-7. https://doi.org/10.1159/000015165.

75. Dietrich A, Gudermann T. TRPC6: Physiological Function and Pathophysiological Relevance. In: Nilius B, Flockerzi V, editors. Mammalian Transient Receptor Potential (TRP) Cation Channels: Volume I. Berlin, Heidelberg: Springer Berlin Heidelberg; 2014. p. 157-88.

76. Proteinatlas. TRPC6 [Webpage]. [cited Dec-21-2022]. Available from: https://www.proteinatlas.org/ENSG00000137672-TRPC6/single+cell+type.

77. Hofmann T, Schaefer M, Schultz G, Gudermann T. Transient receptor potential channels as molecular substrates of receptor-mediated cation entry. Journal of Molecular Medicine. 2000;78(1):14-25. https://doi.org/10.1007/s001099900070.

78. Winn MP, Conlon PJ, Lynn KL, Farrington MK, Creazzo T, Hawkins AF, et al. A Mutation in the TRPC6 Cation Channel Causes Familial Focal Segmental Glomerulosclerosis. Science. 2005;308(5729):1801-4. https://doi.org/10.1126/science.1106215.

79. Kwon Y, Hofmann T, Montell C. Integration of Phosphoinositide- and Calmodulin-Mediated Regulation of TRPC6. Molecular Cell. 2007;25(4):491-503. https://doi.org/10.1016/j.molcel.2007.01.021.

80. Tang Q, Guo W, Zheng L, Wu J-X, Liu M, Zhou X, et al. Structure of the receptor-activated human TRPC6 and TRPC3 ion channels. Cell Research. 2018;28(7):746-55. https://doi.org/10.1038/s41422-018-0038-2.

81. Dietrich A, Mederos y Schnitzler M, Emmel J, Kalwa H, Hofmann T, Gudermann T. N-Linked Protein Glycosylation Is a Major Determinant for Basal TRPC3 and TRPC6 Channel Activity *. Journal of Biological Chemistry. 2003;278(48):47842-52. https://doi.org/10.1074/jbc.M302983200.

82. Lichtenegger M, Stockner T, Poteser M, Schleifer H, Platzer D, Romanin C, et al. A novel homology model of TRPC3 reveals allosteric coupling between gate and selectivity filter. Cell Calcium. 2013;54(3):175-85. https://doi.org/10.1016/j.ceca.2013.05.010.

83. Jung S, Strotmann R, Schultz G, Plant TD. TRPC6 is a candidate channel involved in receptor-stimulated cation currents in A7r5 smooth muscle cells. Am J Physiol Cell Physiol. 2002;282(2):C347-59. https://doi.org/10.1152/ajpcell.00283.2001.

84. Shi J, Mori E, Mori Y, Mori M, Li J, Ito Y, et al. Multiple regulation by calcium of murine homologues of transient receptor potential proteins TRPC6 and TRPC7 expressed in HEK293 cells. The Journal of Physiology. 2004;561(2):415-32. https://doi.org/10.1113/jphysiol.2004.075051.

85. Bai Y, Yu X, Chen H, Horne D, White R, Wu X, et al. Structural basis for pharmacological modulation of the TRPC6 channel. eLife. 2020;9:e53311. https://doi.org/10.7554/eLife.53311.

86. Ryazanov AG, Pavur KS, Dorovkov MV. Alpha-kinases: a new class of protein kinases with a novel catalytic domain. Current Biology. 1999;9(2):R43-R5. https://doi.org/10.1016/S0960-9822(99)80006-2.

87. Ryazanova LV, Pavur KS, Petrov AN, Dorovkov MV, Ryazanov AG. Novel Type of Signaling Molecules: Protein Kinases Covalently Linked with Ion Channels. Molecular Biology. 2001;35(2):271-83. https://doi.org/10.1023/A:1010499720185.

88. Runnels LW, Yue L, Clapham DE. TRP-PLIK, a Bifunctional Protein with Kinase and Ion Channel Activities. Science. 2001;291(5506):1043-7. https://doi.org/10.1126/science.1058519.

89. Nadler MJS, Hermosura MC, Inabe K, Perraud A-L, Zhu Q, Stokes AJ, et al. LTRPC7 is a Mg·ATP-regulated divalent cation channel required for cell viability. Nature. 2001;411(6837):590-5. https://doi.org/10.1038/35079092.

90. Yamaguchi H, Matsushita M, Nairn AC, Kuriyan J. Crystal Structure of the Atypical Protein Kinase Domain of a TRP Channel with Phosphotransferase Activity. Molecular Cell. 2001;7(5):1047-57. https://doi.org/10.1016/S1097-2765(01)00256-8.

91. Perraud A-L, Fleig A, Dunn CA, Bagley LA, Launay P, Schmitz C, et al. ADP-ribose gating of the calcium-permeable LTRPC2 channel revealed by Nudix motif homology. Nature. 2001;411(6837):595-9. https://doi.org/10.1038/35079100.

92. Schlingmann KP, Weber S, Peters M, Niemann Nejsum L, Vitzthum H, Klingel K, et al. Hypomagnesemia with secondary hypocalcemia is caused by mutations in TRPM6, a new member of the TRPM gene family. Nature Genetics. 2002;31(2):166-70. https://doi.org/10.1038/ng889.

93. Walder RY, Landau D, Meyer P, Shalev H, Tsolia M, Borochowitz Z, et al. Mutation of TRPM6 causes familial hypomagnesemia with secondary hypocalcemia. Nature Genetics. 2002;31(2):171-4. https://doi.org/10.1038/ng901.

94. NCBI. TRPM7 (Homo sapiens) [Webpage]. National Center for Biotechnology Information; [updated Dec-13-2022; cited Dec-21-2022]. Available from: https://www.ncbi.nlm.nih.gov/gene/54822.

95. NCBI. Trpm7 (Mus musculus) [Webpage]. National Center for Biotechnology Information; [updated Dec-13-2022; cited Dec-21-2022]. Available from: https://www.ncbi.nlm.nih.gov/gene/58800.

96. Fonfria E, Murdock PR, Cusdin FS, Benham CD, Kelsell RE, McNulty S. Tissue Distribution Profiles of the Human TRPM Cation Channel Family. Journal of Receptors and Signal Transduction. 2006;26(3):159-78. https://doi.org/10.1080/10799890600637506.

97. Proteinatlas. TRPM7 [Webpage]. [cited Dec-21-2022]. Available from: https://www.proteinatlas.org/ENSG00000092439-TRPM7.

References

98. Jin J, Desai BN, Navarro B, Donovan A, Andrews NC, Clapham DE. Deletion of Trpm7 Disrupts Embryonic Development and Thymopoiesis Without Altering Mg2+ Homeostasis. Science. 2008;322(5902):756-60. https://doi.org/10.1126/science.1163493.

99. Jin J, Wu L-J, Jun J, Cheng X, Xu H, Andrews NC, et al. The channel kinase, TRPM7, is required for early embryonic development. Proceedings of the National Academy of Sciences. 2012;109(5):E225-E33. https://doi.org/10.1073/pnas.1120033109.

100. Aarts M, Iihara K, Wei W-L, Xiong Z-G, Arundine M, Cerwinski W, et al. A Key Role for TRPM7 Channels in Anoxic Neuronal Death. Cell. 2003;115(7):863-77. https://doi.org/10.1016/S0092-8674(03)01017-1.

101. Paravicini TM, Chubanov V, Gudermann T. TRPM7: A unique channel involved in magnesium homeostasis. The International Journal of Biochemistry & Cell Biology. 2012;44(8):1381-4. https://doi.org/10.1016/j.biocel.2012.05.010.

102. Fleig A, Chubanov V. TRPM7. In: Nilius B, Flockerzi V, editors. Mammalian Transient Receptor Potential (TRP) Cation Channels: Volume I. Berlin, Heidelberg: Springer Berlin Heidelberg; 2014. p. 521-46.

103. Schmitz C, Perraud A-L, Johnson CO, Inabe K, Smith MK, Penner R, et al. Regulation of Vertebrate Cellular Mg2+ Homeostasis by TRPM7. Cell. 2003;114(2):191-200. https://doi.org/10.1016/S0092-8674(03)00556-7.

104. Ryazanova LV, Rondon LJ, Zierler S, Hu Z, Galli J, Yamaguchi TP, et al. TRPM7 is essential for Mg2+ homeostasis in mammals. Nature Communications. 2010;1(1):109. https://doi.org/10.1038/ncomms1108.

105. Monteilh-Zoller MK, Hermosura MC, Nadler MJS, Scharenberg AM, Penner R, Fleig A. TRPM7 Provides an Ion Channel Mechanism for Cellular Entry of Trace Metal Ions. Journal of General Physiology. 2002;121(1):49-60. https://doi.org/10.1085/jgp.20028740.

106. Fujiwara Y, Minor DL. X-ray Crystal Structure of a TRPM Assembly Domain Reveals an Antiparallel Four-stranded Coiled-coil. Journal of Molecular Biology. 2008;383(4):854-70. https://doi.org/10.1016/j.jmb.2008.08.059.

107. Abiria SA, Krapivinsky G, Sah R, Santa-Cruz AG, Chaudhuri D, Zhang J, et al. TRPM7 senses oxidative stress to release Zn2+ from unique intracellular vesicles. Proceedings of the National Academy of Sciences. 2017;114(30):E6079-E88. https://doi.org/10.1073/pnas.1707380114.

108. Hofmann T, Schäfer S, Linseisen M, Sytik L, Gudermann T, Chubanov V. Activation of TRPM7 channels by small molecules under physiological conditions. Pflügers Archiv - European Journal of Physiology. 2014;466(12):2177-89. https://doi.org/10.1007/s00424-014-1488-0.

109. Demeuse P, Penner R, Fleig A. TRPM7 Channel Is Regulated by Magnesium Nucleotides via its Kinase Domain. Journal of General Physiology. 2006;127(4):421-34. https://doi.org/10.1085/jgp.200509410.

110. Chokshi R, Matsushita M, Kozak JA. Sensitivity of TRPM7 channels to Mg2+ characterized in cell-free patches of Jurkat T lymphocytes. American Journal of Physiology-Cell Physiology. 2012;302(11):C1642-C51. https://doi.org/10.1152/ajpcell.00037.2012.

111. Chokshi R, Matsushita M, Kozak JA. Detailed examination of Mg2+ and pH sensitivity of human TRPM7 channels. American Journal of Physiology-Cell Physiology. 2012;302(7):C1004-C11. https://doi.org/10.1152/ajpcell.00422.2011.

112. Kozak JA, Cahalan MD. MIC Channels Are Inhibited by Internal Divalent Cations but Not ATP. Biophys J. 2003;84(2):922-7. https://doi.org/10.1016/S0006-3495(03)74909-1.

113. Runnels LW, Yue L, Clapham DE. The TRPM7 channel is inactivated by PIP2 hydrolysis. Nature Cell Biology. 2002;4(5):329-36. https://doi.org/10.1038/ncb781.

114. Crawley SW, Côté GP. Identification of dimer interactions required for the catalytic activity of the TRPM7 alpha-kinase domain. Biochemical Journal. 2009;420(1):115-22. https://doi.org/10.1042/bj20081405.

115. Desai Bimal N, Krapivinsky G, Navarro B, Krapivinsky L, Carter Brett C, Febvay S, et al. Cleavage of TRPM7 Releases the Kinase Domain from the Ion Channel and Regulates Its Participation in Fas-Induced Apoptosis. Developmental Cell. 2012;22(6):1149-62. https://doi.org/10.1016/j.devcel.2012.04.006.

116. Matsushita M, Kozak JA, Shimizu Y, McLachlin DT, Yamaguchi H, Wei F-Y, et al. Channel Function Is Dissociated from the Intrinsic Kinase Activity and Autophosphorylation of TRPM7/ChaK1 *. Journal of Biological Chemistry. 2005;280(21):20793-803. https://doi.org/10.1074/jbc.M413671200.

117. Kim TY, Shin SK, Song M-Y, Lee JE, Park K-S. Identification of the phosphorylation sites on intact TRPM7 channels from mammalian cells. Biochemical and Biophysical Research Communications. 2012;417(3):1030-4. https://doi.org/10.1016/j.bbrc.2011.12.085.

118. Clark K, Middelbeek J, Morrice NA, Figdor CG, Lasonder E, van Leeuwen FN. Massive autophosphorylation of the Ser/Thr-rich domain controls protein kinase activity of TRPM6 and TRPM7. PloS one [Internet]. 2008 2008/03//; 3(3):[e1876 p.]. Available from: https://europepmc.org/articles/PMC2267223?pdf=render.

119. Ryazanova LV, Dorovkov MV, Ansari A, Ryazanov AG. Characterization of the Protein Kinase Activity of TRPM7/ChaK1, a Protein Kinase Fused to the Transient Receptor Potential Ion Channel *. Journal of Biological Chemistry. 2004;279(5):3708-16. https://doi.org/10.1074/jbc.M308820200.

120. Dorovkov MV, Ryazanov AG. Phosphorylation of Annexin I by TRPM7 Channel-Kinase*. Journal of Biological Chemistry. 2004;279(49):50643-6. https://doi.org/10.1074/jbc.C400441200.

121. Clark K, Middelbeek J, Dorovkov MV, Figdor CG, Ryazanov AG, Lasonder E, et al. The α-kinases TRPM6 and TRPM7, but not eEF-2 kinase, phosphorylate the assembly domain of myosin IIA, IIB and IIC. FEBS Letters. 2008;582(20):2993-7. https://doi.org/10.1016/j.febslet.2008.07.043.

References

122. Deason-Towne F, Perraud A-L, Schmitz C. Identification of Ser/Thr phosphorylation sites in the C2-domain of phospholipase C γ2 (PLCγ2) using TRPM7-kinase. Cellular Signalling. 2012;24(11):2070-5. https://doi.org/10.1016/j.cellsig.2012.06.015.

123. Nadolni W, Zierler S. The Channel-Kinase TRPM7 as Novel Regulator of Immune System Homeostasis. Cells. 2018;7(8):109. https://doi.org/10.3390/cells7080109.

124. Berridge MJ, Lipp P, Bootman MD. The versatility and universality of calcium signalling. Nature Reviews Molecular Cell Biology. 2000;1(1):11-21. https://doi.org/10.1038/35036035.

125. Carafoli E. Calcium signaling: A tale for all seasons. Proceedings of the National Academy of Sciences. 2002;99(3):1115-22. https://doi.org/10.1073/pnas.032427999.

126. Berridge MJ, Bootman MD, Roderick HL. Calcium signalling: dynamics, homeostasis and remodelling. Nature Reviews Molecular Cell Biology. 2003;4(7):517-29. https://doi.org/10.1038/nrm1155.

127. Raraty M, Ward J, Erdemli G, Vaillant C, Neoptolemos JP, Sutton R, et al. Calcium-dependent enzyme activation and vacuole formation in the apical granular region of pancreatic acinar cells. Proceedings of the National Academy of Sciences. 2000;97(24):13126-31. https://doi.org/10.1073/pnas.97.24.13126.

128. Rizzuto R, Pozzan T. Microdomains of Intracellular Ca2+: Molecular Determinants and Functional Consequences. Physiological Reviews. 2006;86(1):369-408. https://doi.org/10.1152/physrev.00004.2005.

129. Gilabert J. Cytoplasmic Calcium Buffering: An Integrative Crosstalk. In: Islam S, editor. Calcium Signaling. Advances in Experimental Medicine and Biology. 1. 2 ed: Springer Cham; 2019. p. 163-82.

130. Parekh AB. Decoding cytosolic Ca2+ oscillations. Trends in Biochemical Sciences. 2011;36(2):78-87. https://doi.org/10.1016/j.tibs.2010.07.013.

131. Dietrich A, Kalwa H, Rost BR, Gudermann T. The diacylgylcerol-sensitive TRPC3/6/7 subfamily of cation channels: functional characterization and physiological relevance. Pflügers Archiv. 2005;451(1):72-80. https://doi.org/10.1007/s00424-005-1460-0.

132. Berridge MJ. Rapid accumulation of inositol trisphosphate reveals that agonists hydrolyse polyphosphoinositides instead of phosphatidylinositol. Biochemical Journal. 1983;212(3):849-58. https://doi.org/10.1042/bj2120849.

133. Berridge MJ, Irvine RF. Inositol trisphosphate, a novel second messenger in cellular signal transduction. Nature. 1984;312(5992):315-21. https://doi.org/10.1038/312315a0.

134. Burgess GM, Godfrey PP, McKinney JS, Berridge MJ, Irvine RF, Putney JW. The second messenger linking receptor activation to internal Ca release in liver. Nature. 1984;309(5963):63-6. https://doi.org/10.1038/309063a0.

135. Putney JW. A model for receptor-regulated calcium entry. Cell Calcium. 1986;7(1):1-12. https://doi.org/10.1016/0143-4160(86)90026-6.

136. Parekh AB, James W. Putney J. Store-Operated Calcium Channels. Physiological Reviews. 2005;85(2):757-810. https://doi.org/10.1152/physrev.00057.2003.

137. Furuichi T, Yoshikawa S, Miyawaki A, Wada K, Maeda N, Mikoshiba K. Primary structure and functional expression of the inositol 1,4,5-trisphosphate-binding protein P400. Nature. 1989;342(6245):32-8. https://doi.org/10.1038/342032a0.

138. Streb H, Irvine RF, Berridge MJ, Schulz I. Release of Ca2+ from a nonmitochondrial intracellular store in pancreatic acinar cells by inositol-1,4,5-trisphosphate. Nature. 1983;306(5938):67-9. https://doi.org/10.1038/306067a0.

139. Parekh AB, Penner R. Store depletion and calcium influx. Physiological Reviews. 1997;77(4):901-30. https://doi.org/10.1152/physrev.1997.77.4.901.

140. Hoth M, Penner R. Depletion of intracellular calcium stores activates a calcium current in mast cells. Nature. 1992;355(6358):353-6. https://doi.org/10.1038/355353a0.

141. Roos J, DiGregorio PJ, Yeromin AV, Ohlsen K, Lioudyno M, Zhang S, et al. STIM1, an essential and conserved component of store-operated Ca2+ channel function. Journal of Cell Biology. 2005;169(3):435-45. https://doi.org/10.1083/jcb.200502019.

142. Liou J, Kim ML, Do Heo W, Jones JT, Myers JW, Ferrell JE, Jr., et al. STIM Is a Ca2+ Sensor Essential for Ca2+-Store-Depletion-Triggered Ca2+ Influx. Current Biology. 2005;15(13):1235-41. https://doi.org/10.1016/j.cub.2005.05.055.

143. Takemura H, Hughes AR, Thastrup O, Putney JW. Activation of Calcium Entry by the Tumor Promoter Thapsigargin in Parotid Acinar Cells: Evidence that an intracellular calcium pool, and not an inositol phosphate, regulates calcium fluxes at the plasma membrane. Journal of Biological Chemistry. 1989;264(21):12266-71. https://doi.org/10.1016/S0021-9258(18)63852-9.

144. Zhang SL, Yu Y, Roos J, Kozak JA, Deerinck TJ, Ellisman MH, et al. STIM1 is a Ca2+ sensor that activates CRAC channels and migrates from the Ca2+ store to the plasma membrane. Nature. 2005;437(7060):902-5. https://doi.org/10.1038/nature04147.

145. Stathopulos PB, Li G-Y, Plevin MJ, Ames JB, Ikura M. Stored Ca2+ Depletion-induced Oligomerization of Stromal Interaction Molecule 1 (STIM1) via the EF-SAM Region. Journal of Biological Chemistry. 2006;281(47):35855-62. https://doi.org/10.1074/jbc.M608247200.

146. Feske S, Gwack Y, Prakriya M, Srikanth S, Puppel S-H, Tanasa B, et al. A mutation in Orai1 causes immune deficiency by abrogating CRAC channel function. Nature. 2006;441(7090):179-85. https://doi.org/10.1038/nature04702.

147. Yeromin AV, Zhang SL, Jiang W, Yu Y, Safrina O, Cahalan MD. Molecular identification of the CRAC channel by altered ion selectivity in a mutant of Orai. Nature. 2006;443(7108):226-9. https://doi.org/10.1038/nature05108.

References

148. Vig M, Peinelt C, Beck A, Koomoa DL, Rabah D, Koblan-Huberson M, et al. CRACM1 Is a Plasma Membrane Protein Essential for Store-Operated Ca2+ Entry. Science. 2006;312(5777):1220-3. https://doi.org/10.1126/science.1127883.

149. Liou J, Fivaz M, Inoue T, Meyer T. Live-cell imaging reveals sequential oligomerization and local plasma membrane targeting of stromal interaction molecule 1 after Ca2+ store depletion. Proceedings of the National Academy of Sciences. 2007;104(22):9301-6. https://doi.org/10.1073/pnas.0702866104.

150. Mullins FM, Park CY, Dolmetsch RE, Lewis RS. STIM1 and calmodulin interact with Orai1 to induce Ca2+-dependent inactivation of CRAC channels. Proceedings of the National Academy of Sciences. 2009;106(36):15495-500. https://doi.org/10.1073/pnas.0906781106.

151. Shaw JP, Utz PJ, Durand DB, Toole JJ, Emmel EA, Crabtree GR. Identification of a putative regulator of early T cell activation genes. Science. 1988;241(4862):202-5. https://doi.org/10.1126/science.3260404.

152. Hogan PG, Chen L, Nardone J, Rao A. Transcriptional regulation by calcium, calcineurin, and NFAT. Genes & Development. 2003;17(18):2205-32. https://doi.org/10.1101/gad.1102703.

153. Cheng KT, Ong HL, Liu X, Ambudkar IS. Chapter Seven - Contribution and Regulation of TRPC Channels in Store-Operated Ca2+ Entry. In: Prakriya M, editor. Current Topics in Membranes. 71: Academic Press; 2013. p. 149-79.

154. Hoth M, Penner R. Calcium release-activated calcium current in rat mast cells. The Journal of Physiology. 1993;465(1):359-86. https://doi.org/10.1113/jphysiol.1993.sp019681.

155. Voets T, Prenen J, Fleig A, Vennekens R, Watanabe H, Hoenderop JGJ, et al. CaT1 and the Calcium Release-activated Calcium Channel Manifest Distinct Pore Properties *. Journal of Biological Chemistry. 2001;276(51):47767-70. https://doi.org/10.1074/jbc.C100607200.

156. Huang GN, Zeng W, Kim JY, Yuan JP, Han L, Muallem S, et al. STIM1 carboxyl-terminus activates native SOC, Icrac and TRPC1 channels. Nature Cell Biology. 2006;8(9):1003-10. https://doi.org/10.1038/ncb1454.

157. Zeng W, Yuan JP, Kim MS, Choi YJ, Huang GN, Worley PF, et al. STIM1 Gates TRPC Channels, but Not Orai1, by Electrostatic Interaction. Molecular Cell. 2008;32(3):439-48. https://doi.org/10.1016/j.molcel.2008.09.020.

158. Lee KP, Choi S, Hong JH, Ahuja M, Graham S, Ma R, et al. Molecular Determinants Mediating Gating of Transient Receptor Potential Canonical (TRPC) Channels by Stromal Interaction Molecule 1 (STIM1) *. Journal of Biological Chemistry. 2014;289(10):6372-82. https://doi.org/10.1074/jbc.M113.546556.

159. Ong HL, Cheng KT, Liu X, Bandyopadhyay BC, Paria BC, Soboloff J, et al. Dynamic Assembly of TRPC1-STIM1-Orai1 Ternary Complex Is Involved in Store-operated Calcium Influx: EVIDENCE FOR SIMILARITIES IN STORE-OPERATED AND CALCIUM RELEASE-ACTIVATED CALCIUM CHANNEL COMPONENTS. Journal of Biological Chemistry. 2007;282(12):9105-16. https://doi.org/10.1074/jbc.M608942200.

160. Liao Y, Erxleben C, Yildirim E, Abramowitz J, Armstrong DL, Birnbaumer L. Orai proteins interact with TRPC channels and confer responsiveness to store depletion. Proceedings of the National Academy of Sciences. 2007;104(11):4682-7. https://doi.org/10.1073/pnas.0611692104.

161. Liao Y, Erxleben C, Abramowitz J, Flockerzi V, Zhu MX, Armstrong DL, et al. Functional interactions among Orai1, TRPCs, and STIM1 suggest a STIM-regulated heteromeric Orai/TRPC model for SOCE/Icrac channels. Proceedings of the National Academy of Sciences. 2008;105(8):2895-900. https://doi.org/10.1073/pnas.0712288105.

162. Liao Y, Plummer NW, George MD, Abramowitz J, Zhu MX, Birnbaumer L. A role for Orai in TRPC-mediated Ca2+ entry suggests that a TRPC:Orai complex may mediate store and receptor operated Ca2+ entry. Proceedings of the National Academy of Sciences. 2009;106(9):3202-6. https://doi.org/10.1073/pnas.0813346106.

163. Albarrán L, Lopez JJ, Dionisio N, Smani T, Salido GM, Rosado JA. Transient receptor potential ankyrin-1 (TRPA1) modulates store-operated Ca(2+) entry by regulation of STIM1-Orai1 association. Biochim Biophys Acta. 2013;1833(12):3025-34. https://doi.org/10.1016/j.bbamcr.2013.08.014.

164. Souza Bomfim GH, Costiniti V, Li Y, Idaghdour Y, Lacruz RS. TRPM7 activation potentiates SOCE in enamel cells but requires ORAI. Cell Calcium. 2020;87:102187. https://doi.org/10.1016/j.ceca.2020.102187.

165. Faouzi M, Kilch T, Horgen FD, Fleig A, Penner R. The TRPM7 channel kinase regulates store-operated calcium entry. The Journal of Physiology. 2017;595(10):3165-80. https://doi.org/10.1113/JP274006.

166. Beesetty P, Wieczerzak KB, Gibson JN, Kaitsuka T, Luu CT, Matsushita M, et al. Inactivation of TRPM7 kinase in mice results in enlarged spleens, reduced T-cell proliferation and diminished store-operated calcium entry. Scientific Reports. 2018;8(1):3023. https://doi.org/10.1038/s41598-018-21004-w.

167. Guillot L, Nathan N, Tabary O, Thouvenin G, Le Rouzic P, Corvol H, et al. Alveolar epithelial cells: Master regulators of lung homeostasis. The International Journal of Biochemistry & Cell Biology. 2013;45(11):2568-73. https://doi.org/10.1016/j.biocel.2013.08.009.

168. Bousquet J, Czarlewski W, Zuberbier T, Mullol J, Blain H, Cristol JP, et al. Potential Interplay between Nrf2, TRPA1, and TRPV1 in Nutrients for the Control of COVID-19. International Archives of Allergy and Immunology. 2021;182(4):324-38. https://doi.org/10.1159/000514204.

169. Leidinger G, Flockerzi F, Hohneck J, Bohle RM, Fieguth A, Tschernig T. TRPC6 is altered in COVID-19 pneumonia. Chemico-Biological Interactions. 2022;362:109982. https://doi.org/10.1016/j.cbi.2022.109982.

170. Ojo AS, Balogun SA, Williams OT, Ojo OS. Pulmonary Fibrosis in COVID-19 Survivors: Predictive Factors and Risk Reduction Strategies. Pulmonary Medicine. 2020;2020:6175964. https://doi.org/10.1155/2020/6175964.

References

171. Wendisch D, Dietrich O, Mari T, von Stillfried S, Ibarra IL, Mittermaier M, et al. SARS-CoV-2 infection triggers profibrotic macrophage responses and lung fibrosis. Cell. 2021;184(26):6243-61.e27. https://doi.org/10.1016/j.cell.2021.11.033.

172. Vasarmidi E, Tsitoura E, Spandidos DA, Tzanakis N, Antoniou KM. Pulmonary fibrosis in the aftermath of the COVID-19 era (Review). Exp Ther Med. 2020;20(3):2557-60. https://doi.org/10.3892/etm.2020.8980.

173. NIH. Respiratory System [Webpage]. U. S. National Institutes of Health, National Cancer Institute; [cited Dec-12-2022]. Available from: https://training.seer.cancer.gov/anatomy/respiratory/.

174. Hogan B, Tata PR. Cellular organization and biology of the respiratory system. Nature Cell Biology. 2019. https://doi.org/10.1038/s41556-019-0357-7.

175. Matthys H, Seeger W. Klinische Pneumologie. 4 ed. Heidelberg: Springer Berlin, Heidelberg; 2008. 754 p.

176. MASON RJ. Biology of alveolar type II cells. Respirology. 2006;11(s1):S12-S5. https://doi.org/10.1111/j.1440-1843.2006.00800.x.

177. Stone KC, Mercer RR, Gehr P, Stockstill B, Crapo JD. Allometric Relationships of Cell Numbers and Size in the Mammalian Lung. American Journal of Respiratory Cell and Molecular Biology. 1992;6(2):235-43. https://doi.org/10.1165/ajrcmb/6.2.235.

178. Rooney SA, Young SL, Mendelson CR. Molecular and cellular processing of lung surfactant1. The FASEB Journal. 1994;8(12):957-67. https://doi.org/10.1096/fasebj.8.12.8088461.

179. Kopf M, Schneider C, Nobs SP. The development and function of lung-resident macrophages and dendritic cells. Nature Immunology. 2015;16(1):36-44. https://doi.org/10.1038/ni.3052.

180. Kleinstreuer C, Zhang Z, Donohue JF. Targeted Drug-Aerosol Delivery in the Human Respiratory System. Annual Review of Biomedical Engineering. 2008;10(1):195-220. https://doi.org/10.1146/annurev.bioeng.10.061807.160544.

181. Ushakumary MG, Riccetti M, Perl A-KT. Resident interstitial lung fibroblasts and their role in alveolar stem cell niche development, homeostasis, injury, and regeneration. STEM CELLS Translational Medicine. 2021;10(7):1021-32. https://doi.org/10.1002/sctm.20-0526.

182. Plikus MV, Wang X, Sinha S, Forte E, Thompson SM, Herzog EL, et al. Fibroblasts: Origins, definitions, and functions in health and disease. Cell. 2021;184(15):3852-72. https://doi.org/10.1016/j.cell.2021.06.024.

183. McGowan SE, Torday JS. The pulmonary lipofibroblast (lipid interstitial cell) and its contributions to alveolar development. Annu Rev Physiol. 1997;59:43-62. https://doi.org/10.1146/annurev.physiol.59.1.43.

184. Hynes RO, Naba A. Overview of the Matrisome—An Inventory of Extracellular Matrix Constituents and Functions. Cold Spring Harbor Perspectives in Biology. 2012;4(1). https://doi.org/10.1101/cshperspect.a004903.

185. Naba A, Clauser KR, Hoersch S, Liu H, Carr SA, Hynes RO. The Matrisome: In Silico Definition and In Vivo Characterization by Proteomics of Normal and Tumor Extracellular Matrices Molecular & Cellular Proteomics. 2012;11(4). https://doi.org/10.1074/mcp.M111.014647.

186. White ES. Lung Extracellular Matrix and Fibroblast Function. Annals of the American Thoracic Society. 2015;12(Supplement 1):S30-S3. https://doi.org/10.1513/AnnalsATS.201406-240MG.

187. Matthes SA, Hadley R, Roman J, White ES. Chapter 20 - Comparative Biology of the Normal Lung Extracellular Matrix. In: Parent RA, editor. Comparative Biology of the Normal Lung (Second Edition). San Diego: Academic Press; 2015. p. 387-402.

188. Onursal C, Dick E, Angelidis I, Schiller HB, Staab-Weijnitz CA. Collagen Biosynthesis, Processing, and Maturation in Lung Ageing. Frontiers in Medicine. 2021;8. https://doi.org/10.3389/fmed.2021.593874.

189. Zhou Y, Horowitz JC, Naba A, Ambalavanan N, Atabai K, Balestrini J, et al. Extracellular matrix in lung development, homeostasis and disease. Matrix Biology. 2018;73:77-104. https://doi.org/10.1016/j.matbio.2018.03.005.

190. Campbell ID, Humphries MJ. Integrin Structure, Activation, and Interactions. Cold Spring Harbor Perspectives in Biology. 2011;3(3). https://doi.org/10.1101/cshperspect.a004994.

191. Hynes RO. Integrins: Bidirectional, Allosteric Signaling Machines. Cell. 2002;110(6):673-87. https://doi.org/10.1016/S0092-8674(02)00971-6.

192. George EL, Georges-Labouesse EN, Patel-King RS, Rayburn H, Hynes RO. Defects in mesoderm, neural tube and vascular development in mouse embryos lacking fibronectin. Development. 1993;119(4):1079-91. https://doi.org/10.1242/dev.119.4.1079.

193. Georges-Labouesse EN, George EL, Rayburn H, Hynes RO. Mesodermal development in mouse embryos mutant for fibronectin. Developmental Dynamics. 1996;207(2):145-56. https://doi.org/10.1002/(SICI)1097-0177(199610)207:2<145::AID-AJA3>3.0.CO;2-H.

194. Schwarzbauer JE, DeSimone DW. Fibronectins, Their Fibrillogenesis, and In Vivo Functions. Cold Spring Harbor Perspectives in Biology. 2011;3(7). https://doi.org/10.1101/cshperspect.a005041.

195. Schwartz MA. Integrins and Extracellular Matrix in Mechanotransduction. Cold Spring Harbor Perspectives in Biology. 2010;2(12). https://doi.org/10.1101/cshperspect.a005066.

196. Yurchenco PD. Basement Membranes: Cell Scaffoldings and Signaling Platforms. Cold Spring Harbor Perspectives in Biology. 2011;3(2). https://doi.org/10.1101/cshperspect.a004911.

197. Sarrazin S, Lamanna WC, Esko JD. Heparan Sulfate Proteoglycans. Cold Spring Harbor Perspectives in Biology. 2011;3(7). https://doi.org/10.1101/cshperspect.a004952.

References

198. Hynes RO. The Extracellular Matrix: Not Just Pretty Fibrils. Science. 2009;326(5957):1216-9. https://doi.org/10.1126/science.1176009.

199. Miles LA, Dahlberg CM, Plescia J, Felez J, Kato K, Plow EF. Role of cell-surface lysines in plasminogen binding to cells: identification of alpha-enolase as a candidate plasminogen receptor. Biochemistry. 1991;30(6):1682-91. https://doi.org/10.1021/bi00220a034.

200. Andreasen* PA, Egelund R, Petersen HH. The plasminogen activation system in tumor growth, invasion, and metastasis. Cellular and Molecular Life Sciences CMLS. 2000;57(1):25-40. https://doi.org/10.1007/s000180050497.

201. Deryugina EI, Quigley JP. Cell surface remodeling by plasmin: a new function for an old enzyme. J Biomed Biotechnol. 2012;2012:564259. https://doi.org/10.1155/2012/564259.

202. Papp B, Kovács T, Léránt I, Nagy Z, Machovich R. Conditions of formation of the heparin-fibronectin-collagen complex and the effect of plasmin. Biochim Biophys Acta. 1987;925(3):241-7. https://doi.org/10.1016/0304-4165(87)90188-7.

203. Pins GD, Collins-Pavao ME, Van De Water L, Yarmush ML, Morgan JR. Plasmin triggers rapid contraction and degradation of fibroblast-populated collagen lattices. J Invest Dermatol. 2000;114(4):647-53. https://doi.org/10.1046/j.1523-1747.2000.00858.x.

204. Bharadwaj AG, Holloway RW, Miller VA, Waisman DM. Plasmin and Plasminogen System in the Tumor Microenvironment: Implications for Cancer Diagnosis, Prognosis, and Therapy. Cancers (Basel). 2021;13(8):1838. https://doi.org/10.3390/cancers13081838.

205. Beachley VZ, Wolf MT, Sadtler K, Manda SS, Jacobs H, Blatchley MR, et al. Tissue matrix arrays for high-throughput screening and systems analysis of cell function. Nature Methods. 2015;12(12):1197-204. https://doi.org/10.1038/nmeth.3619.

206. Cortini F, Villa C, Marinelli B, Combi R, Pesatori AC, Bassotti A. Understanding the basis of Ehlers–Danlos syndrome in the era of the next-generation sequencing. Archives of Dermatological Research. 2019;311(4):265-75. https://doi.org/10.1007/s00403-019-01894-0.

207. King TE, Jr., Pardo A, Selman M. Idiopathic pulmonary fibrosis. The Lancet. 2011;378(9807):1949-61. https://doi.org/10.1016/S0140-6736(11)60052-4.

208. Abe R, Donnelly SC, Peng T, Bucala R, Metz CN. Peripheral Blood Fibrocytes: Differentiation Pathway and Migration to Wound Sites1. The Journal of Immunology. 2001;166(12):7556-62. https://doi.org/10.4049/jimmunol.166.12.7556.

209. Bainbridge P.1 BBC. Wound healing and the role of fibroblasts. Journal of Wound Care. 2013;22(8):407-12. https://doi.org/10.12968/jowc.2013.22.8.407.

210. Soo C, Shaw WW, Zhang X, Longaker MT, Howard EW, Ting K. Differential Expression of Matrix Metalloproteinases and Their Tissue-Derived Inhibitors in Cutaneous Wound Repair. Plastic and Reconstructive Surgery. 2000;105(2):638-47.

211. Moses HL, Branum EL, Proper JA, Robinson RA. Transforming Growth Factor Production by Chemically Transformed Cells1. Cancer Research. 1981;41(7):2842-8.

212. Roberts AB, Anzano MA, Lamb LC, Smith JM, Sporn MB. New class of transforming growth factors potentiated by epidermal growth factor: isolation from non-neoplastic tissues. Proceedings of the National Academy of Sciences. 1981;78(9):5339-43. https://doi.org/10.1073/pnas.78.9.5339.

213. Sporn MB, Roberts AB, Shull JH, Smith JM, Ward JM, Sodek J. Polypeptide Transforming Growth Factors Isolated from Bovine Sources and Used for Wound Healing in Vivo. Science. 1983;219(4590):1329-31. https://doi.org/10.1126/science.6572416.

214. Desmoulière A, Geinoz A, Gabbiani F, Gabbiani G. Transforming growth factor-beta 1 induces alpha-smooth muscle actin expression in granulation tissue myofibroblasts and in quiescent and growing cultured fibroblasts. Journal of Cell Biology. 1993;122(1):103-11. https://doi.org/10.1083/jcb.122.1.103.

215. Rønnov-Jessen L, Petersen OW. Induction of alpha-smooth muscle actin by transforming growth factor-beta 1 in quiescent human breast gland fibroblasts. Implications for myofibroblast generation in breast neoplasia. Lab Invest. 1993;68(6):696-707.

216. WERNER S, GROSE R. Regulation of Wound Healing by Growth Factors and Cytokines. Physiological Reviews. 2003;83(3):835-70. https://doi.org/10.1152/physrev.2003.83.3.835.

217. Gabbiani G, Ryan GB, Majno G. Presence of modified fibroblasts in granulation tissue and their possible role in wound contraction. Experientia. 1971;27(5):549-50. https://doi.org/10.1007/BF02147594.

218. Majno G, Gabbiani G, Hirschel BJ, Ryan GB, Statkov PR. Contraction of Granulation Tissue in vitro: Similarity to Smooth Muscle. Science. 1971;173(3996):548-50. https://doi.org/10.1126/science.173.3996.548.

219. Sappino AP, Schürch W, Gabbiani G. Differentiation repertoire of fibroblastic cells: expression of cytoskeletal proteins as marker of phenotypic modulations. Lab Invest. 1990;63(2):144-61.

220. Grinnell F. Fibroblasts, myofibroblasts, and wound contraction. J Cell Biol. 1994;124(4):401-4. https://doi.org/10.1083/jcb.124.4.401.

221. Tomasek JJ, Gabbiani G, Hinz B, Chaponnier C, Brown RA. Myofibroblasts and mechano-regulation of connective tissue remodelling. Nature Reviews Molecular Cell Biology. 2002;3(5):349-63. https://doi.org/10.1038/nrm809.

222. Hinz B, Phan SH, Thannickal VJ, Galli A, Bochaton-Piallat M-L, Gabbiani G. The Myofibroblast: One Function, Multiple Origins. The American Journal of Pathology. 2007;170(6):1807-16. https://doi.org/10.2353/ajpath.2007.070112.

223. Desmoulière A, Redard M, Darby I, Gabbiani G. Apoptosis mediates the decrease in cellularity during the transition between granulation tissue and scar. Am J Pathol. 1995;146(1):56-66.

References

224. Grinnell F, Zhu M, Carlson MA, Abrams JM. Release of Mechanical Tension Triggers Apoptosis of Human Fibroblasts in a Model of Regressing Granulation Tissue. Experimental Cell Research. 1999;248(2):608-19. https://doi.org/10.1006/excr.1999.4440.

225. PFF. Radiation-Induced Pulmonary Fibrosis [Webpage]. Pulmonary Fibrosis Foundation [cited Dec-24-2022]. Available from: https://www.pulmonaryfibrosis.org/understanding-pff/types-of-pulmonary-fibrosis/radiation-induced.

226. Richeldi L, Collard HR, Jones MG. Idiopathic pulmonary fibrosis. The Lancet. 2017;389(10082):1941-52. https://doi.org/10.1016/S0140-6736(17)30866-8.

227. Moss BJ, Ryter SW, Rosas IO. Pathogenic Mechanisms Underlying Idiopathic Pulmonary Fibrosis. Annual Review of Pathology: Mechanisms of Disease. 2022;17(1):515-46. https://doi.org/10.1146/annurev-pathol-042320-030240.

228. Glass DS, Grossfeld D, Renna HA, Agarwala P, Spiegler P, DeLeon J, et al. Idiopathic pulmonary fibrosis: Current and future treatment. The Clinical Respiratory Journal. 2022;16(2):84-96. https://doi.org/10.1111/crj.13466.

229. Mora AL, Rojas M, Pardo A, Selman M. Emerging therapies for idiopathic pulmonary fibrosis, a progressive age-related disease. Nature Reviews Drug Discovery. 2017;16(11):755-72. https://doi.org/10.1038/nrd.2017.170.

230. Wynn TA, Ramalingam TR. Mechanisms of fibrosis: therapeutic translation for fibrotic disease. Nature Medicine. 2012;18(7):1028-40. https://doi.org/10.1038/nm.2807.

231. King TE, Bradford WZ, Castro-Bernardini S, Fagan EA, Glaspole I, Glassberg MK, et al. A Phase 3 Trial of Pirfenidone in Patients with Idiopathic Pulmonary Fibrosis. New England Journal of Medicine. 2014;370(22):2083-92. https://doi.org/10.1056/NEJMoa1402582.

232. Noble PW, Albera C, Bradford WZ, Costabel U, Glassberg MK, Kardatzke D, et al. Pirfenidone in patients with idiopathic pulmonary fibrosis (CAPACITY): two randomised trials. Lancet. 2011;377(9779):1760-9. https://doi.org/10.1016/s0140-6736(11)60405-4.

233. Richeldi L, du Bois RM, Raghu G, Azuma A, Brown KK, Costabel U, et al. Efficacy and Safety of Nintedanib in Idiopathic Pulmonary Fibrosis. New England Journal of Medicine. 2014;370(22):2071-82. https://doi.org/10.1056/NEJMoa1402584.

234. Richeldi L, Costabel U, Selman M, Kim DS, Hansell DM, Nicholson AG, et al. Efficacy of a tyrosine kinase inhibitor in idiopathic pulmonary fibrosis. N Engl J Med. 2011;365(12):1079-87. https://doi.org/10.1056/NEJMoa1103690.

235. Selvaggio AS, Noble PW. Pirfenidone Initiates a New Era in the Treatment of Idiopathic Pulmonary Fibrosis. Annual Review of Medicine. 2016;67(1):487-95. https://doi.org/10.1146/annurev-med-120214-013614.

236. Martinez FJ, Collard HR, Pardo A, Raghu G, Richeldi L, Selman M, et al. Idiopathic pulmonary fibrosis. Nature Reviews Disease Primers. 2017;3(1):17074. https://doi.org/10.1038/nrdp.2017.74.

237. Heldin C-H, Moustakas A. Role of Smads in TGFβ signaling. Cell and Tissue Research. 2012;347(1):21-36. https://doi.org/10.1007/s00441-011-1190-x.

238. Zhao J, Shi W, Wang Y-L, Chen H, Pablo Bringas J, Datto MB, et al. Smad3 deficiency attenuates bleomycin-induced pulmonary fibrosis in mice. American Journal of Physiology-Lung Cellular and Molecular Physiology. 2002;282(3):L585-L93. https://doi.org/10.1152/ajplung.00151.2001.

239. Vindevoghel L, Lechleider RJ, Kon A, de Caestecker MP, Uitto J, Roberts AB, et al. SMAD3/4-dependent transcriptional activation of the human type VII collagen gene (COL7A1) promoter by transforming growth factor beta. Proc Natl Acad Sci U S A. 1998;95(25):14769-74. https://doi.org/10.1073/pnas.95.25.14769.

240. Rahaman SO, Grove LM, Paruchuri S, Southern BD, Abraham S, Niese KA, et al. TRPV4 mediates myofibroblast differentiation and pulmonary fibrosis in mice. The Journal of Clinical Investigation. 2014;124(12):5225-38. https://doi.org/10.1172/JCI75331.

241. Ramires FJ, Sun Y, Weber KT. Myocardial fibrosis associated with aldosterone or angiotensin II administration: attenuation by calcium channel blockade. J Mol Cell Cardiol. 1998;30(3):475-83. https://doi.org/10.1006/jmcc.1997.0612.

242. Du J, Xie J, Zhang Z, Tsujikawa H, Fusco D, Silverman D, et al. TRPM7-Mediated Ca2+ Signals Confer Fibrogenesis in Human Atrial Fibrillation. Circulation Research. 2010;106(5):992-1003. https://doi.org/10.1161/CIRCRESAHA.109.206771.

243. Davis J, Burr Adam R, Davis Gregory F, Birnbaumer L, Molkentin Jeffery D. A TRPC6-Dependent Pathway for Myofibroblast Transdifferentiation and Wound Healing In Vivo. Developmental Cell. 2012;23(4):705-15. https://doi.org/10.1016/j.devcel.2012.08.017.

244. Park S, Lee S, Park E-J, Kang M, So I, Jeon J-H, et al. TGFβ1 induces stress fiber formation through upregulation of TRPC6 in vascular smooth muscle cells. Biochemical and Biophysical Research Communications. 2017;483(1):129-34. https://doi.org/10.1016/j.bbrc.2016.12.179.

245. Lin BL, Matera D, Doerner JF, Zheng N, del Camino D, Mishra S, et al. In vivo selective inhibition of TRPC6 by antagonist BI 749327 ameliorates fibrosis and dysfunction in cardiac and renal disease. Proceedings of the National Academy of Sciences. 2019;116(20):10156-61. https://doi.org/10.1073/pnas.1815354116.

246. Zhang Y, Yin N, Sun A, Wu Q, Hu W, Hou X, et al. Transient Receptor Potential Channel 6 Knockout Ameliorates Kidney Fibrosis by Inhibition of Epithelial–Mesenchymal Transition. Frontiers in Cell and Developmental Biology. 2021;8. https://doi.org/10.3389/fcell.2020.602703.

247. Zheng Z, Xu Y, Krügel U, Schaefer M, Grune T, Nürnberg B, et al. In Vivo Inhibition of TRPC6 by SH045 Attenuates Renal Fibrosis in a New Zealand Obese (NZO) Mouse Model of Metabolic Syndrome. International Journal of Molecular Sciences. 2022;23(12):6870. https://doi.org/10.3390/ijms23126870.

References

248. Kim EY, Yazdizadeh Shotorbani P, Dryer SE. Trpc6 inactivation confers protection in a model of severe nephrosis in rats. Journal of Molecular Medicine. 2018;96(7):631-44. https://doi.org/10.1007/s00109-018-1648-3.

249. Kong W, Haschler TN, Nürnberg B, Krämer S, Gollasch M, Markó L. Renal Fibrosis, Immune Cell Infiltration and Changes of TRPC Channel Expression after Unilateral Ureteral Obstruction in Trpc6-/- Mice. Cell Physiol Biochem. 2019;52(6):1484-502. https://doi.org/10.33594/000000103.

250. Gu L-f, Ge H-t, Zhao L, Wang Y-j, Zhang F, Tang H-t, et al. Huangkui Capsule Ameliorates Renal Fibrosis in a Unilateral Ureteral Obstruction Mouse Model Through TRPC6 Dependent Signaling Pathways. Frontiers in Pharmacology. 2020;11. https://doi.org/10.3389/fphar.2020.00996.

251. Wu Y-L, Xie J, An S-W, Oliver N, Barrezueta NX, Lin M-H, et al. Inhibition of TRPC6 channels ameliorates renal fibrosis and contributes to renal protection by soluble klotho. Kidney International. 2017;91(4):830-41. https://doi.org/10.1016/j.kint.2016.09.039.

252. Su Y, Chen Q, Ju Y, Li W, Li W. Palmitate induces human glomerular mesangial cells fibrosis through CD36-mediated transient receptor potential canonical channel 6/nuclear factor of activated T cell 2 activation. Biochimica et Biophysica Acta (BBA) - Molecular and Cell Biology of Lipids. 2020;1865(12):158793. https://doi.org/10.1016/j.bbalip.2020.158793.

253. Kurahara LH, Sumiyoshi M, Aoyagi K, Hiraishi K, Nakajima K, Nakagawa M, et al. Intestinal Myofibroblast TRPC6 Channel May Contribute to Stenotic Fibrosis in Crohn's Disease. Inflammatory Bowel Diseases. 2015;21(3):496-506. https://doi.org/10.1097/mib.0000000000000295.

254. Kurahara LH, Hiraishi K, Sumiyoshi M, Doi M, Hu Y, Aoyagi K, et al. Significant contribution of TRPC6 channel-mediated Ca2+ influx to the pathogenesis of Crohn's disease fibrotic stenosis. Journal of Smooth Muscle Research. 2016;52:78-92. https://doi.org/10.1540/jsmr.52.78.

255. Kuwahara K, Wang Y, McAnally J, Richardson JA, Bassel-Duby R, Hill JA, et al. TRPC6 fulfills a calcineurin signaling circuit during pathologic cardiac remodeling. The Journal of Clinical Investigation. 2006;116(12):3114-26. https://doi.org/10.1172/JCI27702.

256. Bogdanova E, Beresneva O, Galkina O, Zubina I, Ivanova G, Parastaeva M, et al. Myocardial Hypertrophy and Fibrosis Are Associated with Cardiomyocyte Beta-Catenin and TRPC6/Calcineurin/NFAT Signaling in Spontaneously Hypertensive Rats with 5/6 Nephrectomy. International Journal of Molecular Sciences. 2021;22(9):4645. https://doi.org/10.3390/ijms22094645.

257. Sassoli C, Chellini F, Squecco R, Tani A, Idrizaj E, Nosi D, et al. Low intensity 635 nm diode laser irradiation inhibits fibroblast–myofibroblast transition reducing TRPC1 channel expression/activity: New perspectives for tissue fibrosis treatment. Lasers in Surgery and Medicine. 2016;48(3):318-32. https://doi.org/10.1002/lsm.22441.

258. Wei Y, Wu Y, Feng K, Zhao Y, Tao R, Xu H, et al. Astragaloside IV inhibits cardiac fibrosis via miR-135a-TRPM7-TGF-β/Smads pathway. Journal of Ethnopharmacology. 2020;249:112404. https://doi.org/10.1016/j.jep.2019.112404.

259. Jia T, Wang X, Tang Y, Yu W, Li C, Cui S, et al. Sacubitril Ameliorates Cardiac Fibrosis Through Inhibiting TRPM7 Channel. Frontiers in Cell and Developmental Biology. 2021;9. https://doi.org/10.3389/fcell.2021.760035.

260. Fang L, Zhan S, Huang C, Cheng X, Lv X, Si H, et al. TRPM7 channel regulates PDGF-BB-induced proliferation of hepatic stellate cells via PI3K and ERK pathways. Toxicology and Applied Pharmacology. 2013;272(3):713-25. https://doi.org/10.1016/j.taap.2013.08.009.

261. Fang L, Huang C, Meng X, Wu B, Ma T, Liu X, et al. TGF-β1-elevated TRPM7 channel regulates collagen expression in hepatic stellate cells via TGF-β1/Smad pathway. Toxicology and Applied Pharmacology. 2014;280(2):335-44. https://doi.org/10.1016/j.taap.2014.08.006.

262. Cai S, Wu L, Yuan S, Liu G, Wang Y, Fang L, et al. Carvacrol alleviates liver fibrosis by inhibiting TRPM7 and modulating the MAPK signaling pathway. European Journal of Pharmacology. 2021;898:173982. https://doi.org/10.1016/j.ejphar.2021.173982.

263. Lu J, Wang Q-y, Zhou Y, Lu X-c, Liu Y-h, Wu Y, et al. AstragalosideⅣ against cardiac fibrosis by inhibiting TRPM7 channel. Phytomedicine. 2017;30:10-7. https://doi.org/10.1016/j.phymed.2017.04.002.

264. Guo J-L, Yu Y, Jia Y-Y, Ma Y-Z, Zhang B-Y, Liu P-Q, et al. Transient Receptor Potential Melastatin 7 (TRPM7) Contributes to H2O2-Induced Cardiac Fibrosis via Mediating Ca2+ Influx and Extracellular Signal–Regulated Kinase 1/2 (ERK1/2) Activation in Cardiac Fibroblasts. Journal of Pharmacological Sciences. 2014;125(2):184-92. https://doi.org/10.1254/jphs.13224FP.

265. Dolivo DM, Larson SA, Dominko T. Crosstalk between mitogen-activated protein kinase inhibitors and transforming growth factor-β signaling results in variable activation of human dermal fibroblasts. Int J Mol Med. 2019;43(1):325-35. https://doi.org/10.3892/ijmm.2018.3949.

266. Saraiva M, O'Garra A. The regulation of IL-10 production by immune cells. Nature Reviews Immunology. 2010;10(3):170-81. https://doi.org/10.1038/nri2711.

267. Inoue R, Kurahara L-H, Hiraishi K. TRP channels in cardiac and intestinal fibrosis. Seminars in Cell & Developmental Biology. 2019;94:40-9. https://doi.org/10.1016/j.semcdb.2018.11.002.

268. Virk HS, Biddle MS, Smallwood DT, Weston CA, Castells E, Bowman VW, et al. TGFβ1 induces resistance of human lung myofibroblasts to cell death via down-regulation of TRPA1 channels. British Journal of Pharmacology. 2021;178(15):2948-62. https://doi.org/10.1111/bph.15467.

269. Kurahara LH, Hiraishi K, Hu Y, Koga K, Onitsuka M, Doi M, et al. Activation of Myofibroblast TRPA1 by Steroids and Pirfenidone Ameliorates Fibrosis in Experimental Crohn's Disease. Cell Mol Gastroenterol Hepatol. 2018;5(3):299-318. https://doi.org/10.1016/j.jcmgh.2017.12.005.

References

270. Li W, Zhang Z, Li X, Cai J, Li D, Du J, et al. CGRP derived from cardiac fibroblasts is an endogenous suppressor of cardiac fibrosis. Cardiovasc Res. 2020;116(7):1335-48. https://doi.org/10.1093/cvr/cvz234.

271. Hiraishi K, Kurahara L-H, Sumiyoshi M, Hu Y-P, Koga K, Onitsuka M, et al. Daikenchuto (Da-Jian-Zhong-Tang) ameliorates intestinal fibrosis by activating myofibroblast transient receptor potential ankyrin 1 channel. World Journal of Gastroenterology. 2018;24(35):4036. https://doi.org/10.3748/wjg.v24.i35.4036.

272. Ma S, Wang DH. Knockout of Trpa1 accelerates age-related cardiac fibrosis and dysfunction. PLOS ONE. 2022;17(9):e0274618. https://doi.org/10.1371/journal.pone.0274618.

273. Schaefer EA, Stohr S, Meister M, Aigner A, Gudermann T, Buech TR. Stimulation of the chemosensory TRPA1 cation channel by volatile toxic substances promotes cell survival of small cell lung cancer cells. Biochem Pharmacol. 2013;85(3):426-38. https://doi.org/10.1016/j.bcp.2012.11.019.

274. Wang Z, Xu Y, Wang M, Ye J, Liu J, Jiang H, et al. TRPA1 inhibition ameliorates pressure overload-induced cardiac hypertrophy and fibrosis in mice. eBioMedicine. 2018;36:54-62. https://doi.org/10.1016/j.ebiom.2018.08.022.

Acknowledgements